Capacity assessment of a single span arch bridge with backfill

- A case study of the Glomman Bridge

HENRIK BJURSTRÖM
JOHAN LASELL

KTH Architecture and the Built Environment

Master of Science Thesis
Stockholm, Sweden 2009

KTH Architecture and
the Built Environment

Capacity assessment of a single span arch bridge with backfill

- A case study of the Glomman Bridge

Henrik Bjurström & Johan Lasell

February 2009
TRITA-BKN. Master Thesis 271, 2009
ISSN 1103-4297
ISRN KTH/BKN/EX-271-SE

Royal Institute of Technology (KTH)
Department of Civil and Architectural Engineering
Division of Structural Design and Bridges
Stockholm, Sweden, 2009

Preface

The research presented in this thesis was initiated by Reinertsen Sverige AB. The work has been carried out at the Department of Civil and Architectural Engineering at the Royal Institute of Technology, KTH, and at Reinertsen's office in Stockholm.

We would like to give our sincere gratitude to our supervisor Andreas Andersson, Ph.D. student at the Department of Civil and Architectural Engineering at KTH. Thank you for all the hours spent giving us invaluable advice in different situations and for the guidance during the work with this thesis.

Thanks to Ph.D. Henrik Gabrielsson, our supervisor at Reinertsen Sverige AB and to our examiner Professor Raid Karoumi for advices and discussions.

Special thanks go to Richard Malm, Ph.D. student at the Department of Civil and Architectural Engineering, KTH, for devoted time spent helping us.

We would also like to thank our families and friends, who have always been supporting and understanding during this work.

Stockholm, February 2009

Henrik Bjurström & Johan Lasell

Abstract

The aim of this Master Thesis is to assess the load carrying capacity of the Glomman Bridge outside of the Swedish city Örebro. The Glomman Bridge is an unreinforced concrete single span arch bridge with backfill. The bridge was constructed in 1923 on assignment from the Swedish National Railways (SJ).

The failure criteria used in this thesis is that the bridge collapses when any cross section in the concrete arch reaches its ultimate capacity. In reality, the bridge may manage heavier loads than this. When the capacity is reached in a cross section, a hinge is formed and the arch relocates the forces to other parts of the arch that can carry higher stresses. The real bridge will not collapse until a fourth hinge is formed, and by that a mechanism. To be able to calculate the cross section forces in the arch, it was necessary to know the influences of the loads on the arch when they were run along the bridge. For this purpose, influence lines were obtained from a 2D finite element model created in ABAQUS, a general FE-analyses software. A calculation routine to find the least favourable load combination was then created in MATLAB, a numerical calculation software. The routine was made to find the worst case among different load cases and to combine the standardized axle pressures with the present number of axles.

A parametric survey was also performed because the material properties for the different parts of the bridge are very uncertain. In the survey, the initial values were changed one at a time to study the outcome on the load factor. The load factor is the ratio between the ultimate limit load and the actual load. The studied parameters are the compressive strength, the Young's modulus, the density and the Poisson's ratio of the different parts of the bridge. The parameters are studied individually irrespective of possible correlation. The studied parts of the bridge are the backfill, the arch, the abutments and the asphalt. The clearly most important component is found to be the backfill. With increased stiffness or increased Poisson's ratio in the backfill follows increased load factor.

The equations behind the failure envelope can be derived from equilibrium equations for the unreinforced cross section. The influence lines are normalised with respect to the capacity of the cross section to get the degree of efficiency along the whole length of the arch, instead of the common influence lines that give the cross section forces. This is done because the failure is not caused by large cross section forces but by an exceeded ultimate stress. As the different loads are run along the bridge, the largest positive and negative efficiency for bending moment and normal force are localised. The normalised cross section forces are plotted together with the failure envelope and the load factor is then calculated.

Several masonry arch bridges were loaded until collapse in a study performed by the British Transport and Road Research Laboratory. One of the bridges in the study, the Prestwood Bridge, has been used in this thesis as a comparison to the Glomman Bridge. The load carrying capacity of the Prestwood Bridge is known, and is used to verify that the method using the failure envelope is applicable.

To compare the results from the cross section analysis from the failure envelope model to another method, the Glomman Bridge and the Prestwood Bridge were also tested in the commercial software RING 2.0. The method used in RING 2.0 differs from the failure mode in this thesis by calculating the load factor when four different cross sections reach their capacity and the bridge collapses.

The results in this report are discussed and compared to results obtained by Reinertsen Sverige AB. The studied method allows higher axle- and bogie loads than the method used by Reinertsen. The big difference is the failure mode. While the equilibrium equations used in this report allow increased loading until the eccentric normal force does not manage to balance the bending moment, Reinertsen uses a failure criterion that failure occurs when the tensile strength is exceeded.

When using the worst conceivable parameters and just letting the concrete compressive strength in the arch vary, load factors were calculated stated as a worst-case scenario. The load factors are shown in the figure below.

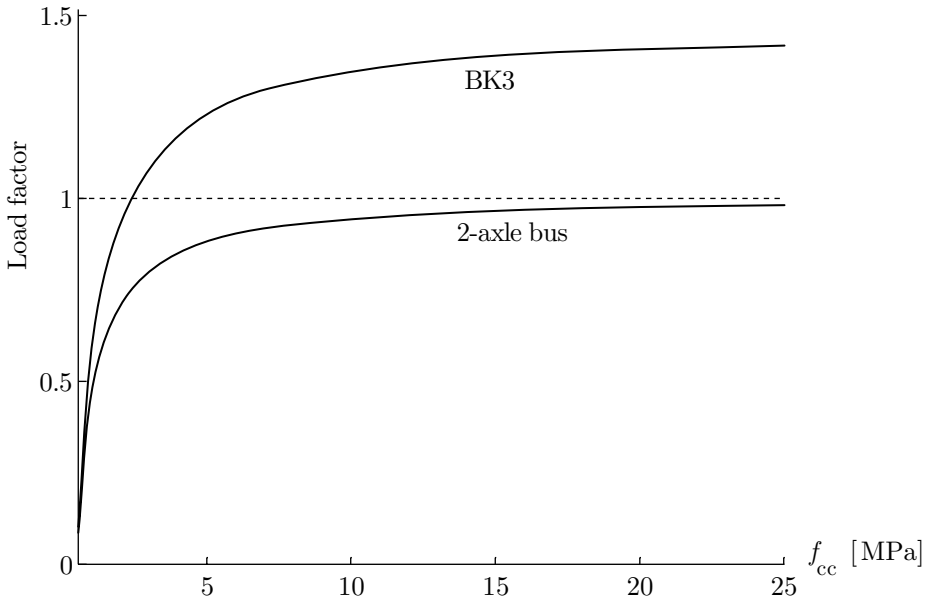

The failure envelope method allows an A/B-value (Axle- and Bogie load) of 102 kN/147 kN when using very poor values of the parameters and 181 kN/226 kN when using a reference case with normal parameters.

Although the load capacity is found to be acceptable, the uncertainties are still large. To get a more accurate apprehension of the condition of the actual bridge, further research should be carried out, such as e.g. a non-linear model.

Keywords: Arch bridge, vault, finite element, backfill, failure envelope, masonry, capacity assessment.

Sammanfattning

Syftet med föreliggande examensarbete är att uppskatta bärförmågan hos bron Glomman utanför Örebro. Glomman är en oarmerad betongvalvbro i ett spann med ovanliggande jordfyllning. Bron byggdes 1926 på uppdrag av Statens Järnvägar (SJ).

Brottkriteriet i detta examensarbete är att bron går till brott när något tvärsnitt i betongbågen uppnår sin kapacitet. I själva verket är det möjligt att bron kan klara tyngre last än detta. När kapaciteten nås i ett tvärsnitt uppstår en led och bågen omlagrar krafterna till andra bågdelar som klarar större spänningar. Den verkliga bron rasar inte förrän en fjärde led har utvecklats, och därmed en mekanism. För att kunna beräkna tvärsnittskrafterna i bågen, var det nödvändigt att känna till trafiklasternas påverkan på bågen när de kördes över bron. För detta ändamål erhölls influenslinjer från en tvådimensionell finita elementmodell skapad i ABAQUS, ett generellt FE-program. En beräkningsrutin för att finna värsta tänkbara lastkombinering skapades i MATLAB, ett numeriskt beräkningsprogram. Rutinen utformades för att hitta värsta fallet bland olika lastfall samt för att kombinera standardiserade axeltryck med det aktuella antalet axlar.

En parameterstudie utfördes också då materialegenskaperna för de olika delarna i bron är mycket osäkra. I parameterstudien ändrades ingångsvärdena ett åt gången för att studera utslaget på lastfaktorn. Lastfaktorn är förhållandet mellan brottgränslasten och den verkliga lasten. De parametrar som studeras är tryckhållfastheten, E-modulen, densiteten och tvärkontraktionen för de olika brodelarna. Parametrarna studeras enskilt utan hänsyn till eventuell korrelation. De brodelar som studeras är fyllningen, bågen, fundamenten och asfalten. Den klart viktigaste komponenten visar sig vara fyllningen. Med ökad styvhet eller ökad tvärkontraktion i fyllningen följer ökad lastfaktor.

Ekvationerna bakom brottenveloppet kan härledas ur jämviktsekvationer för det oarmerade tvärsnittet. Influenslinjerna normeras med avseende på tvärsnittets kapacitet för att få ut utnyttjandegraden längs hela bågen. Detta görs då det egentligen inte är för stor tvärsnittskraft som orsakar brott utan för stor spänning. Högsta och lägsta utnyttjandegrad för böjande moment och normalkraft lokaliseras när de olika typlasterna körs över bron. Utnyttjandegraderna placeras i brottenveloppet för att sedan räkna fram en lastfaktor.

Ett flertal liknande broar har lastats till brott i en studie genomförd av British Transport and Road Research Laboratory. En av broarna i studien, Prestwood Bridge, har använts i denna rapport som jämförelse med Glomman. Då bärförmågan hos Prestwood Bridge är känd används den till att bekräfta att metoden med brottenveloppet är tillämpbar.

För att jämföra resultaten från tvärsnittsanalysen i brottenveloppmetoden med en annan metod, testades även Glomman och Prestwood Bridge i det kommersiella programmet RING 2.0. Metoden som används i RING 2.0 skiljer sig från brottmoden i denna rapport genom att istället beräkna lastfaktorn när fyra olika tvärsnitt har uppnått sina kapaciteter och bron kollapsar.

Resultaten i denna rapport diskuteras och jämförs med resultat erhållna av Reinertsen Sverige AB. Den använda modellen tillåter högre axel- och boggitryck än metoden som används av Reinertsen. Den stora skillnaden är brottmoden. Medan jämviktsekvationer i denna rapport tillåter fortsatt pålastning tills den excentriska normalkraften inte klarar av att balansera det böjande momentet, använder Reinertsen ett brottkriterium som innebär att brott uppstår när draghållfastheten överskrids.

När sämsta tänkbara parametrar används och endast betongens tryckhållfasthet i bågen tillåts variera, beräknas lastfaktorerna som ett sämsta fall. Lastfaktorerna visas i figuren nedan.

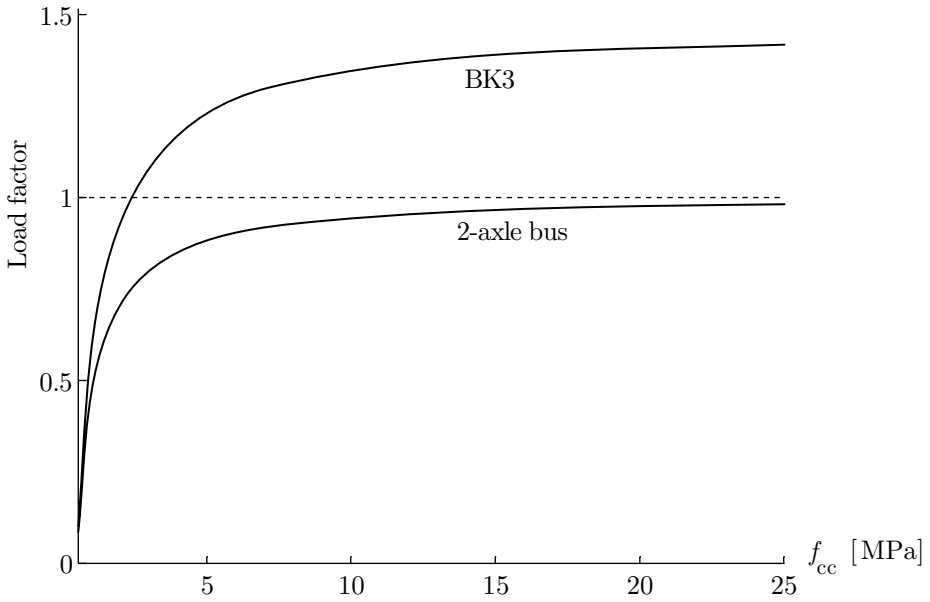

Metoden med brottenvelopp tillåter ett A/B-värde (Axel- och Boggitryck) på 102 kN/147 kN när mycket dåliga parametervärden används och 181 kN/226 kN när referensfallet med normala parametervärden används.

Även om bärförmågan kan anses vara acceptabel är osäkerheterna stora. För att få en nogrannare uppfattning om brons faktiska tillstånd bör fortsatta studier utföras, som t.ex. en icke-linjär modell.

Nyckelord: Bågbro, valv, finita element, fyllning, brottenvelopp, stenvalv, klassningsberäkning.

Contents

Chapter 1

Introduction

1.1 Introduction

The aim of this thesis is to assess the load carrying capacity for the Glomman Bridge outside of Örebro in Sweden. The studied bridge, shown in Figure 1.1, is a single span arch bridge with backfill. It was constructed in 1923 by request from the Swedish National Railways (SJ). It is a public road bridge but it is currently owned by the Swedish Rail Administration (Banverket). The arch is a combination of a stone vault and a concrete arch.

Today, the traffic passing the bridge is restricted by a maximum vehicle total weight of 3.5 tonnes with the exception for buses in regular traffic. The main task in this thesis is to determine if this restriction of the vehicle weight is too conservative or if it is not enough. A parameter study was also done since the input parameters of the bridge contain large uncertainties.

The course of action was to create a two-dimensional finite element model in ABAQUS to obtain influence lines for the bridge, using amplitude functions. A routine that calculate the load factors in every arch node when the loads were run along the pavement was then created. The load factor is the ratio between the ultimate load capacity and the actual load. The routine finds the least favourable load position, taking the different axle pressures and the number of axles of the load types into consideration.

The condition of the bridge was assessed during an inspection, further presented in Chapter 3.6. The inspection of the bridge was performed in October 2008. An earlier inspection and capacity assessment have been performed by Reinertsen Sverige AB, which has been referred to in this thesis.

Figure 1.1: The Glomman Bridge.

1.2 Aims of the study

The main purpose of this thesis is to investigate the load carrying capacity with the failure envelope also considering the backfill. Therefore, e.g. snow load and temperature load are of subordinate meaning and not considered in this thesis. To study the sensitivity of the carrying capacity for different values of the parameters, a parametric survey was performed. A reference case was created with certain initial values and the load carrying capacity was calculated by means of the created model. The initial values were changed individually within a given interval to study how the carrying capacity differs from the reference case.

An obstacle with the Glomman Bridge is the limited total weight of the vehicles allowed today on the bridge. An exception from this is however made; buses in regular traffic are allowed to pass the bridge even though they are much heavier than the rest of the vehicles. This thesis deals with the question if heavier vehicles can be allowed, knowing that the bridge can manage the buses.

1.3 Structure of the thesis

The main structure of the thesis is described below to give the reader an idea of the content in the different chapters.

A literature survey was performed and presented in Chapter 2. A history of arch constructions presented. The object for comparison used in the thesis, the Prestwood Bridge, is also mentioned. Some facts and statistics about arch bridges in Sweden and the rest of Europe are also brought up. The main part of the chapter presents different methods of assessment and commercial software such as the finite element method and RING 2.0. Both are used in this thesis when calculating the load carrying capacity.

In Chapter 3, the Glomman Bridge is described. Some simplifications that were made in this thesis are presented and discussed. The original design drawings are also found in this chapter. The cross-sectional variations are calculated with an adjustment to a polynomial. The variation is then compared with known structural engineers' cross-sectional variation curves. Since the concrete quality is of great importance, the obtained concrete core samples are presented and analysed. Maintenance of the bridge concerning among other things, the replacement of the edge beam and the concrete layer on the intrados is presented.

Chapter 4 presents the basic idea with the failure envelope used in this thesis, what theory lies behind the method and some limitations. The failure envelope shows what combination of cross section forces that causes a failure in the arch. It is explained how the model is created in ABAQUS and what type of elements and constraints that are used. To find a suitable mesh, a test of convergence was performed and presented in Chapter 4. The different load cases and the work done in MATLAB, the way of finding the least favourable load combination, are also explained.

In Chapter 5, the results from the study are presented. The results from the ABAQUS model in terms of influence lines are discussed and analysed. The load factors for different load types are calculated for a parameter configuration that serves as a reference case. A parametric survey to find the most important parameters are presented and intervals for the studied parameters are identified. The load factor for the worst possible parameter configuration is calculated. A comparison with the Prestwood Bridge and the commercial software RING 2.0 is presented.

Conclusions concerning the results are presented in Chapter 6. Limitations and simplifications of the model are discussed. So are the uncertainties that the model contains. Some possible further research is mentioned.

Chapter 2

Literature survey

2.1 Arch bridges

The knowledge to construct vaults and arches is very old. It is possible that arches were used in China as early as 2900 BC. In Campbell's tomb in Egypt, a four-ring arch was found which could be dated to 1540 BC, (Howe, 1897). Despite the considerable age of the vault, it has its precursor in the corbelled arch. A corbelled arch can be described as a series of stones positioned so that each stone project a bit from its previous. The principle in which the stones can be placed becomes clear in Figure 2.1. It is possible to build corbels with large spans but because of the divergence of the arithmetic series in Equation (2.1), it takes a lot of height to construct. The corbelled arch does not generate any horizontal forces. (Sundquist, 2007)

$$x_i = x_{i-1} + h/2i \tag{2.1}$$

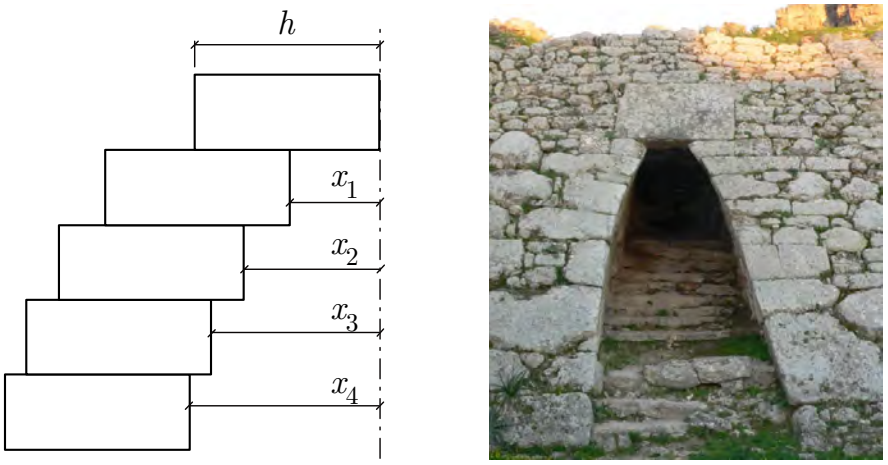

a) b)

Figure 2.1: a) Outline of a corbelled arch (reproduced from Sundquist, 2007), b) The Ugarit Palace entrance[1].

[1] www.answers.com/corbel%20arch

More effective and not as demanding in height is the vault construction. The difference between a corbelled arch and a vault is not always obvious. The idea of the vault is that the material only should be exposed to compressive forces and not to tensile forces. The vault can thus be built in a material, which has no or very low tensile strength, such as brick or stone wall. A more daring architecture is of course possible if a material with a tensile strength is used. When the first arch bridges were built, the arches were constructed on top of a temporary framework, known as a centering. A key stone was used, in the arch crown, to close the arch. It was this key stone that bore the entire dead-weight of the bridge. The structure became stronger the more weight (distributed load) that was put onto the arch, until a certain point when the arch material crushes. Masonry arch bridges use a backfill material to increase the dead-weight of the bridge and make the arch less sensitive to live loads by distributing the load through the backfill onto the arch. (Sundquist, 2007)

In the beginning of the twentieth century, there were several concrete arch bridges constructed in Sweden without reinforcement. Concrete has the properties of high compressive strength and very low tensile strength, about 1/15 of the compressive strength. This is the reason why reinforcement bars are used to manage the tensile forces. Nowadays concrete is nearly always reinforced, but this has obviously not always been the case. Unreinforced concrete arch bridges can be compared to the older masonry arch bridges. In masonry structures, the units are either bonded with mortar or, as in the case with dry stone walling, selected to dovetail together. Mortar can be compared to unreinforced concrete regarding the very low tensile strength while dry stone walls have no tensile strength at all.

In the United Kingdom, a lot of research regarding masonry arches has been undertaken. There has also been some experimental testing, where a few full-scale bridges were loaded to failure. One of them, The Prestwood Bridge, shown in Figure 2.2, has been subject for several papers and reports. (Sowden, 1990)

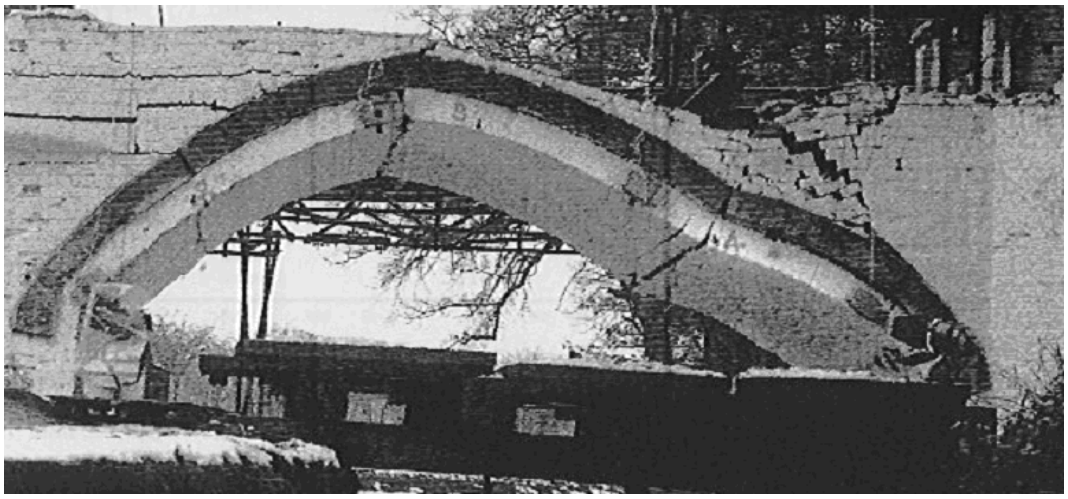

Figure 2.2: The Prestwood Bridge during failure at the haunch, (Sowden, 1990).

2.2 The backfill

In the early work, the backfill was only considered as vertical deadweight due to the difficulties to compute the direction and magnitude of forces caused by the fill. However, now it is well known that the resistance of the backfill has great importance for the load carrying capacity. The backfill creates an earth pressure, which counteracts heaving of the haunches. The load distributing effect of the fill, shown simplified in Figure 2.3, should also be taken into account. According to Betti *et al.* 2008, a model with non-resistant fill gives a collapse load that is only 35% of the collapse load from a model with resistant fill.

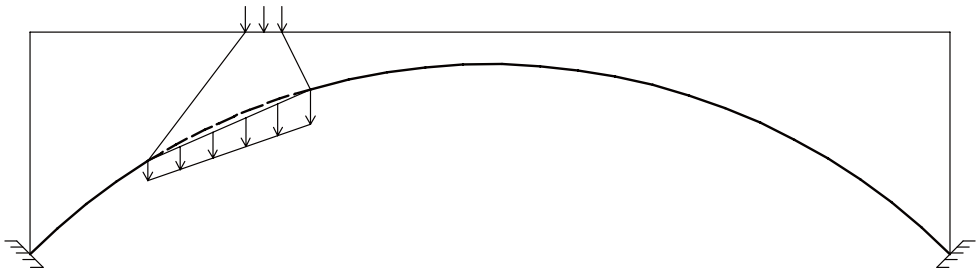

Figure 2.3: Load distribution through the fill. (Reproduced from Sowden, 1990)

2.3 Arch bridges in Europe

According to a survey of railway bridges carried out in 2004 within the EU-funded project Sustainable Bridges, 41% of the railway bridges in Europe are arch bridges. The survey included 220 000 bridges from 17 European railway administrations. This gives that the number of arch bridges in the survey was around 90 000. From these, 52% had vaults made of bricks and 33% vaults made of stone. Because of some insecurity, it was assumed that no more than 5% of the arch bridges were made of concrete. The survey shows that the age of the arch bridges is rather high. The majority, 64% are older than 100 years and 35% are 50 – 100 years old. This is however far from a surprise since concrete has more or less replaced the bricks and stones as a load carrying construction material. It is also shown in the survey that arch bridges are most often used in spans less than 10 m, more specifically 75%. In the case with spans between 10 m and 40 m, the share is 24%. Arch bridges with long spans are thus rather unusual with only 1% greater than 40 m.

In Sweden, 150 of 3 620 railway bridges are arch bridges. This gives that 4% of the railway bridges in Sweden are arch bridges. This can be compared with the earlier mentioned 41% in the rest of Europe. From the 150 railway arch bridges in Sweden 115 are made of stone, 35 are made of concrete and no railway bridges are made of bricks. Of the railway bridges in Sweden, 76% are less than 50 years old while the corresponding number in Europe is 33%. For the arch bridges, the number older than 50 years is 91%. Arch bridges are also here mainly used in shorter spans. A large majority of 87% is used in spans less than 10 m, 10% in spans between 10 – 40 m and 3% for spans larger than 40 m. (Sustainable bridges D1.2)

2.4 Design methods

Earlier design methods were related to collapse mechanisms and the line of thrust. For a collapse mechanism to arise, it has to consist of four hinges. When the line of thrust reaches the edge of the arch a hinge arise and when four hinges has developed, the arch collapses. For an arch to carry its own weight, the optimal shape is a catenary. If an arch has different geometry, it is supported because some form of catenary shape is included within the thickness of the arch. (Sowden, 1990)

To determine the load carrying capacity in a masonry arch bridge, there are three general analytical methods that differ rather much from one to another. There are also semi-empirical methods, which only give approximate values of the load carrying capacity. A large number of test results have formed simple approximate equations that together with some theoretical assumptions build a basis for analytical solutions. One semi-empirical method, the MEXE-method, is discussed below. (Sustainable Bridges D4.7.3)

2.4.1 The maximum stress analyses

The basic principle of the maximum stress analyses is to determine the maximum stresses in the elements and to compare these with the material strength. Several models are used for this type of analyses and common for all of them is that they consist of one-dimensional bar elements. The differences in the applied method algorithms depend on the material model. Usage of maximum stress analyses is mainly orientated against single-span arch bridges or to multi-span bridges where one span is treated at the time.

An approach to analyse masonry arch spans is to consider them as arch ribs made of an elastic material. This way, the solution procedure is made into a problem of solving a static calculation. This method gives reasonable results as long as the calculated forces are relatively small in comparison with the material strength. The choice of method when it comes to solving the equation depends on the number of hinges in the structure. If the structure is statically determinate, with three hinges Figure 2.4a, it can be solved using only equilibrium equations for horizontal and vertical forces and bending moment. If the structure however is statically indeterminate, with two or no hinges, Figure 2.4b and Figure 2.4c, it is necessary to solve the problem by integration of equilibrium equations, force method or displacement method.

a) b) c)

Figure 2.4: Position of the hinges in the arch.
(Reproduced from Sustainable Bridges D4.7.3)

The inelastic arch rib method is a method that allows non-linear behaviour of masonry. This method is based on the same static calculations as above. The arch is divided into segments and calculations are made in the internal nodes between these segments. An increment of the total load is placed somewhere on the arch and elastic analysis are carried out, giving internal forces in the nodes as the result. From these forces, an effective arch thickness x_i as shown in Figure 2.5 is calculated for each segment by using the average values of internal forces, one force from each side of the segment. The effective thickness, the thickness without the possible tensile zone and/or crushed area, is set to be its segment thickness before applying the next load increment. This routine is repeated until the entire load is applied onto the arch. Between two adjacent segments, the connection is infinitely rigid. (Sustainable Bridges D4.7.3)

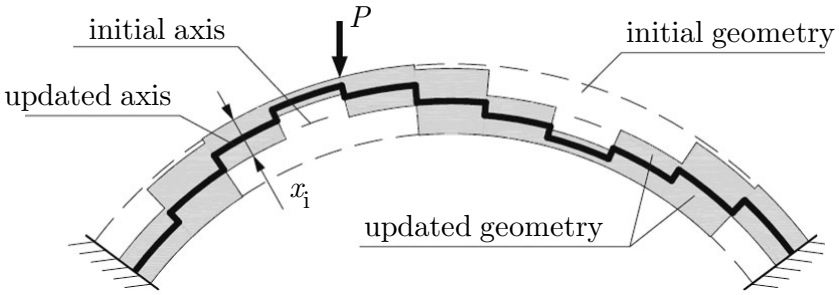

Figure 2.5: The position of the thrust line and thrust zone in the segments. (Sustainable Bridges D4.7.3)

2.4.2 The thrust line analyses

The line of thrust method is a static approach, which analyses the location of the thrust line within the arch. The thrust line shows where the resultant from the normal force is located in a cross section. The location of the line is calculated by dividing the moment by the normal force, which gives the eccentricity of the normal force. The load carrying capacity is then defined by limiting the zone where the resultant force is allowed to be positioned. The earliest version of this method used the limits of Navier's middle third rule, which said that if the resultant force is positioned in the middle third of a wall or foundation no tension is developed. With this limit however, the method was extremely conservative. Therefore the middle half limit was used instead, which increased the zone to half the cross section. The last version of the method has the entire cross section as allowed zone and requires that the line of thrust reaches the edge of the arch in four sections before a mechanism arise and the structure collapse. This method however presumes infinite compressive strength, which is not true but since the mean stress in masonry arch bridges in general are low in proportion to its compressive strength, the result is close to reality.

A similar method is the zone of thrust method. It presumes a finite compressive strength that makes it impossible for the normal force resultant to be positioned on the edge of the arch. Instead, there is a rectangular area created around the force resultant. The height of the rectangle is calculated with Equation (2.2) where N is the normal force, f_c is the compressive strength and B is the width of the arch. The resultant force is positioned at $t/2$ as shown in Figure 2.6. The failure criterion is then calculated with Equation (2.3). (Sustainable Bridges D4.7.3)

$$t = \frac{N}{f_c \cdot B} \tag{2.2}$$

$$e = \left|\frac{M}{N}\right| \leq \frac{d-t}{2} \tag{2.3}$$

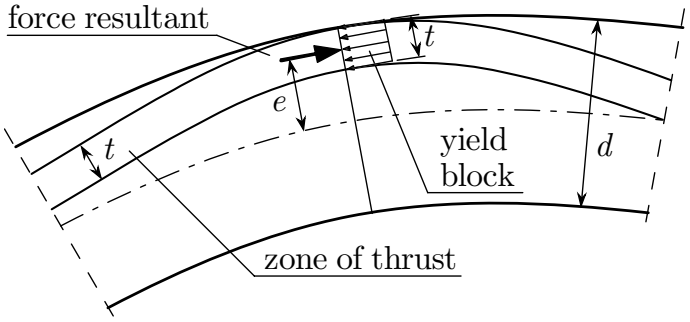

Figure 2.6: The zone of thrust. (Sustainable bridges D4.7.3)

2.4.3 The Mechanism method

The mechanism method is a kinematical method, which uses the assumption that an arch needs four plastic hinges to become a mechanism. The position of these hinges has to be computed. In a simplified analysis with only a concentrated force on the arch, the first three hinges can be assumed to be located under the load and at the springing. The position of the fourth hinge is then possible to calculate with moment equilibrium at the hinges or with the equations of virtual work. This has to be done for several positions for the fourth hinge to find the minimum load.

Another analysis using the mechanism method is the rigid blocks analysis. It uses a number of blocks to model the arch. The blocks have infinite strength and are infinitely rigid. At collapse, the blocks can either slide or rotate about the edges. Using minimal energy for the global deformation makes it possible to calculate the movements of all blocks.

A similar mechanism method analysis is to use rigid-plastic blocks with a finite compressive strength. This makes the hinge unable to lay on the edge of the arch. Instead, there is a zone between the edge and the hinge where the material is crushed. This gives a non-linear analysis instead of the earlier linear, which complicates the calculation.

There is also a three dimensional version of the mechanism method which uses volumetric blocks to model the arch, but similar assumptions as the analysis with plane blocks. This is the most complicated mechanism method. (Sustainable Bridges D4.7.3)

2.4.4 The MEXE method

The MEXE method is a semi-empirical method, which was developed during the Second World War and into the 1950s because the British Ministry of Supply wanted to classify the bridges after what military loads they could carry. The method was developed from a number of full scale tests and analytical calculations and is valid for a number of assumptions: (Sowden 1990)

- the arch is parabolic,
- the arch is two pinned,
- the arch is in perfect condition,
- the load is applied as a point load in the crown,
- the span is less than 20 m,
- the rise at the crown is larger than ¼ of the span,
- the depth of the fill lies between 30-105 cm in the arch crown.

Through the tests and calculations, diagrams for the relations between the span L, the depth of the fill above crown h, the thickness at the crown d, and the provisional axle load (PAL) were created. Later the diagrams were replaced with Equation 2.4.

$$PAL = \frac{740(d+h)^2}{L^{1.3}} \text{ (tonnes)} \tag{2.4}$$

The provisional axle load is then to be multiplied with five factors that take *e.g.* the material properties, the condition of the bridge and the ratio between the span and the rise into consideration. The result is a modified axle load, which represents a double-axle bogie. Allowed single axle pressures and triple-axle pressures can then be calculated. (Sustainable bridges D4.7.3 and Sowden, 1990)

2.5 Commercial software

Several commercial softwares use different part of the analytical theory explained above. Common for all programs is that they are used only on masonry arches. Depending on what output and results that is wanted, different methods and programs are chosen.

2.5.1 Archie-M

Archie-M is a software that uses the thrust line analysis, or the zone of thrust that uses a finite material strength, to be accurate. The program uses a three hinge arch and places the hinges where it is most likely for the given load pattern. Archie-M presents the thrust line location in the arch when the load is applied. As long as the thrust line lies within the arch along the whole length, the structure is in equilibrium. When the thrust line however touches the edge at any place along the arch, a fourth node, and

thus a mechanism, is created and the structure will collapse. The load carrying capacity is given by the magnitude of the load when the fourth hinge arises. Archie-M presents internal forces and zone of thrust for each segment in the structure. It also places the load in the worst location, which gives the fourth hinge. (Sustainable Bridges D4.7.3)

2.5.2 RING 2.0

RING 2.0 is a software developed for assessment of single- or multi-span masonry arch bridges. It uses a two-dimensional model that allows a chosen load to increase in magnitude until a mechanism is formed. The design method used in RING 2.0 is the mechanism method with rigid plastic blocks. A quality that makes the software special is the ability to handle the problem of separation of masonry rings. RING 2.0 is also able to model local defects such as brick- or stone loss. The program presents the thrust line together with the failure mode. It also shows the earth pressure in terms of vectors graphically. (LimitState Ltd, 2007)

2.5.3 FEM systems

Finite element method (FEM) is not a certain program but a calculation technique that is applicable on any type of structure. The programs most used in calculation of masonry arch structures are ANSYS, ABAQUS and DIANA. Depending on the accuracy of the results and the workload, one-, two- or three-dimensional elements are possible to use. Maybe the most difficult part of this type of calculation is to construct the model in a good way. Smaller elements in general give a more exact result but only to a certain point. After a while, the result will converge and the decreasing of element dimensions will only increase the calculation time. It is therefore important to try to get a good balance between the element dimensions and the calculation time. A good way to do this is to try different number of elements and examine when a certain result converge. The choice of method can also be dependent of material model; FEM makes it possible to create detailed material properties. (Sustainable Bridges D4.7.3)

2.5.4 DEM systems

Discrete Element Method (DEM) is a method that is suitable when a large part of the deformation can be imposed the internal motion between blocks. The model is usually created in two dimensions, containing rigid as well as deformable blocks. These are allowed to move in relation to one another and interact when they have contact with each other. The idea of DEM is to let equilibrium equations between blocks, be solved by explicit algorithms. The new deflected position of the arch and the new internal forces are used to solve new equations. The number and type of contacts between blocks may vary during the calculation. (Sustainable Bridges D4.7.3)

2.5.5 Explicit formula analysis

There are several simplified calculation methods where the only thing needed is a formula. The background for this is tests that have been done on hundreds of masonry arch bridges with different measurements and material properties. The load carrying capacity was examined with FEM and formulas were created for a point load and a distributed load. Equation (2.5) is valid for a point load.

$$P_{\text{ult}} = \left(AL^2 + BL + C\right)K_1K_2 \tag{2.5}$$

A, B and C are coefficients depending on the ratio between the arch barrel depth and the span, K_1 is a coefficient regarding the rise and the span and K_2 is a coefficient that depends on the fill height in the crown. (Sustainable Bridges D4.7.3)

Chapter 3

Description of the studied bridge

3.1 Introduction

The studied bridge is located just to the south of the Swedish city Örebro, where the road Glomman crosses the railway. The bridge was constructed in 1926. At that time, concrete was introduced as a construction material replacing stone, which was the usual material. The design of the arch was done entirely without reinforcement and the arch was made as a combination of a stone- and concrete arch. The abutment and the ground wall of the bridge are mainly mortared with large blocks. The arch is probably also consisting of a stone vault and the transition between the arch and the abutment was made of in situ concrete. The bridge is completely unreinforced except for the wing walls consisting of round reinforcement bars.

The bridge is a single span arch bridge with backfill. The span is 17.5 m and the width is 8.4 m. It was constructed in unreinforced concrete with rocks embedded in the arch as shown in Figure 3.3. The arch is a fixed end arch but was according to the design drawings considered as a three-hinge arch with hinges at the springing and the crown. This was probably done to simplify the calculations.

The owner of the bridge is The Swedish Rail Administration and its exact position is Bdl 524, km 219+359. The road that runs over the bridge is a public road with a restriction regarding the weight of passing vehicles. The maximum allowed vehicle weight is set to 3.5 tonnes, with an exception for buses (two certain kinds of buses explained in Chapter 4.3) in regular traffic, that are heavier. (Reinertsen, 2006)

3.2 Construction of the bridge

According to the design drawing in Figure 3.2 and Figure 3.3, the concrete mixing proportions are 1:5:7 in the lower part of the abutments and 1:4:6 in the upper part of the abutments. These proportions are by volume. The mixing proportions are given in volume and corresponding weights in Table 3.1.

Table 3.1: Concrete mixing proportions, (BVS 583.11, Appendix 5)

Mixing proportions by volume	Material consumption per m^3 concrete						σ_{B28} $\left[\text{kp/cm}^2\right]$
	Cement		Sand		Macadam		
	litres	kg	litres	kg	litres	kg	
1c:4s:6m	130	185	520	830	780	1015	105
1c:5s:7m	110	155	550	880	770	1000	85

The compressive strength of 105 kp/cm^2 and 85 kp/cm^2 equals to 10.3 MPa and 8.3 MPa respectively. The concrete strength is difficult to assess, due to the presence of plums. An evaluation of the quality has been done in Chapter 3.4, by analyzing core samples taken on site.

Settlements were estimated to be unlikely when the abutments stand on solid rock. The bridge is defined sideways by a spandrel wall on each side, illustrated in Figure 3.1. The spandrel walls are casted in concrete with an outer layer of plaster. In the model, no consideration of the spandrel walls has been accounted for. The two-dimensional model in this thesis may be seen as a cross section taken lengthwise in the middle of the bridge where only the arch and the fill cooperate. The spandrel walls are rather thick, forming half of the total width of the bridge at the springing, see Figure 3.2. It is likely that the spandrel walls will strengthen the construction and have a positive effect on the load carrying capacity. A way of considering the higher strength of the spandrel walls could be to aggregate the Young's modulus with the backfill to get a united material. On the other hand, it may also be considerable to think that the heavier density of the concrete in the spandrel walls, as an extra load, can have an effect on the load carrying capacity.

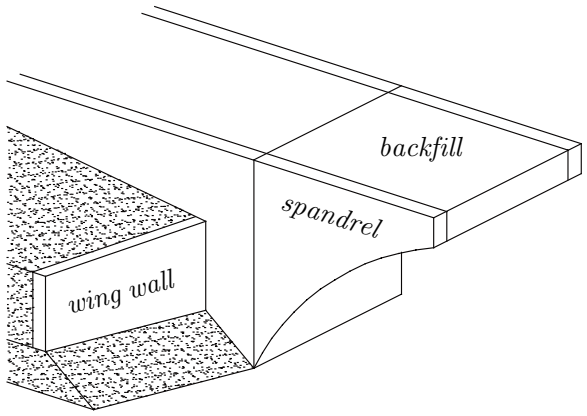

Figure 3.1: The different parts of the arch bridge.

Another simplification made was that the bridge was modelled orthogonal to the ground. According to the design drawing, the bridge is slightly skewed. The bridge and the railway form an angle of 74 ° and are to be seen in Figure 3.2. Since the bridge is not orthogonal to the embankment side, the breaking and accelerating vehicles will cause some forces in the perpendicular direction of the bridge. These forces should not be that large though because of the low weight of the passing vehicles and that the maximum speed allowed on the bridge is 30 km/h.

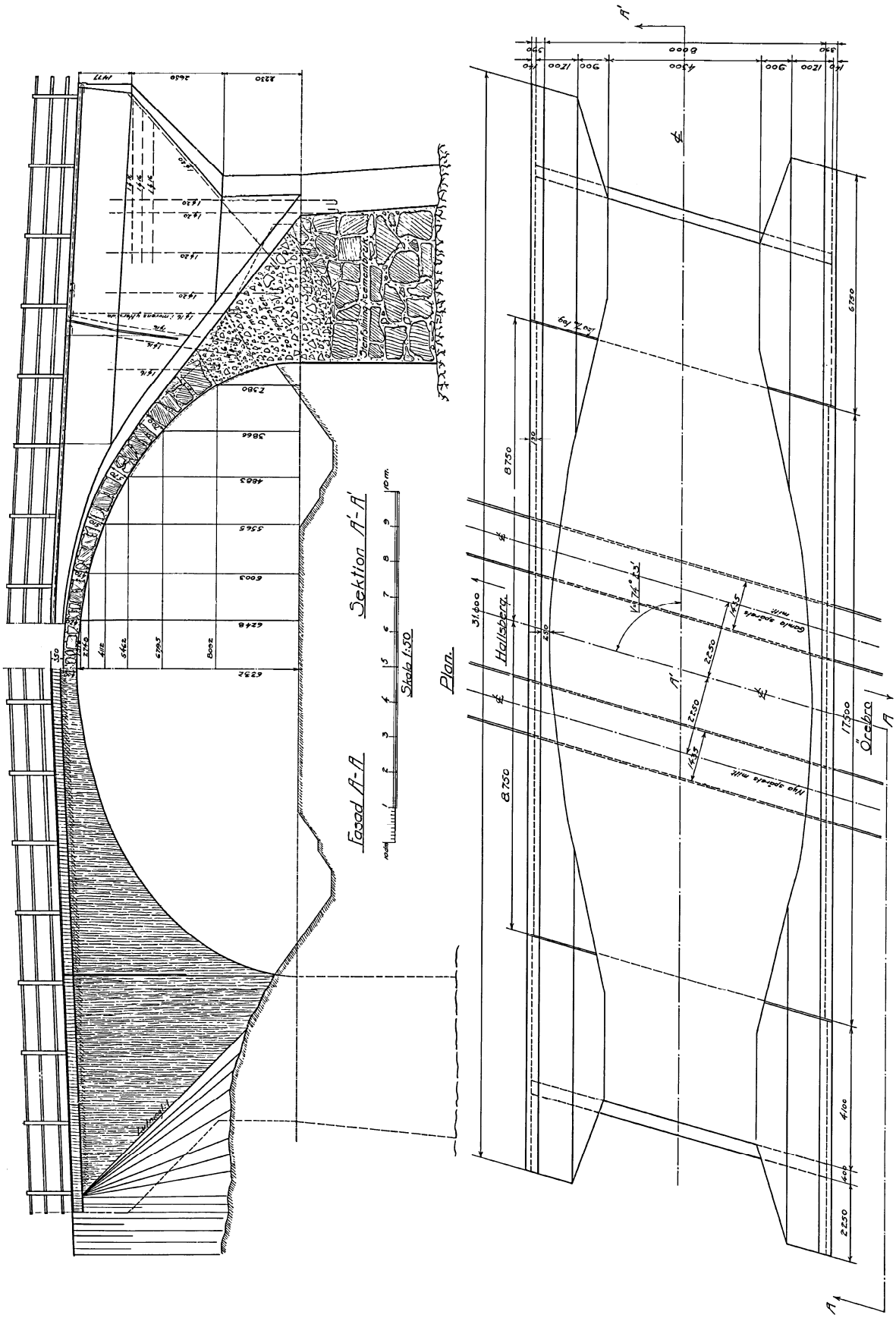

a) b)

Figure 3.2 Geometrical drawing of the Glomman Bridge, a) elevation and b) plane view.

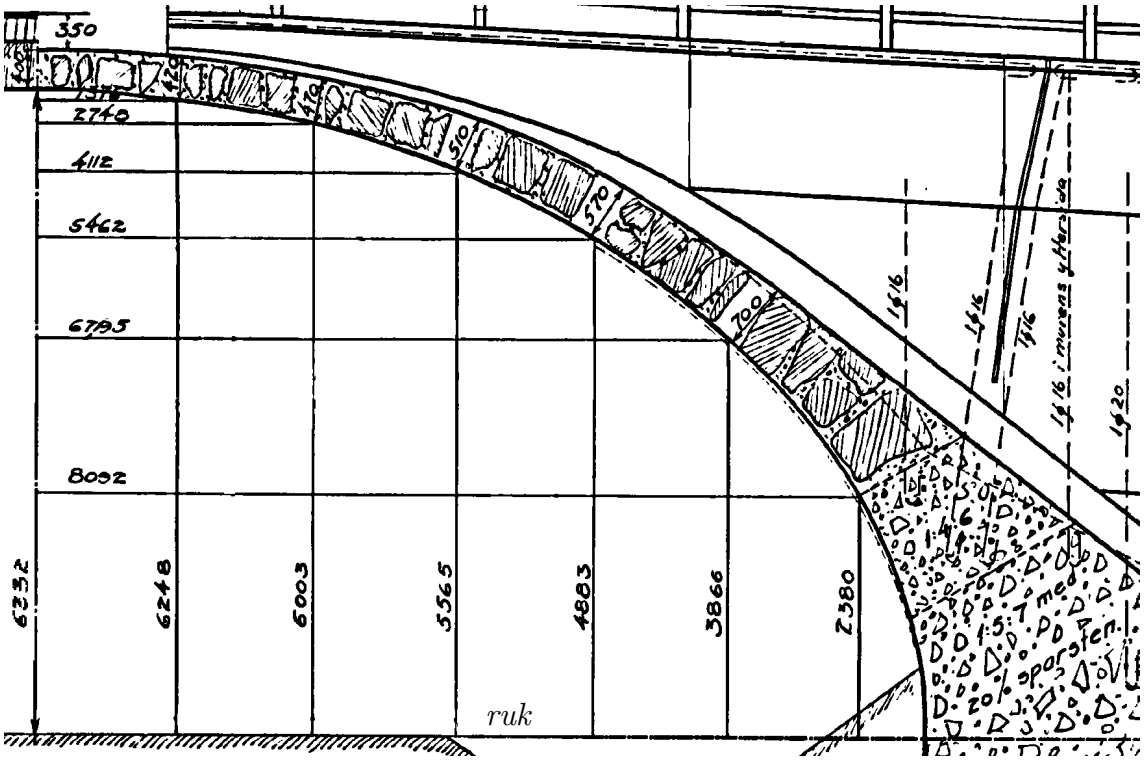

Figure 3.3: Enlargement of Figure 3.2.

3.3 Cross-sectional variation

The thickness of the arch varies continuously along the whole length. According to the existing design drawings, Figure 3.3, there are seven different thicknesses defined at seven different points between the abutment and the crown. These points are given in Table 3.2.

Table 3.2: The thickness variation of the arch. The distances from the abutment is calculated between points in the frame line.

Distance from the abutment [m]	0.000	1.610	3.019	4.426	5.837	7.232	8.633
Thickness [m]	1.100	0.700	0.570	0.510	0.470	0.420	0.400

Between these seven points, a curve fitting was made as shown in Figure 3.4. To avoid the usage of a too high degree of polynomials, the fitting was divided into two parts. Different degrees of the polynomials and different breakpoints between the curves were tried. A suitable breakpoint was found to be the third point from the left, fitted by a second and third degree polynomial respectively. The polynomial for the second part of the curve was calculated first. The curve can be represented by Equation 3.1.

$$t = a_0 + a_1 x + a_2 x^2 \tag{3.1}$$

To find the coefficients a_0, a_1 and a_2 a system of equations was set up.

$$\begin{bmatrix} 1 & x_3 & x_3^2 \\ 1 & x_4 & x_4^2 \\ 1 & x_5 & x_5^2 \\ 1 & x_6 & x_6^2 \\ 1 & x_7 & x_7^2 \end{bmatrix} \cdot \begin{bmatrix} a_0 \\ a_1 \\ a_2 \end{bmatrix} = \begin{bmatrix} t_1 \\ t_2 \\ t_3 \\ t_4 \\ t_5 \end{bmatrix} \tag{3.2}$$

The vector $\boldsymbol{a}$ was calculated by Equation 3.3.

$$\boldsymbol{a} = \left(\boldsymbol{X}^{\mathrm{T}} \cdot \boldsymbol{X}\right)^{-1} \cdot \left(\boldsymbol{X}^{\mathrm{T}} \cdot \boldsymbol{t}\right) \tag{3.3}$$

The first part of the arch thickness was represented by a similar system of equations. Although the curve was supposed to be continuous, another two conditions had to be added. In the breakpoint between the two curve parts, continuity in thickness and thickness rate were stated as boundary conditions.

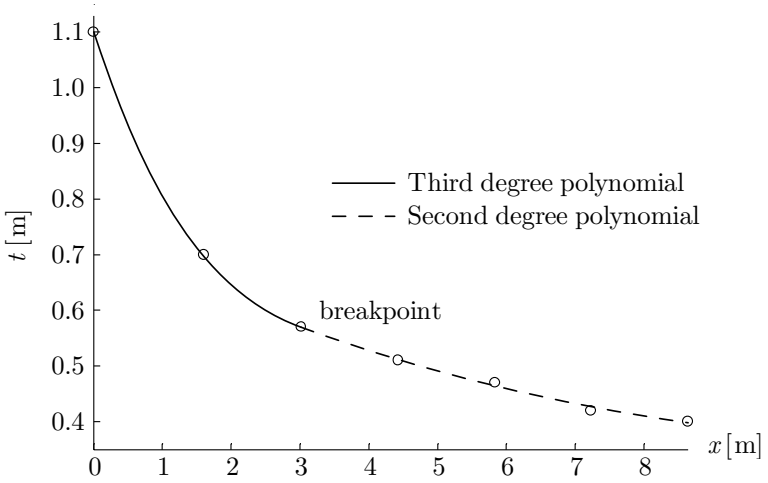

Figure 3.4 The curve describes the thickness variation of the arch. The seven different measured thicknesses according to the construction plan are marked with rings. The plotted curve describes half the arch's length.

The resulting equations are presented in Equation 3.4.

$$t_1(x) = -5.96 \cdot 10^{-3} x^3 + 7.93 \cdot 10^{-2} x^2 - 0.36x + 1.10 \tag{3.4a}$$

$$t_2(x) = 2.51 \cdot 10^{-3} x^2 - 5.98 \cdot 10^{-2} x + 0.73 \tag{3.4b}$$

Several structural engineers have developed certain appropriate cross-sectional variations and influence lines so that they are easy to find in different specialist literature. The cross-sectional variation usually found in the literature can be summarised in Equation (3.5). (Sundquist, 2007)

$$\frac{D_x}{D_0} = \frac{EI_x \cos\phi}{EI_0} = \frac{1}{1-\left(1-\frac{D_0}{D_a}\right)\left(1-\frac{2x}{L}\right)^k} \tag{3.5}$$

where ϕ is the angle between the arch and the horizontal plane. *Strassner* uses the value $k=1$ while *Ritter* uses $k=2$. *Kasarnowsky* on the other hand only uses a variation from the springing until a certain point into the arch and then a constant as shown in Equation (3.6) and Equation (3.7).

$$\frac{D_x}{D_0} = \frac{D_0}{D_a}\left(1-\frac{2x}{L}\right)^4, \quad 0 \le x \le \frac{L}{2}\left(1-\sqrt[4]{\frac{D_0}{D_a}}\right) \tag{3.6}$$

$$\frac{D_x}{D_0} = 1, \quad \frac{L}{2}\left(1-\sqrt[4]{\frac{D_0}{D_a}}\right) \le x \le \frac{L}{2} \tag{3.7}$$

Cross-sectional variations according to *Strassner*, *Ritter*, *Kasarnowsky* and Glomman, are plotted in Figure 3.5

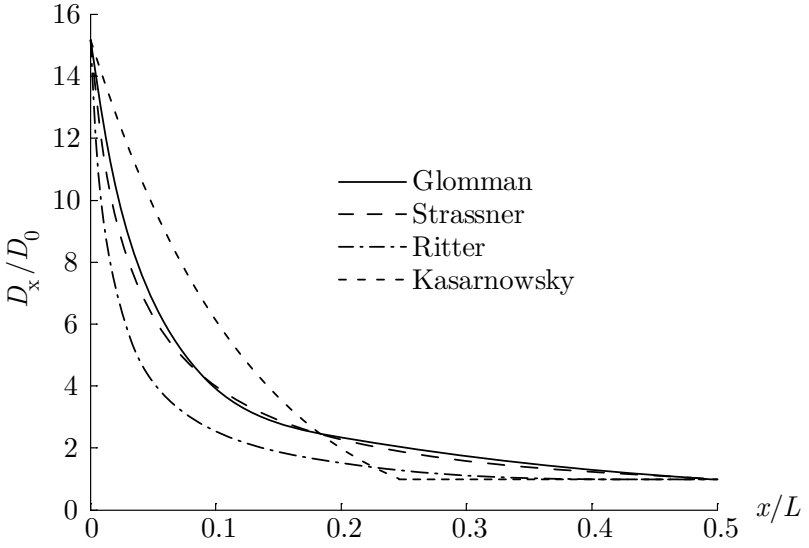

Figure 3.5: Thickness variation of the Glomman arch compared to *Strassner*, *Ritter* and *Kasarnowsky*.

Glomman has a rather large variation of the cross section with $D_x/D_0 = 15$ in the springing and the cross-sectional variation is almost identical to a Strassner arch.

3.4 Concrete quality

By order of the Swedish Rail Administration, Carl Bro AB performed a concrete inspection of the bridge in 2006. Ten core samples were taken from the front wall, from which six of them were picked out and tested regarding compressive strength and splitting strength. The measured strengths are given in Table 3.3. It is shown in Figure 3.6 where the samples were taken. The core samples were cylindrical with a diameter of 100 mm and a length of 300 mm. Since the compressive strength was of great interest, assessment of its distribution were checked and questioned. The entire calculations are given in Appendix A. The characteristic value of the compressive strength was calculated several times, both using different methods and with different number of core samples. (Reinertsen, 2006)

Table 3.3: The six core samples. The presented accuracy of the compressive strength is 0.5 MPa.

Sample no.	1	2	3	4	5	6
Tested compressive strength (MPa)	23.0	45.0	20.5	16.0	13.5	25.0
Tested splitting strength (MPa)	2.4	3.3	2.3	2.5	1.8	2.2

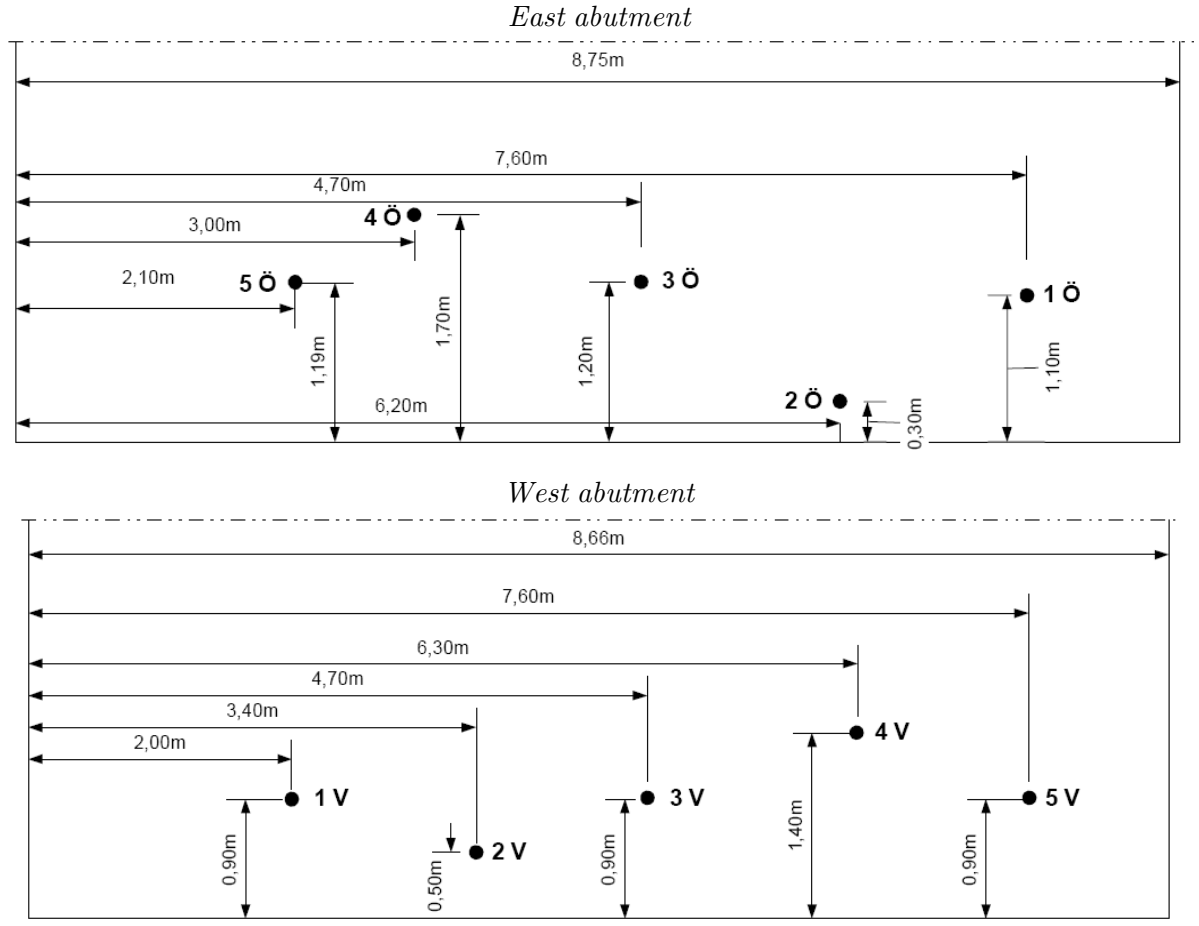

Figure 3.6 An outline of the bridge abutments marked with places where the core samples were taken from. (Reinertsen, 2006)

The first method used was according to Boverket, 1994. The measured values of the compressive strength seemed to have an accuracy of 0.5 MPa. The calculated values in this thesis were rounded to the same accuracy. From the six measured values, a mean compressive strength and a standard deviation were calculated to 23.8 MPa and 11.2 MPa respectively. The covariance was found to be $cov = std/mean = 11.2/23.8 = 0.47$. The statistical limit was set to be the lower five percentile. It resulted in a negative compressive strength of -2.5 MPa, of course a completely unrealistic value. Due to the large scatter of the measured values, the standard deviation was found to be large. The characteristic value will then be very low when searching for a low percentile. In an earlier report by Reinertsen Sverige AB, the highest and lowest values were neglected when one can suspect that these two samples may have been damaged in some way. The same calculations were performed with these four values and the characteristic compressive strength was found to be 10.5 MPa. When in fact it was only one of the tested values (45.0 MPa) that stood out from the rest more than the others, the calculations were performed once again. This time sample no. two was deleted and the five samples left resulted in a characteristic compressive strength of 8.0 MPa.

Another assessment method was also used. According to Boverket, 2004, the characteristic compressive strength was estimated to 15.5 MPa when all six samples were included. Also with this method, the calculations were made without the highest and lowest values and a second time without only the highest value. The characteristic value was then estimated to be 13.5 MPa and 12.0 MPa respectively.

The characteristic compressive strengths using the different methods and the different number of samples are summarized in Table 3.4. The number of samples used is given in the first row.

Table 3.4: Characteristic compressive strengths, given in MPa, calculated with two different methods and different number of core samples.

Number of core samples	6	4	5
Boverket, 1994	-2.5	10.5	8.0
Boverket, 2004	15.5	13.5	12.0

The reason why the results according to Boverket, 1994 show a larger scatter is that this method uses the standard deviation to find the lower five-percentage percentile. "BBK 04, Appendix A" uses another method that does not consider the standard deviation. Instead, it uses either the minimum test value or the mean value to calculate a characteristic strength.

It is obvious that the real value cannot be negative. The characteristic compressive strength can therefore be assumed to lie between 8.0 MPa and 15.5 MPa. The two concrete classes with the lowest strength according to Boverket, 2004, C12/15 and C16/20, are represented by characteristic compressive strengths of 11.5 MPa and 15.5 MPa respectively. The tested concrete from the Glomman Bridge was therefore assumed closer to C12/15 concrete than C16/20 concrete.

3.5 Maintenance and repairs

The only known repair that has been made was in 1986 when the edge beams were replaced. In 2004, Carl Bro AB performed a maintenance inspection of the Glomman Bridge by order of the Swedish Rail Administration. During the inspection, some defects in the concrete were detected. This caused the Swedish Rail Administration to close the bridge for all traffic and decided to do a capacity assessment. It was also decided to perform a scaling of the intrados, after which they could see that it was only the concrete surface that was damaged. It was also discussed to cover the intrados with for example corrugated sheet, to prevent concrete to fall down on the rail. This was however never done. When the new capacity assessment was finished, it showed that the bridge could resist some traffic load. One month later when these measures had been carried out the bridge was opened for traffic again, but only for vehicles with a weight less than 3.5 tons and buses in regular service. (Reinertsen, 2006)

3.6 Inspection of the bridge

An ocular inspection of the bridge was made by the authors 2008-10-03, with the purpose of examine the condition and take pictures of the bridge.

The bridge has a joint that separates the vault and the spandrel from the abutment as shown in Figure 3.7. The side wall of the abutment has moved perpendicular to the bridge but it is uncertain if it is still moving. The diagonal wing wall, see Figure 3.1, have probably been placed there later to hold a larger mass of soil in order to create a larger earth pressure which counteracts the moving of the side wall.

Figure 3.7: The joint between the spandrel and the side wall of the abutment.

The edge beam and the rail have been replaced. This has unfortunately not been working that well, when the grouting already has been exposed to frost erosion and large visible cracks have developed as seen in Figure 3.8.

Figure 3.8: Cracks in the edge beam caused by frost erosion.

In Figure 3.9, another crack is clearly visible in the spandrel concrete just above the arch. The reason of this crack is unknown. However, it is possible that it is due to a too large earth pressure from the backfill on spandrel. Another explanation can be that water has found its way through the backfill.

Figure 3.9: Crack between the arch barrel and the spandrel.

A new layer of concrete has been casted on the inside of the intrados. There is no information about when this repair was done. After the new casting, a searching for empty parts was made by cutting the concrete. The result was that parts of the new concrete fell down and left holes that uncover rather large plums as seen in Figure 3.10.

Figure 3.10: Uncovered plum.

A layer of isolation has been laid on top of the arch to prevent water to pour through the backfill and in to the concrete in the arch. Since the bridge was built, the endurance of the isolation has been passed. The consequence is leakage when water pours through the concrete and out through cracks, which leaves white marks from lime precipitate, see Figure 3.11. Furthermore, this water could cause frost erosion when the temperature gets below freezing.

Figure 3.11: The leakage is seen as white marks on the concrete.

Chapter 4

Methods of analysis

4.1 The failure envelope

Arch bridges can manage three hinges and not until the fourth hinge is developed will the bridge collapse. When a hinge is developed, the forces are distributed to other parts of the bridge. The model studied in this thesis was however based on the assumption that the bridge has reached its load carrying capacity as soon as one cross section attains its capacity and the first hinge was formed. In this manner, a safe side assumption of the load carrying capacity of the bridge is obtained.

To begin with, a few assumptions have to be made.

1. The concrete has no tensile strength. This assumption is not exaggerated when the actual concrete used, has been tested with a very poor compressive strength and it only seems natural to assume that the tensile strength is poor as well. This is an assumption on the safe side, which had to be made in lack of real test values.
2. Shear failure is not possible.

If furthermore another assumption can be made, that the concrete compressive strength is infinite, that only leaves one failure mode possible. The only way the arch can collapse is by hinging at a free edge, see Figure 4.1 a). If a normal force N act in the centre line and the thickness of the concrete is h, a hinge will occur at a free edge resulting in a bending moment $M = hN/2$.

The two straight lines OA and OB in Figure 4.1 b) are represented by this bending moment $M = \pm hN/2$. A point within the triangle OAB is therefore safe on condition that the three assumptions named above are true.

When one however realizes that the final assumption is unrealistic, adjusting has to be made to the figure. The actual concrete has a limited compressive strength which implies that the rupture curve after a certain point decreases until it finally reaches the N-axis again. This final point C in Figure 4.1 b) would be represented of a pure compressive rupture, the concrete crushes.

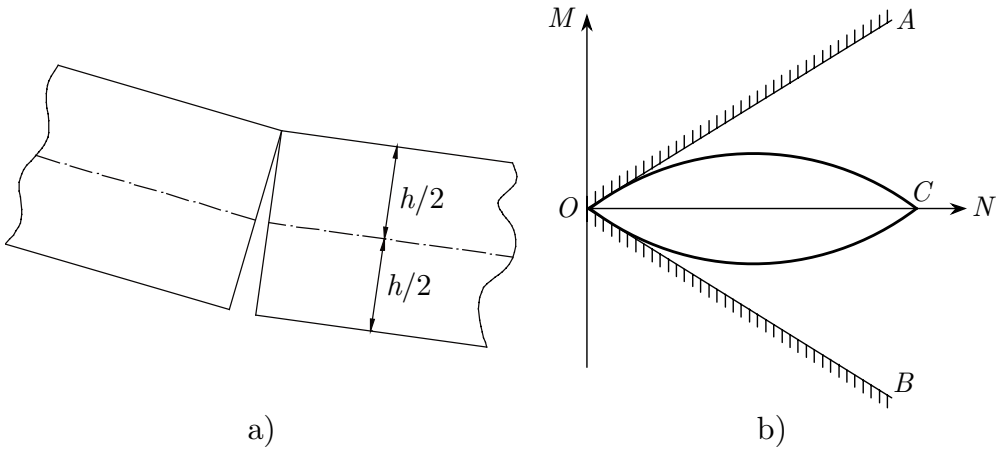

Figure 4.1: a) hinge, b) failure envelope.

To derive the failure envelope, we first need to know the expressions for the normal force and for the bending moment in the arch cross section. The equilibrium equations can be written as Equation (4.1) and Equation (4.2).

$$N = F_c = \alpha \cdot f_{cc} \cdot x \cdot b \tag{4.1}$$

$$M = N \cdot e = \alpha \cdot f_{cc} \cdot x \cdot b \cdot e = \alpha \cdot f_{cc} \cdot x \cdot b \cdot \left(\frac{h}{2} - \beta x \right) \tag{4.2}$$

The expressions in Equation (4.1) and Equation (4.2) are derived by means of Figure 4.2.

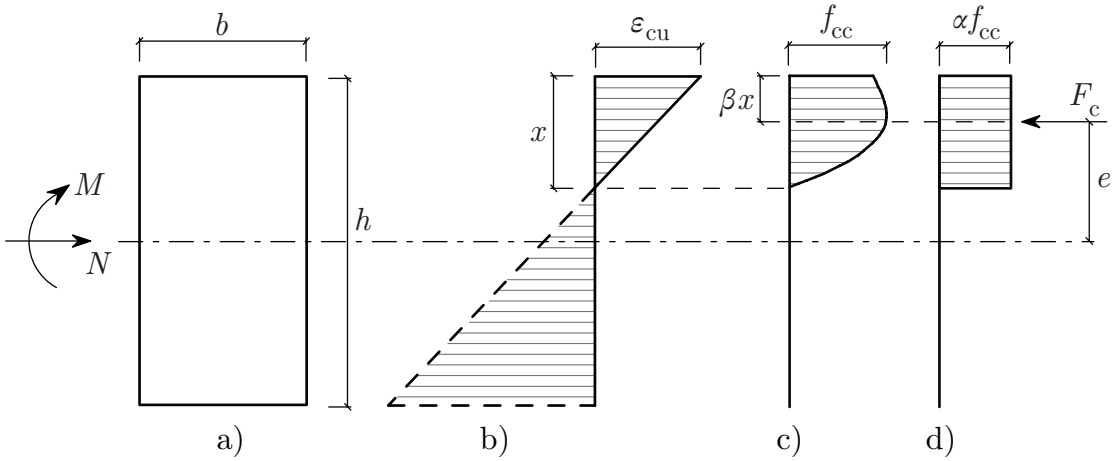

Figure 4.2: a) An arbitrary cross section with outer forces, b) the strain distribution, c) the stress distribution and d) simplified rectangular stress distribution and its resultant force.

The real stress distribution shown in Figure 4.2c is equal to the stress-strain diagram for the concrete, see Figure 4.3.

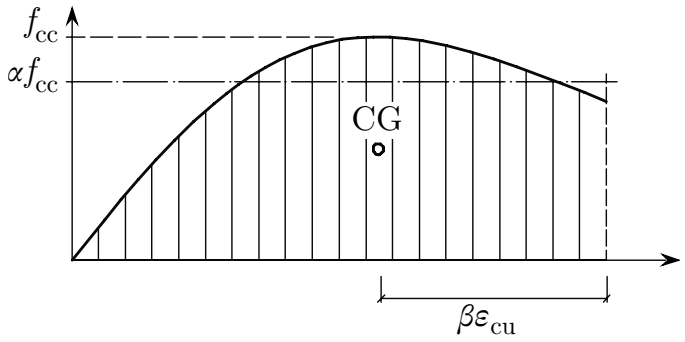

Figure 4.3: Stress-strain diagram of a bent concrete cross section. (Reproduced from Sundquist, 2007)

In accordance with Holmgren *et al.* 2007, a simplification has been made from Figure 4.2 c) to get Figure 4.2 d). According to Boverket 2004, the average strain in a cross section is limited to $2^0/_{00}$. This will cause a change in the shape of the failure envelope, as shown in Figure 4.4.

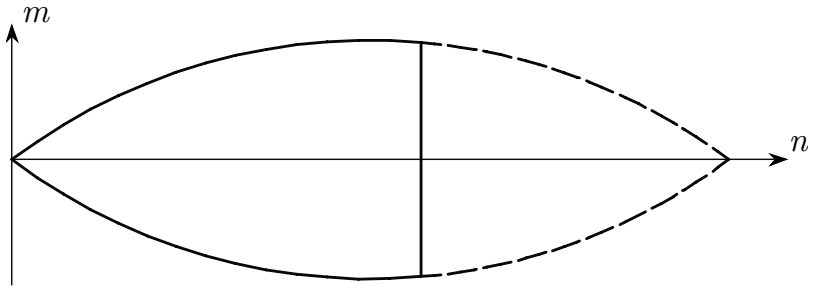

Figure 4.4 Modified failure envelope where the right part is cut off to illustrate the restriction that the average strain in the cross section is limited to be maximum $2^0/_{00}$.

When the point C in Figure 4.1 b), where the failure curve meets the n-axis represents a completely compressed cross section with a compressive strain of $3.5^0/_{00}$, a new restrictive line must cross the n-axis at 2/3.5 of the total length of the n-interval.

To normalise the section forces, the normal force was divided by its capacity $f_{cc} \cdot b \cdot h$ and the bending moment by $f_{cc} \cdot b \cdot h^2$ as shown in Equation (4.3) and Equation (4.4). When it was not really about dividing the bending moment by its capacity $f_{cc} bh^2/6$ but to normalise it, it was unnecessary to divide it by the capacity when that only would bring an extra constant. The denominator is in fact rather insignificant when the normalised values are not important. As long as the normal force and the bending moment in Equation (4.1) and Equation (4.2) are divided by the same expressions as the cross section forces, the denominator does not matter.

$$n = \frac{N}{N_{Rd}} = \frac{\alpha \cdot f_{cc} \cdot x \cdot b}{f_{cc} \cdot b \cdot h} = \alpha \cdot \frac{x}{h} \tag{4.3}$$

$$m = \frac{M}{6 \cdot M_{\mathrm{Rd}}} = \frac{\alpha \cdot f_{\mathrm{cc}} \cdot x \cdot b\left(\frac{h}{2} - \beta x\right)}{f_{\mathrm{cc}} \cdot b \cdot h^2} = \alpha \cdot \frac{x}{h^2}\left(\frac{h}{2} - \beta x\right) \tag{4.4}$$

Insertion of Equation (4.3) in Equation (4.4) leads to Equation (4.5),

$$m(n) = n\left(\frac{1}{2} - \frac{\beta}{\alpha} \cdot n\right) \tag{4.5}$$

which in the ultimate limit state with $\beta/\alpha = 0.5$ yields Equation (4.6).

$$m = \frac{n}{2}(1 - n) \tag{4.6}$$

In Figure 4.5, Equation (4.6) is plotted as an upper limit. As long as the loads lie within this curve, there is no risk for rupture in the arch. The point P_1 is represented by the normal force and the moment from the deadweight of the bridge. If the normal force and the bending moment from the traffic load are multiplied with a factor 1.0, the point P_2 is found. From this point, an extension of the load line $(P_1 \rightarrow P_2)$ can be made to find the point on the failure curve where the arch will break. The number of times the traffic load can be added before the failure curve is reached is defined as the load factor. Hence, it is the ratio between the distance P_3 - P_1 and P_2 - P_1 that determines the load factor.

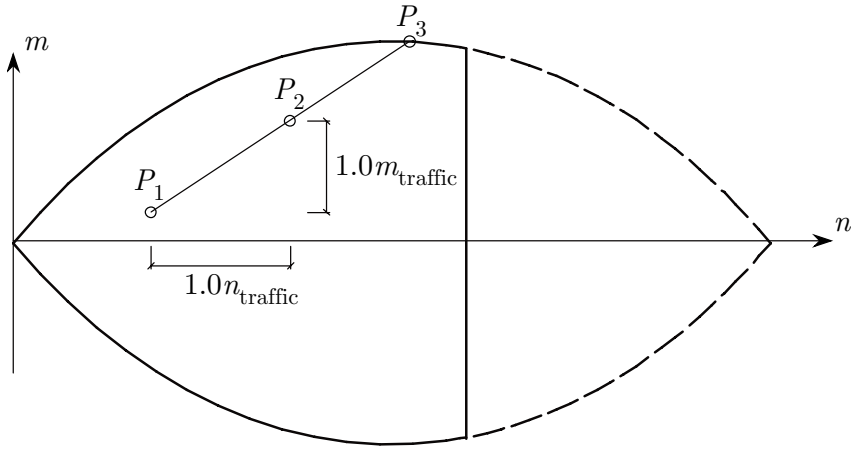

Figure 4.5: The failure envelope.

When the load factor was calculated, the inclination of the load line k between point P_1 and P_2 in Figure 4.5 and the point where this line cut the m-axis p were calculated by Equation (4.7) and (4.8).

$$k = \frac{m_2 - m_1}{n_2 - n_1} \tag{4.7}$$

$$p = m_1 - kn_1 \tag{4.8}$$

Along the extended load line between P_1 and P_2, a new value on n equal to an n on the parabolic curve was searched. This was done by Equation (4.9).

$$m_{\text{curve}} = m_{\text{line}} \rightarrow \frac{n}{2}(1-n) = kn + p \tag{4.9}$$

The equation was solved to find the intersection point at P_3. With a known n, the load factor was calculated by Equation (4.10). Attention had to be paid to multiple crossing points since one of the points was found in the opposite direction of the load line. Appendix D.3, containing the larger part of the code written in MATLAB, ensures that it is the correct crossing point that is found.

$$Load\ factor = \frac{n(P_3) - n(P_1)}{n(P_2) - n(P_1)} \tag{4.10}$$

The limitation of a maximum compressive strain of $2^0/_{00}$ discussed above should not cause any problem for the Glomman Bridge. The limit can only narrow the load factor when the inclination of the load line is such that it cuts the new vertical line. This is caused by a large normal force and small bending moment from the traffic load.

In the model, the normal force was set to be positive when the arch was under compression and negative under tension, thus the opposite of the common sign convention. This change was made to get the failure envelope on the positive n-axis, seeing that the deadweight and live load mainly would cause compression in the arch. The bending moment was set to be positive when sagging and negative when hogging. The positive normal force and bending moment are given in Figure 4.6.

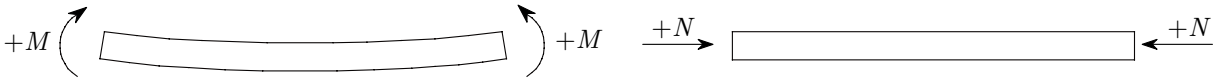

Figure 4.6: Sign convention for bending moment and normal force.

4.2 FE-modelling in ABAQUS

The finite element analyses were carried out in ABAQUS CAE, which is a version of the general-purpose non-linear finite element analysis program ABAQUS. The program was used to create a linear elastic two-dimensional model of the Glomman Bridge. For the most part the graphic interface of the ABAQUS CAE was used to create the model. However, sometimes the ABAQUS input-file was edited. The input

file is created when a job is submitted in ABAQUS CAE and the analysis is then performed using the data of this file. The purpose of the model was to calculate the section forces in the arch with two analyses. One when the bridge was loaded with its deadweight and one when the bridge was loaded with a moving load on the pavement. From the deadweight analysis, section forces in the arch were obtained instantly. In the moving load analysis, influence lines for normal force and moment in the arch were calculated. From the influence lines, section forces were obtained.

In Figure 4.7, the ABAQUS model is shown. It consisted of five parts: pavement, backfill, abutments, rigid beams and the arch. The boundary conditions are also shown in the figure with the abutments on fixed supports and the backfill on roller bearings. To place the abutments on fixed supports was an approximation that could be done because they stand on solid rock. The large friction, which arises due to the high deadweight and presumed rough surface, together with the earth pressure, will prevent the abutments from lateral sliding. The purpose of the pavement was to imitate the real bridge and to consider possible load distribution of the concentrated force to the backfill. Whether it has any effect on the load carrying capacity is shown in Chapter 5.4.

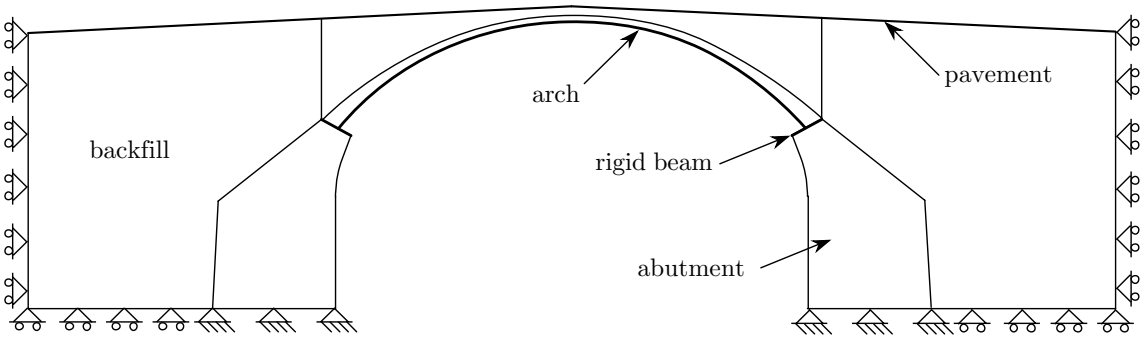

Figure 4.7: Boundary conditions for the Glomman FE-model.

As shown in Table 4.1 the element types used were 2D solid plane stress elements with four nodal points and 2D beam elements. To model the arch, beam elements with varying height were used because it was easier to obtain section forces from beam elements than from solid elements. Between the parts, tie constraints connected the nodes in the edge of each part with a corresponding node in the adjacent part. The tie constraint locked the translations and rotations in each node to the corresponding node. However, since 2D-solid elements do not have rotational degrees of freedom the rotation could not be locked to the beam elements. This however works perfectly between beam elements. Therefore, a rigid beam was connected to the top of the abutment with tie constraints. The rigid beam was connected to the arch beam with a tie constraint with locked translational and rotational degrees of freedom.

Table 4.1: Type of elements for different parts.

Part	Element type
Pavement	2D beam element
Backfill	2D solid plane stress
Abutments	2D solid plane stress
Rigid beams	2D beam element
Arch	2D beam element

The tie constraints used in this model do not consider parts sliding against each other, which is the case in reality. To consider the sliding, the friction between the parts must be taken into account. This was not done when it would have resulted in a non-linear analysis.

To model the backfill as an elastic medium is a rather rough simplification. The backfill has three major purposes: load distribution, increase deadweight and create a passive earth pressure that counteracts heaving. The load distributing effect is shown in Figure 4.8 and Figure 4.9 which shows the reaction forces due to a concentrated load on the backfill when the arch nodes has locked translations.

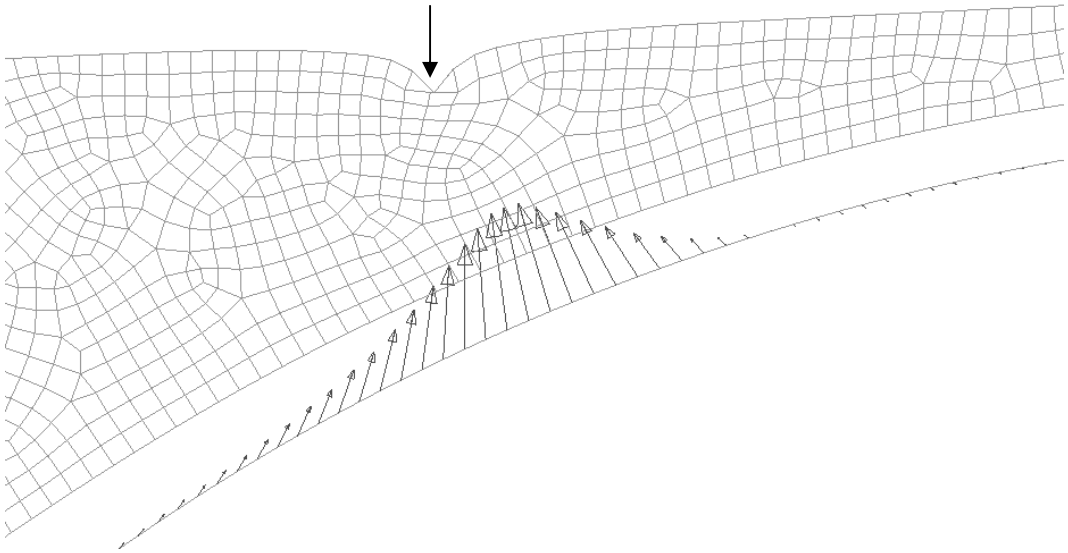

Figure 4.8: Reaction forces in the arch quarter point due to a concentrated load on the backfill.

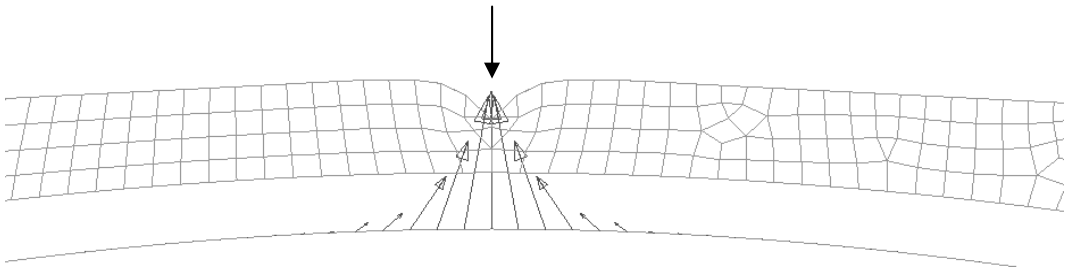

Figure 4.9: Reaction forces in the arch crown due to a concentrated load on the backfill.

The two figures above can be compared to the vertical stress according to Boussinesq, Equation (4.11) where P is a concentrated load, z is the depth and r is the horizontal distance from the concentrated load, (Cernica, 1995). With this equation, a vertical stress distribution as shown in Figure 4.10 was obtained. As seen, the shape is rather similar to the reaction forces in Figure 4.9. Projected on a curved surface, the Boussinesq distribution would be similar to Figure 4.8.

$$\sigma_z = \frac{3P}{2\pi} \cdot \frac{z^3}{(r^2 + z^2)^{5/2}} \tag{4.11}$$

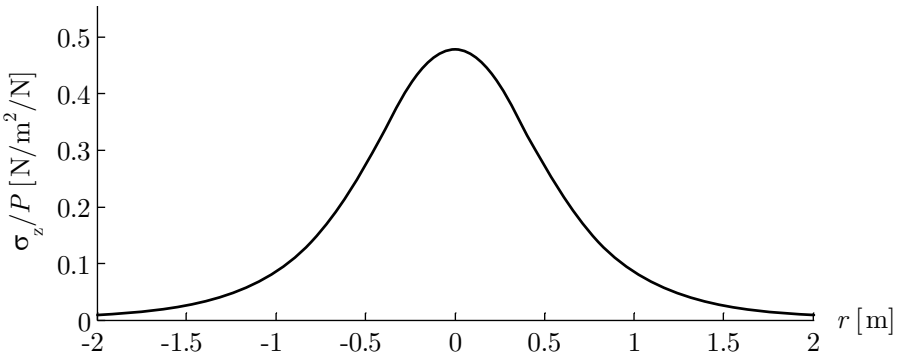

Figure 4.10: Vertical stress distribution on plane, depth $z = 1$ m.

The elasticity of the backfill made it possible for the fill to manage tensile forces that occurred when the concentrated force was positioned alongside the arch. Due to the tie constraints between the arch and the backfill, small tensile forces also occurred in the arch.

A simplified model, as shown in Figure 4.11 has been used to obtain influence lines to compare with influence lines from the literature. In the simplified model, the arch was fixed on supports in both ends with a concentrated force moving directly on the arch.

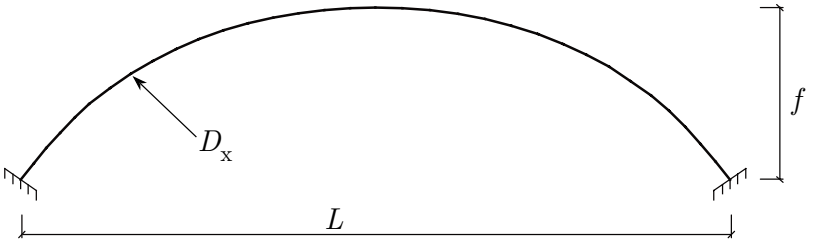

Figure 4.11: Simplified model of the arch.

To create an arch with varying thickness and to create a moving load, the ABAQUS input-file was edited, shown in Appendix D.1. The arch section thickness was generated as a text-file with MATLAB and the text-file was included in the input-file, which was imported into ABAQUS CAE. The moving load was created by using an amplitude function, which were also generated in MATLAB and imported into ABAQUS CAE. The amplitude function activated the load in one node in the pavement for each time increment. Table 4.2 shows the amplitude function used in ABAQUS, where i is the current time increment and n is the total number of increments.

Table 4.2: Amplitude function used in ABAQUS.

Increment No.	Amplitude
0	0
i - 1	0
i	1
i + 1	0
n	0

The mesh is one of the most important parts of a finite element model. The more dense mesh, the more precise the results will be. However, a dense mesh will take longer time to compute than a sparser. To find a suitable mesh, a test of convergence was carried out for the deflection and bending moment in the arch, due to a point load in the crown. The crown was studied due to the small thickness of the fill and therefore few vertical elements. The test was performed with a constant arch thickness of 0.4 m and a point load of 100 kN in the crown. No deadweight was considered. The reason why a point load in the crown was chosen was because the fill distributes concentrated forces and the number of elements in the fill is crucial for a correct distribution. In Figure 4.12, the deflection of the arch is shown with different mesh configuration. No noticeable difference in the deflection can be discerned. Figure 4.13 shows an enlargement of Figure 4.12 where the deflection differs the most which is in the crown of the arch. As seen, the deflection of an arch with a mesh of 200 elements is quite similar to one with 350 elements.

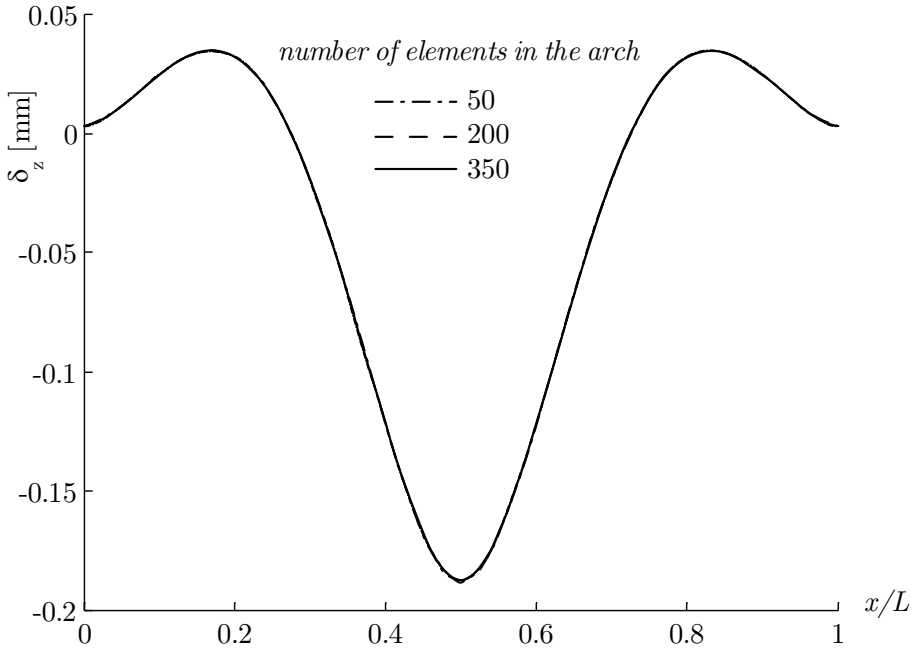

Figure 4.12: Deflection of the arch, due to a point load of 100 kN in the crown, with different meshes.

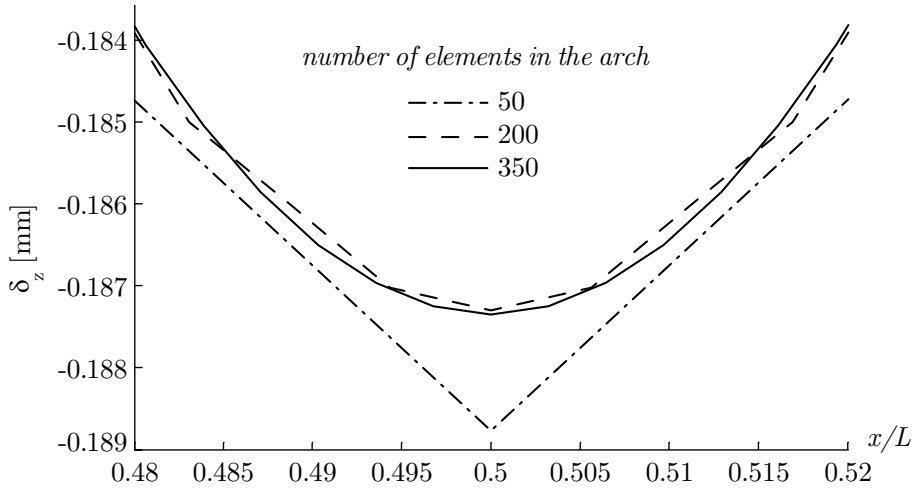

Figure 4.13: Deflection of the crown due to a point load. Enlargement of Figure 4.12.

In Figure 4.14 the bending moment in the arch is shown and as seen the difference in bending moment between the mesh configurations is rather small. Therefore, an enlargement is shown in Figure 4.15. In the figure it shows that the 200 and 350 element meshes correspond fairly well. Hence, it follows that a mesh of 200 elements in the arch gives sufficiently accurate results.

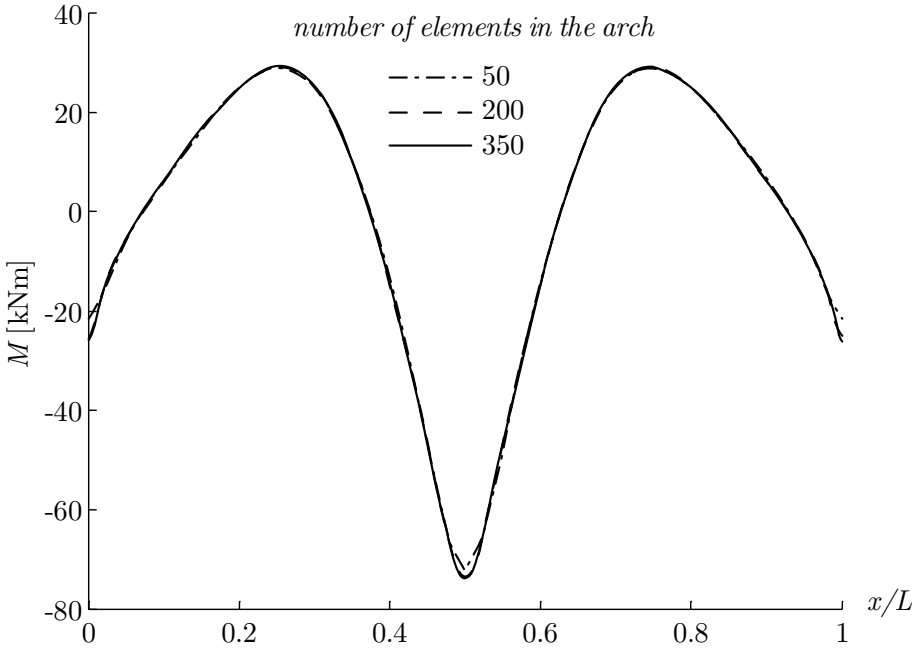

Figure 4.14: Bending moment in arch due to a point load of 100 kN in the crown with different meshes.

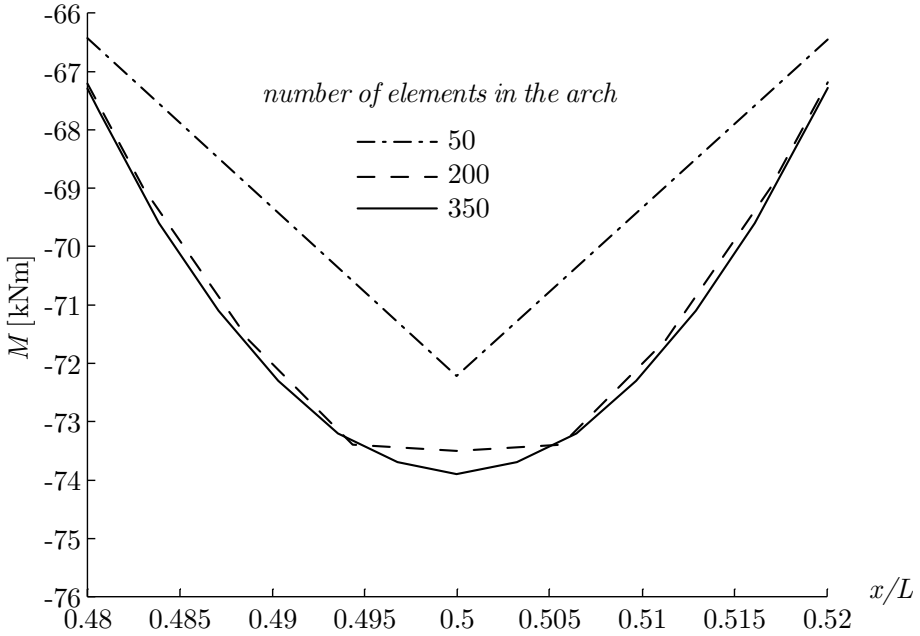

Figure 4.15: Bending moment in crown due to a point load. Enlargement of Figure 4.14.

The mesh configuration finally used is shown in Figure 4.16 with 200 elements in the arch and adjacent fill. This gave an average element size of 0.1 m. As seen, the mesh was denser in the backfill above the arch than alongside the arch. The reason was that the load distribution through the fill is more important where the fill height is low. Therefore, it is crucial to have several elements in height in the crown. In Figure 4.17 an enlargement of the mesh in the crown shows that there were at least four elements in height. The outer parts of the backfill were meshed sparser because of they do not contribute to the section forces in the arch in the same degree as the rest of the model.

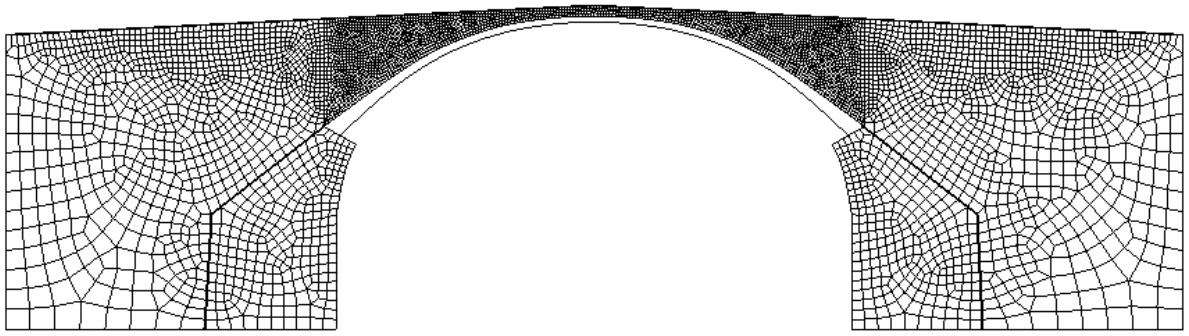

Figure 4.16: The final mesh.

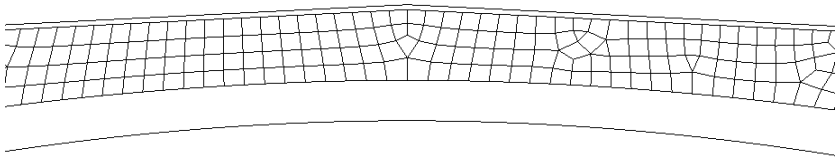

Figure 4.17: The final mesh in the crown. Enlargement of Figure 4.16.

To verify the deadweight results from the ABAQUS model a calculation was carried out by hand, using MATLAB. The calculation was done by dividing the backfill and the arch into stripes with the width of the horizontal distance between the two adjacent nodes in the arch. By this method the stripes in the crown was wider than the stripes in the springing due to the variation in angle of the arch. The stripes were then multiplied by the width of the bridge and by respectively materials unit weight. The force created by each stripe was assumed to act on each of the adjacent arch nodes.

The deadweight from ABAQUS was obtained by locking the translations of the arch nodes and applying gravity force onto the entire model. Then the vertical reaction force in each arch node corresponded to the deadweight. The nodes in the springing of the arch were not considered because of the large influence of the deadweight from the abutments.

In Figure 4.18 a comparison between these two methods is shown. As seen, they correspond fairly well.

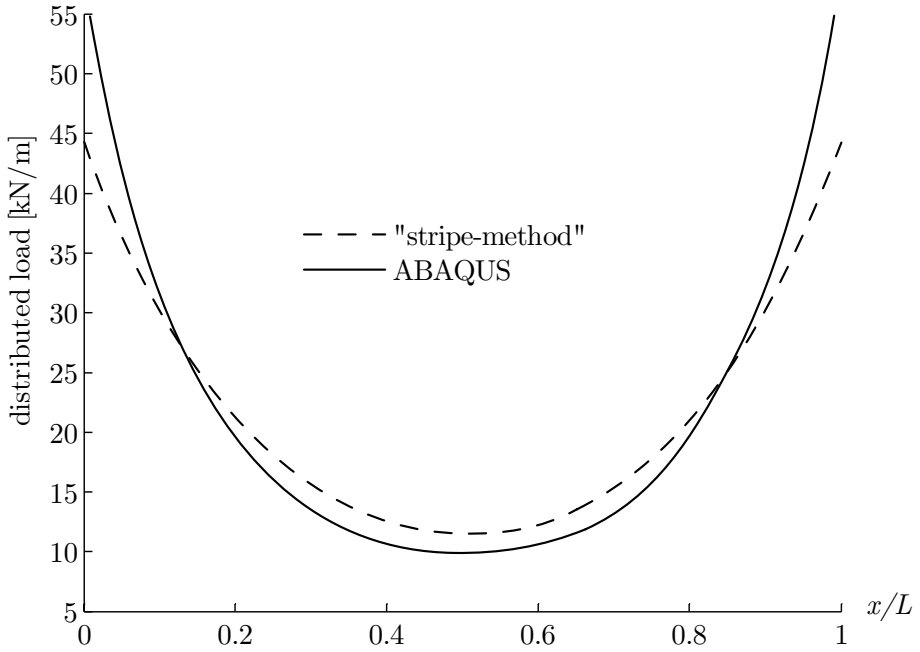

Figure 4.18: Comparison between deadweight on the arch calculated using ABAQUS and by hand using MATLAB.

4.3 Combining loads in MATLAB

By means of the influence lines created in ABAQUS, cross section forces due to the deadweight (permanent load) of the bridge and the traffic (live load) were calculated. According to VV 1998:78, certain pressures on each axle are specified depending on the number of axles on the vehicle travelling over the bridge and the distance between the axles. The main problem is to find the worst combination of normal force and moment in each point of the arch.

The combinations of cross section forces in this thesis were chosen to be the four different extreme cases, namely:

1. The largest positive bending moment $M_{\max}$ and the adherent normal force N_{adh}.
2. The largest negative bending moment $M_{\min}$ and the adherent normal force N_{adh}.
3. The largest positive normal force $N_{\max}$ and the adherent bending moment M_{adh}.
4. The largest negative normal force $N_{\min}$ and the adherent bending moment M_{adh}.

To set such a limit and only examine these four cases may seem like a big restriction, which is further discussed in Chapter 6. The four different extreme cases need qualifying though; it is not too large cross section forces that cause a failure in the arch but too large stresses. To come around this problem it was necessary to take the specific cross section area in every node into consideration. This was done by normalizing the influence lines before searching for the largest positive and negative bending moment and normal force. When the location for the worst cross section forces was unknown, it was necessary to examine the four combinations mentioned above in every node. The flowchart in Figure 4.19 gives a basic view over the routine made in MATLAB.

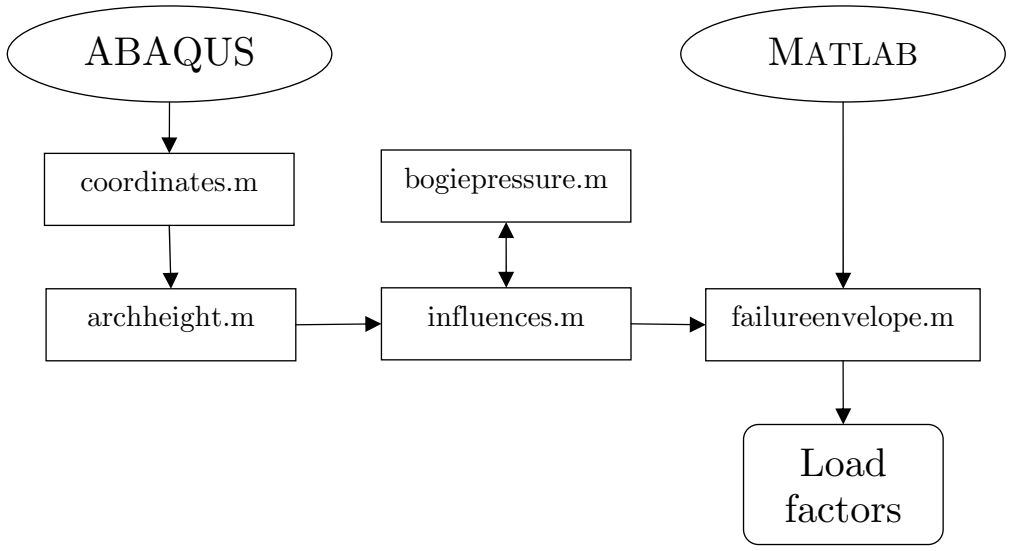

Figure 4.19: Flowchart of the MATLAB routines.

The coordinates for the influence lines were created in ABAQUS and put into MATLAB m-files and were immediately readable to MATLAB. The coordinates were read into the file *archheight*, which then were read into influences. In *archheight* the thickness of the arch was calculated and every element was given a thickness. The file *influences* were used to coordinate the cross section forces calculated in the function file *bogiepressure*. When all the forces were collected in a matrix, the whole file *influences* was read into *failureenvelope* where the load factors were calculated. The failure envelope was also plotted for all four cases mentioned earlier.

4.3.1 Least favourable load combination

A chosen number of axles were placed in one position at the time. The length, which the axles were stepped forward with, was one node in the pavement. Therefore, the steps were shorter over the crown than over the outer parts of the pavement. The four load combinations mentioned earlier were calculated one at the time, starting with the

largest positive bending moment and the adherent normal force. One load combination routine was created, where a single axle was moved along the pavement. For each influence line, its maximum influence and position in the vector (equals the position of the axle on the pavement) were stored in a matrix as shown in Figure 4.20. That matrix contained two columns, one for the maximum influences and one for the adherent positions on the pavement. The maximum influence from the first column and its position (in which node the failure first would occur) in the new vector were then picked out.

$$\begin{bmatrix} i(M_{\max})_{\text{node=1}} & pos_{\text{node=1}} \\ i(M_{\max})_{\text{node=2}} & pos_{\text{node=2}} \\ \downarrow & \downarrow \end{bmatrix}$$

Figure 4.20: Influence matrix.

The maximum influence was then multiplied with the right axle pressure depending on examined classification of the bridge (BK-class). At last, the adherent normal force was picked out and multiplied with the same axle pressure. How large the multipliers were are given in Table 4.3.

Table 4.3: Single axle pressure for different BK-classes given in tonnes. (Trafikförordningen, 1998)

Load class	BK1	BK2	BK3
Not a driving axle	10	10	8
Driving axle	11.5	10	8

A similar load combination routine was made for the bogie. Two axles were run along the pavement, see Figure 4.21 II. In the beginning of the pavement, until one axle distance was reached, only one axle was stepped to simulate just one of the bogie axels. The same was applied in the end of the pavement. As soon as the first axle was stepped further than one axle distance, the second axle was stepped along with the first at this certain axle distance.

Table 4.4: Bogie pressures for different BK-classes given in tonnes. The pressures are supposed to be divided in two, half on each axle. (Trafikförordningen, 1998)

Load class [tonnes]	BK1	BK2	BK3
axle distance<1.0m	11.5	11.5	11.5
1.0 m ≤ axle distance < 1.3 m	16	16	12
1.3 m ≤ axle distance < 1.8 m	18	16	12
1.3 m ≤ axle distance < 1.8 m and the driving axle is equipped with double assembled wheels and air suspension or equivalent suspension, or the driving axles are equipped with double assembled wheels and the weight does not exceed 9.5 tonnes on either axle.	19	16	12
axle distance ≥ 1.8 m	20	16	12

An easier way to accomplish the same result could have been to displace two equal influence lines sideways a distance equivalent to an axle distance. If those two influences are added, the result will be a total influence line for the bogie. Then it is easy to find the maximum influences and multiply it with the right axle pressure to find the cross section forces. The problem with this method is that impossible to make a displacement of a certain distance when the elements do not have the same dimensions. To be able to do this with a reasonable effort, the displacement in the pavement should be formed by a number of whole elements. When the pavement elements in this thesis have varying dimensions, this method was not chosen.

Similar to the single axle, the bending moments from the bogie were saved in a vector, one bending moment for each bogie position. The bogie is different though, because of the unknown axle distance the bogie had to go through the load combination routine one time for each axle distance.

4.3.2 Buses

The maximum weight of the vehicles allowed on the bridge is 3.5 tonnes. The exception is for buses, travelling in regular traffic. According to Länstrafik i Örebro there are two different kinds of buses that are allowed to pass over the bridge today. The first is a two axle bus with six metres between the axles and a pressure on the front- and rear axles of 5 430 kg and 11 290 kg respectively. The other is a bus with three single axles. The distance between the axles is 5.25 metres between the front- and middle axle and 6.75 metres between the middle- and rear axle. The pressure on the axles is 6 120, 7 140 and 11 600 kg respectively. The latter of these two types is illustrated in Figure 4.21 III.

The same method that was used for the bogie load was also used when it came to buses. As long as the first axle had not reached the length of the first axle distance, only the first axle was stepped. In the same way only the two first axles were stepped until the second axle had reached the whole second axle distance. In other words, the routine calculated the largest positive bending moment and adherent normal force from that the first axle runs on the first node of the bridge, until that the last axle leaves the last node.

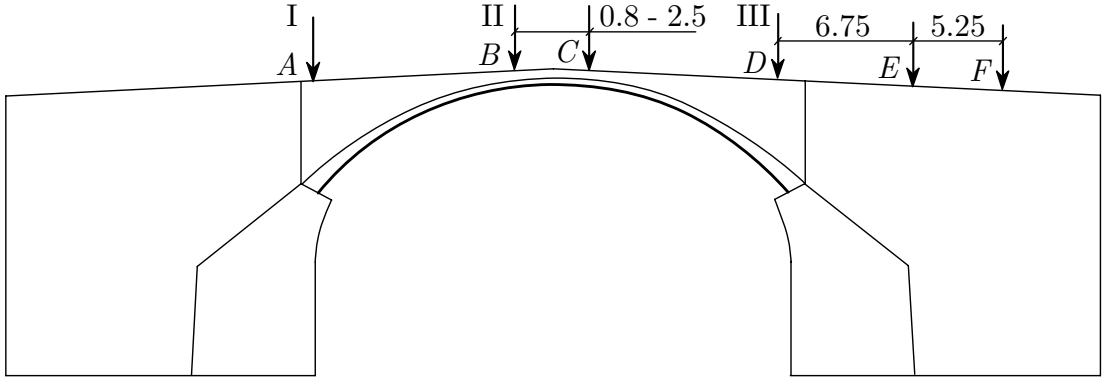

Figure 4.21: The axles and axle distances for the allowed vehicles on the bridge. The axle and bogie pressures I and II are given in Table 4.3 and Table 4.4.

The numbers of load types tested in this thesis were limited to the ones mentioned above. According to VV 1998:78, a number of load types should be tested and run over the bridge. Most of these loads are though spread over a long distance and are low in amplitude so they should not be the decisive load type.

According to VV 1998:78, the load coefficient for the traffic load shall be 1.3. The model was calculated with this coefficient, two vehicles travelling side by side, one in each lane of the bridge. The regulation then says that the load coefficients on these vehicles shall be 1.0 and 0.8 respectively. The total partial coefficient for the traffic load then becomes $1.3 \cdot (1 + 0.8) = 2.34$, which was used for all load types in the thesis.

Chapter 5

Capacity assessment

5.1 Introduction

The only loads considered within this thesis were the deadweight and the vertical traffic load. No consideration of temperature load or snow load etc. was taken. This simplification was done because the main reason with the thesis was not to perform an entire design calculation but to investigate the load carrying capacity with the failure envelope method regarding the effects of the backfill.

The studied traffic loads were BK3 axle load and bogie load with varying distance between the axles and a two- and three-axle bus. A parametric survey for the BK3 bogie load is presented in Chapter 5.4. Parametric surveys for the remaining load types are shown in Appendix C. All load factors were calculated with design concrete compressive strength and the loads was multiplied by 2.34 as mentioned in Chapter 4.3.

5.2 Influence lines

With the reference values presented in Chapter 5.3, the influence lines shown below were obtained. As seen in Figure 5.1 and Figure 5.3 the influence lines reaches outside the arch. This is because when the load is positioned alongside the arch, the backfill distributes the load onto the arch. Figure 5.1 gives an impression that it is the springing that is the most critical section of the arch. This is not the case. It is true that this is where the largest moment arises, however this is also where the moment capacity is largest. To visualize the use of the moment capacity of the arch sections, the influence lines in Figure 5.1 were normalised according to Equation (5.1). The normalised influence lines are shown in Figure 5.2. They, unlike usual influence lines, do not show the variation of the cross section forces. Instead they illustrate the moment efficiency when a unit load is run along the pavement.

$$\eta = \frac{M}{M_{\mathrm{Rd}}} = \frac{i(M)\cdot P}{\frac{f_{\mathrm{cc}} b h^2}{6}} \rightarrow \frac{\eta}{P} = \frac{i(M)\cdot 6}{f_{\mathrm{cc}} b h^2} \tag{5.1}$$

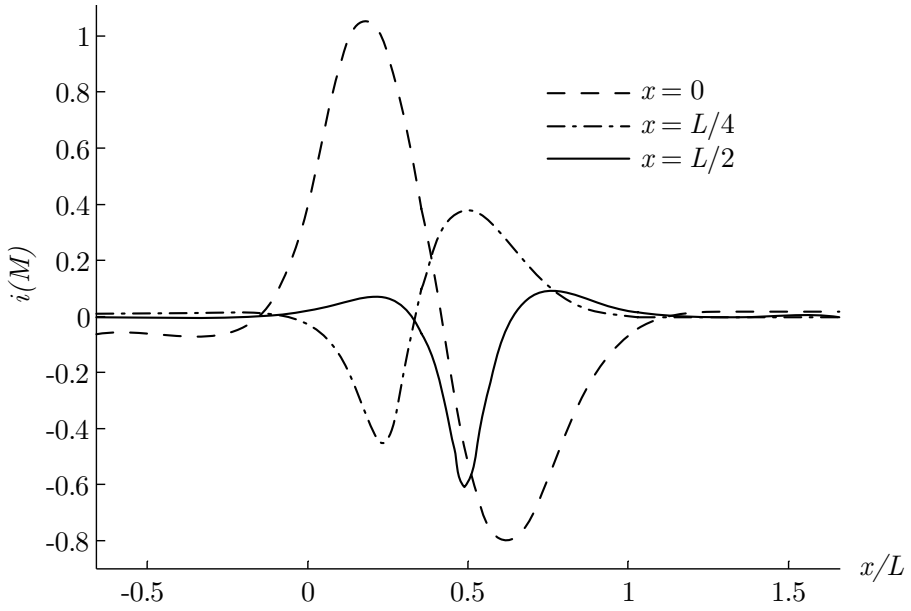

Figure 5.1: Influence lines for bending moment for the Glomman Bridge in the springing, quarter point and crown.

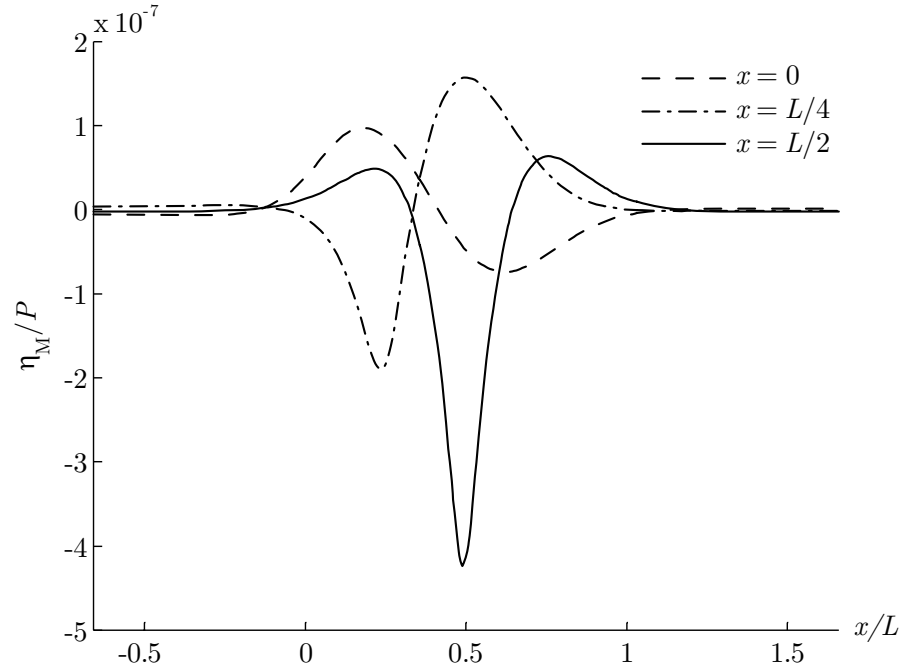

Figure 5.2: Variation of the cross section moment efficiency in the springing, quarter point and crown when the load runs along the arch.

In Figure 5.3, the influence lines for normal force are shown. The influence line $x = L/2$ gave a peak when the load was located in the crown. This was probably because of shear stresses between the arch and the backfill. These stresses arose because the tie constraints did not allow sliding between the parts, which made the arch counteract the movement of the fill. The reason why this was only shown in the crown was the small thickness of the fill at this location. The peak decreased in amplitude when the Poisson's ratio was reduced. When the tie constraints were replaced by coupling constraints, with translation locked only in the normal direction of the arch, the peak disappeared.

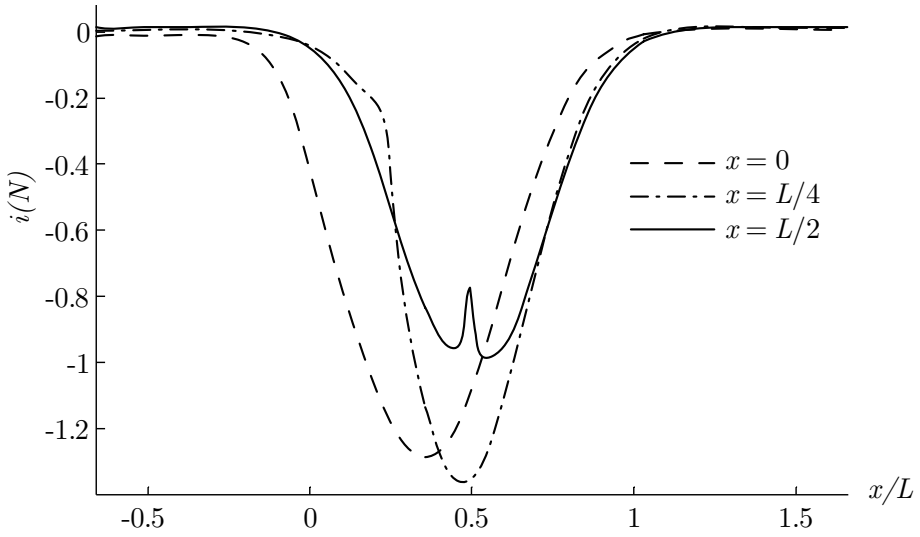

Figure 5.3: Influence lines for normal force for the Glomman Bridge in the springing, quarter point and crown.

The efficiency of the normal force is shown in Figure 5.4. This was calculated by dividing the normal force of each cross section by its normal force capacity, as in Equation (5.2). The largest difference from the influence lines was in the springing where the normal force was large but the efficiency low.

$$\eta = \frac{N}{N_{\mathrm{Rd}}} = \frac{i(N)\cdot P}{f_{\mathrm{cc}} bh} \rightarrow \frac{\eta}{P} = \frac{i(N)}{f_{\mathrm{cc}} bh} \tag{5.2}$$

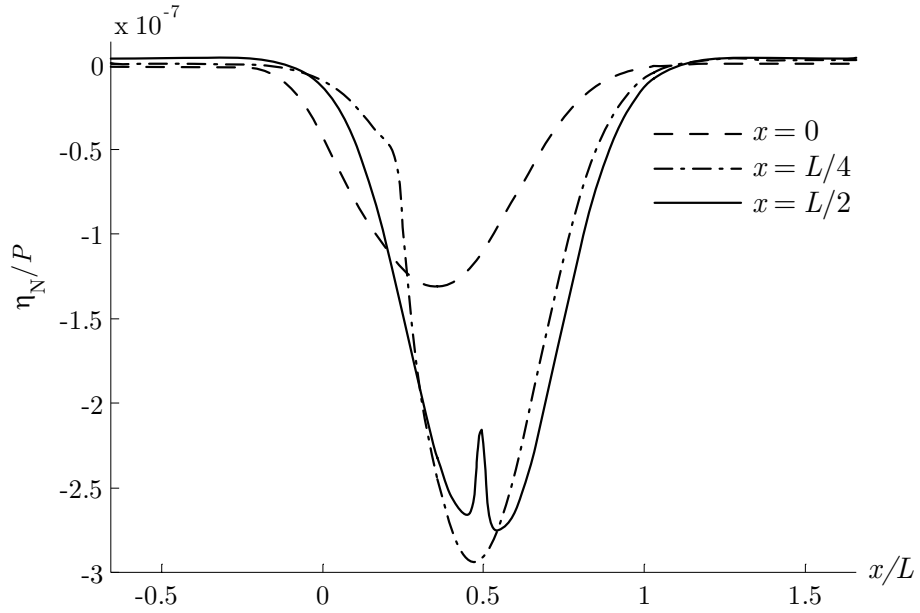

Figure 5.4: Variation of the cross sections normal force efficiency in the springing, quarter point and crown when the load runs along the arch.

Figure 5.5 and Figure 5.6 show the influence lines for the simplified model of the bridge, shown in Figure 4.11. These influence lines are rather similar to the influence lines for the model of the whole bridge shown in Figure 5.1 and Figure 5.3. The difference is that the influence lines above are softer due to the load distribution

through the fill. The influence lines for moment can be compared to Sundquist, 2007 regarding shape but not regarding magnitude. The difference in magnitude was probably the effect of different bending stiffness ratio between the crown and the springing. While Sundquist, 2007 uses a bending stiffness ratio of $D_{\text{springing}}=3D_{\text{crown}}$ the ratio for the Glomman Bridge is, as seen in Figure 3.5, $D_{\text{springing}}=15D_{\text{crown}}$

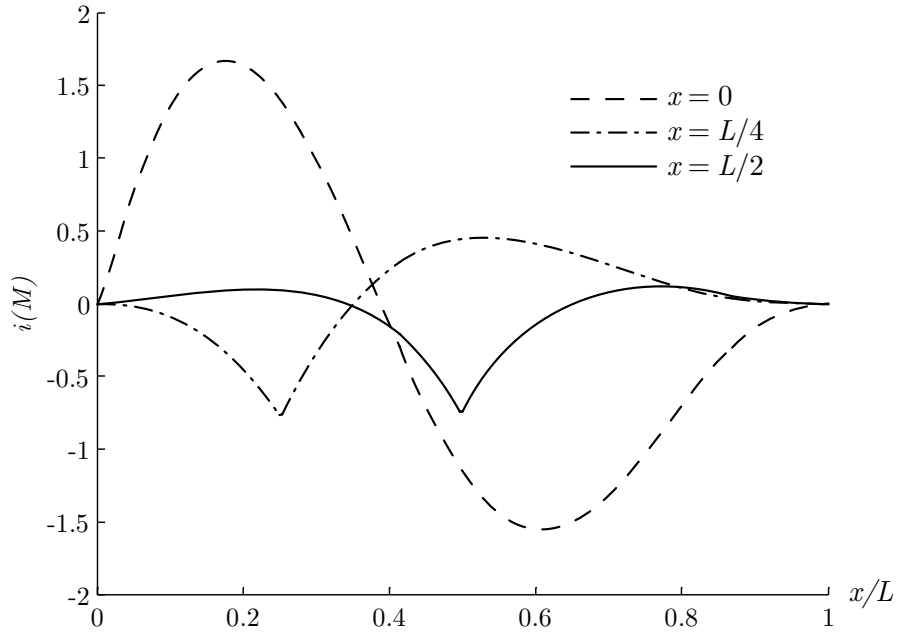

Figure 5.5: Influence lines for bending moment due to a point load directly on the arch.

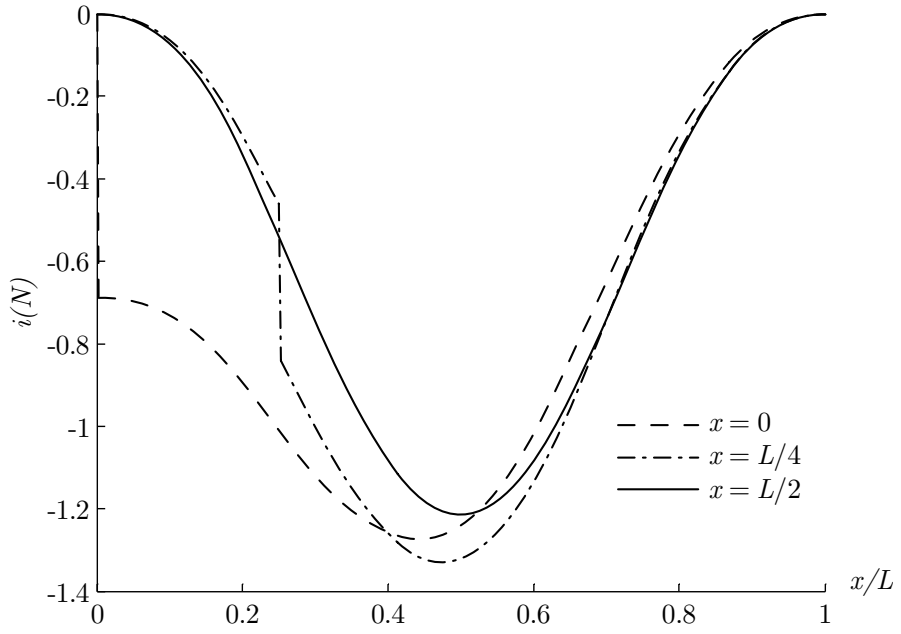

Figure 5.6: Influence lines for normal force due to a point load directly on the arch.

The design influence line for the BK3-load is shown in Figure 5.7. The positions of the axles along the pavement are marked with dotted lines. As seen in the figure, the calculation routine places the axles where they cause the largest influence.

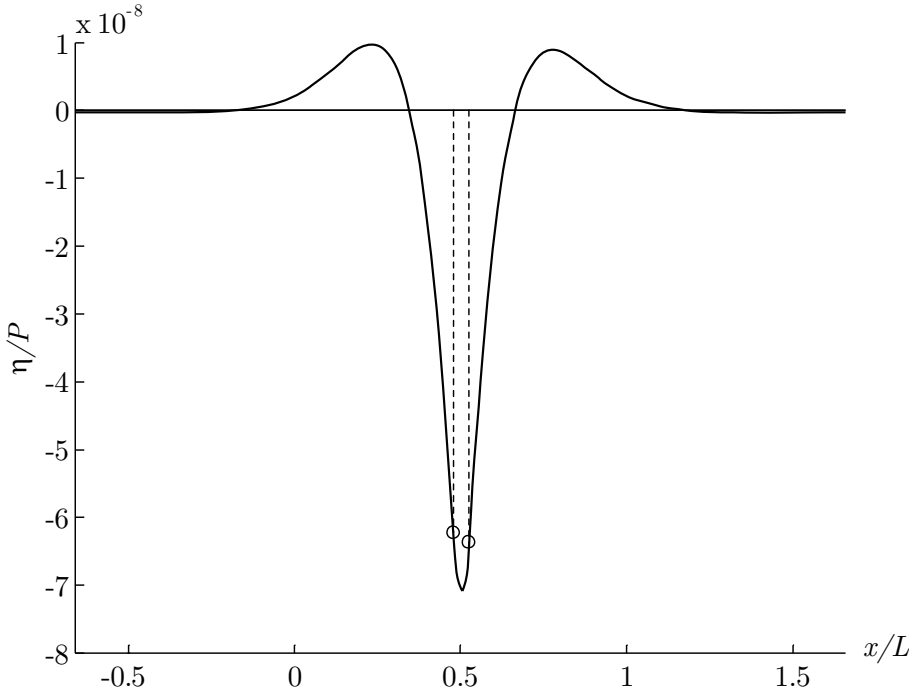

Figure 5.7: BK3-load placed where it causes the largest influence.

In Figure 5.8, the design influence line for the 2-axle bus is shown. The two axles cause bending moment in different directions but it is important to remember that the two influences will be multiplied with different axle pressures.

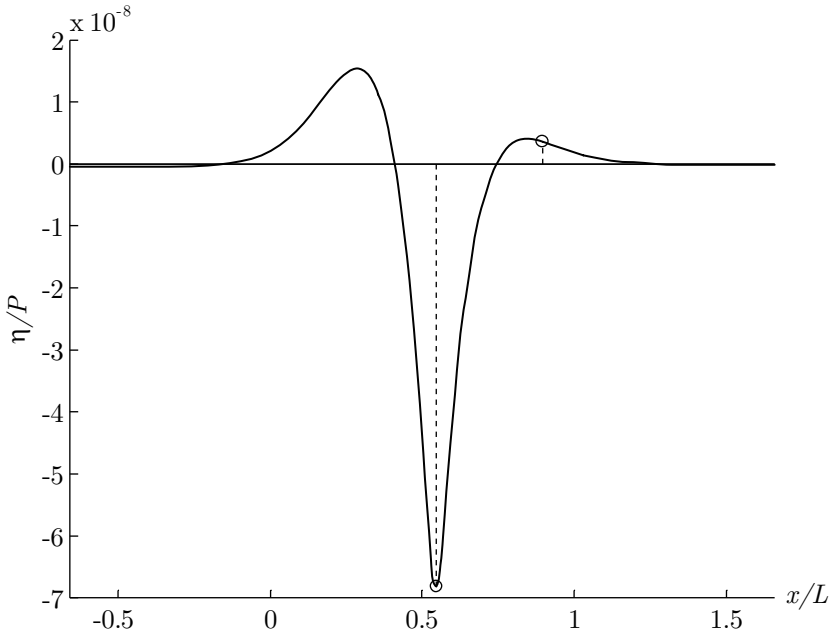

Figure 5.8 The design influence line for the 2-axle bus. Note that the influences from the two axles will be multiplied with different axle pressures.

5.3 Reference case

The reference case was calculated with values for the parameters shown in Table 5.1.

The Young's modulus of the concrete was assigned a reference value of 30 GPa because it is a common value used for concrete. The density of concrete varies between 2200 and 2400 kg/m^3 depending on whether it is reinforced or not. Since the Glomman Bridge has rocks embedded in the concrete, the reference value for the density was chosen to 2400 kg/m^3, which correspond to reinforced concrete. The reference value for the concrete Poisson's ratio was chosen to 0.2 according to Holmgren *et al.* 2007. The characteristic concrete compressive strength was assigned to be the value calculated from the test results in Chapter 3.4. The reference value for the characteristic concrete compressive strength was chosen to 11.5 MPa, which corresponds to the poorest concrete quality, C12/15 according to BBK 04. After dividing with partial safety factors for safety class and uncertainties in the material of 1.2 and 1.5 respectively, this resulted in a design concrete compressive strength of 6.4 MPa.

The Young's modulus of the backfill was assigned a reference value of 225 MPa, which correspond to sand and gravel according to Flener, 2004. The reference value for the backfill density was set to 1500 kg/m^3, which was slightly low. A better value would have been 1800 - 2000 kg/m^3. However, since this value is on the conservative side, it is not a paramount consideration. It still gives an idea of the importance of the fill density. The backfill was assigned a reference value for Poisson's ratio of 0.3 according to GeotechniCAL.

The reference value for the Young's modulus of the pavement was chosen to 1 GPa according to Huang, 2003. The pavement density was estimated to 1200 kg/m^3. This value may as well be a bit low; however, this is also an assumption on the conservative side. The pavement Poisson's ratio was assigned a reference value of 0.3 according to Huang, 2003.

Table 5.1: Reference values for the parametric survey.

Reference values	Arch	Abutments	Backfill	Pavement
E - Young's modulus [GPa]	30	30	0.225	1
ρ - Density [kg/m^3]	2400	2400	1500	1200
ν - Poisson's ratio [-]	0.2	0.2	0.3	0.3
f_{cc} - Concrete compressive strength [MPa]	6.4	6.4	-	-

Figure 5.9 shows the failure envelope for the reference case with the load of a BK3 bogie. As seen in the figure, the design load was two times BK3 bogie and the failure occurred in the crown. This was when the load was positioned symmetric around the crown with an axle distance of 0.8 m.

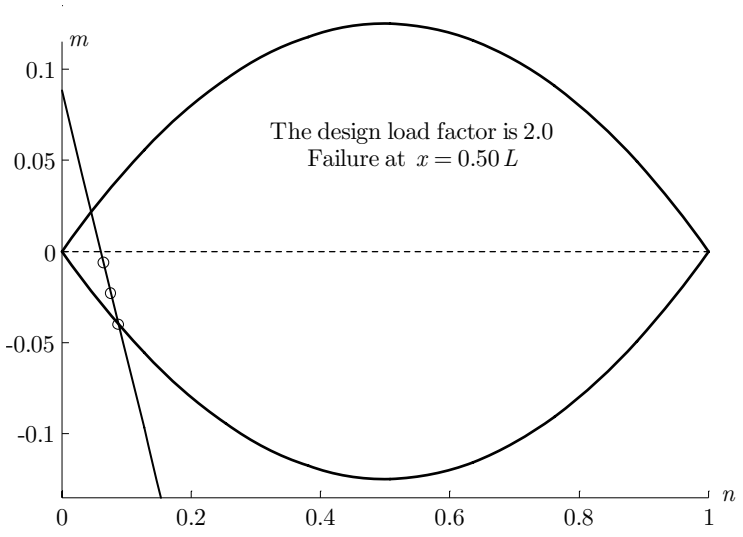

Figure 5.9: The failure envelope for the reference case.

With the used reference values, the load factors shown in Table 5.2 were obtained. As seen in the table, the design load type was the two-axle bus. The load position for the buses describes where the rear axle is positioned. With all load types, failure occurred in the crown.

Table 5.2: Load factors for different load types.

Load type	Load factor	Load position
BK3 Bogie	2.0	Crown
BK3 Axle	2.3	Crown
3-axle bus	1.7	Crown
2-axle bus	1.6	Crown

From Table 5.2, a maximum allowed axle- and bogie pressure could be determined. The load factors, given in the table, gave an allowed axle- and bogie load when they were multiplied with the BK3 axle- and bogie loads. The allowed A/B-value (axle and bogie) became 2.3·8 tonnes = 18.4 tonnes and 2.0·11.5 tonnes=23.0 tonnes, corresponding to 181 kN and 226 kN respectively, given that the safety factor was set to be 1.0.

Even though the safety factor is 1.0, that does not mean that the bridge will collapse if the axle- or bogie loads are exceeded. The partial coefficients for safety class, uncertainties in the material and on traffic load are still included. Besides these, a reduction factor is used considering that two vehicles of the least favourable kind will never be placed with their axles in the least favourable position at the same time. The total safety factor included then becomes $1.2 \cdot 1.5 \cdot 1.3 \cdot (1+1.8)/2 = 2.1$, if two loads of the same type are placed in the least favourable position.

How the load factor is influenced by varying concrete compressive strength when using the parameters of the reference case, is given in Figure 5.10. The load factor 1.0 is marked in the diagram to visualise the needed concrete compressive strength to manage the used traffic load with retained safety.

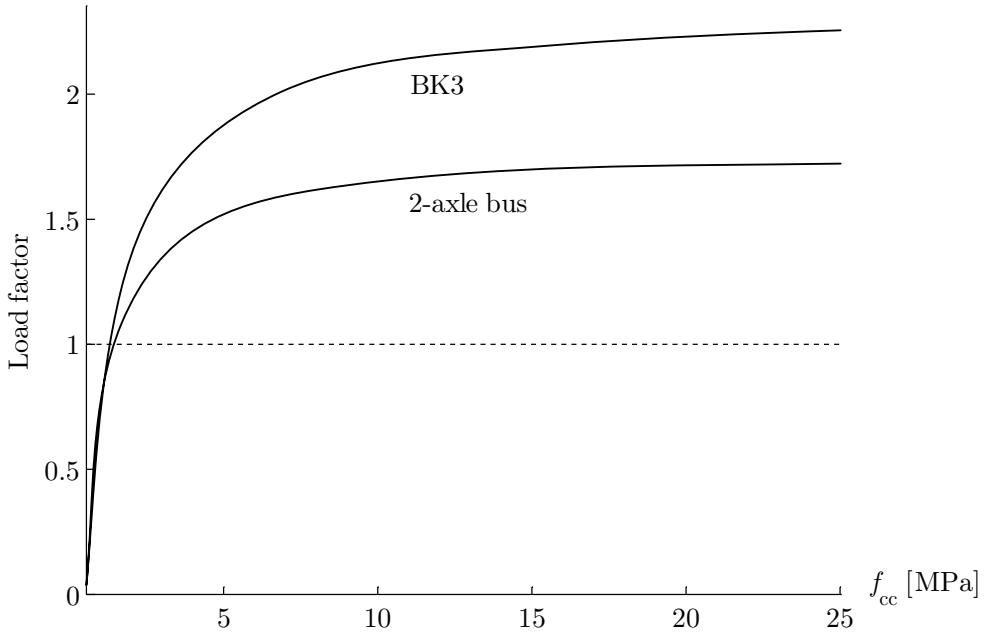

Figure 5.10: The load factor from the reference case as a function of the concrete compressive strength.

Figure 5.11 and Figure 5.12 show the load factor as a function of the concrete compressive strength. However, the values on the load factor axis are not shown. Instead, the positions that correspond to a load factor of 1.0 for different load types are marked. This makes it possible to see the concrete quality needed for different BK-classes. Figure 5.11 shows the quality needed for axle loads and Figure 5.12 shows the quality needed for bogie loads. Using the concrete compressive strength of 6.4 MPa, which was calculated from the core samples, gives a rather large margin to BK1 for both axle and bogie loads. Note that this is valid for the reference case only.

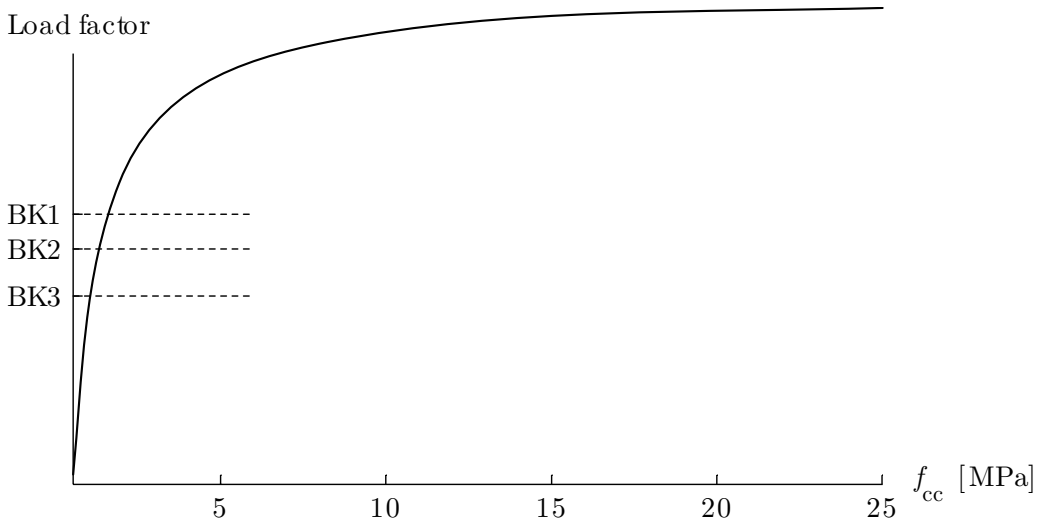

Figure 5.11: The concrete quality needed for different BK-classes when using an axle load.

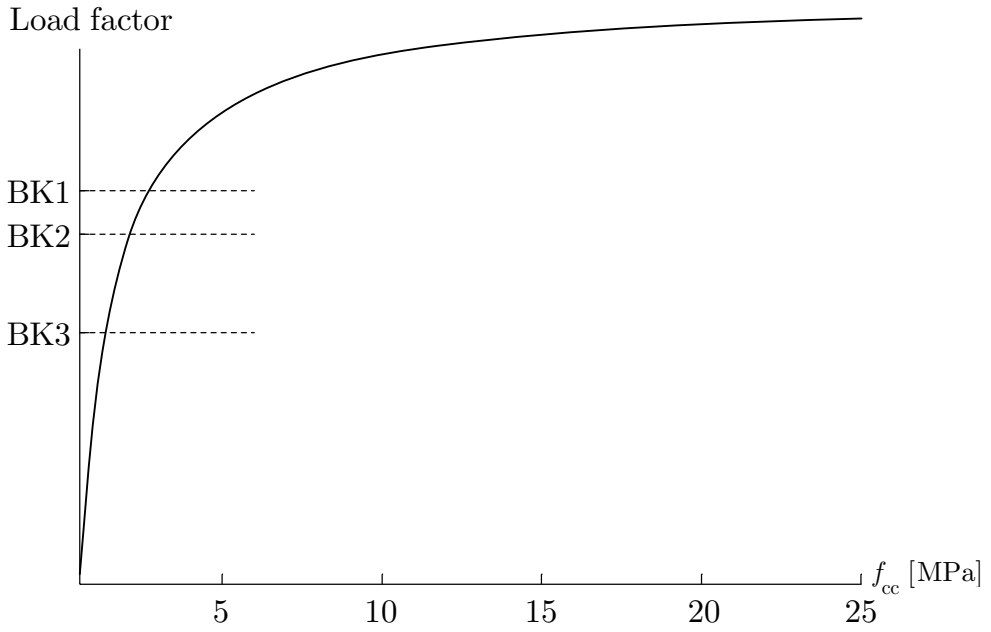

Figure 5.12: The concrete quality needed for different BK-classes when using a bogie load.

The compressive strengths needed for the different BK-classes for an axle load and a bogie load are given in Table 5.3.

Table 5.3: The compressive strengths needed for different BK-classes.

	BK3	BK2	BK1
Axle	1.1 MPa	1.4 MPa	1.6 MPa
Bogie	1.4 MPa	2.1 MPa	2.7 MPa

The positions for the different BK-classes in Figure 5.11 and Figure 5.12 are given in Table 5.4, calculated by dividing the pressures for BK2 and BK1 by the pressure for BK3. The single axle was considered as a driving axle. The bogie pressures used were for BK3 11.5 tonnes, for BK2 16 tonnes and for BK1 18 tonnes. These pressures were chosen because they together with their respective axle distances were found to be the design load case.

Table 5.4: Multipliers to find load factors 1.0 for different BK-classes.

	BK3	BK2	BK1
Axle	1.00	1.25	1.44
Bogie	1.00	1.39	1.57

Figure 5.13 shows the load factors as a function of the compressive strength in the arch. The load factors were calculated for both kinds of buses allowed on the bridge. The other parameters used were all according to the reference case, given in Table 5.1.

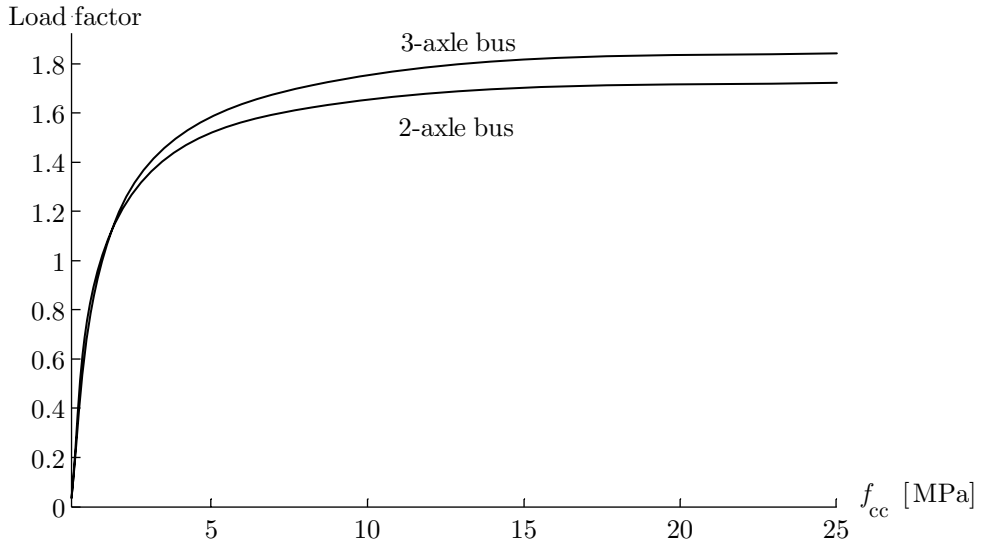

Figure 5.13: The concrete quality needed for different load factors for the two- and three-axle bus.

To visualize the behaviour of the arch when the bridge was loaded with deadweight, a stress analysis was performed. Figure 5.14 shows how the compressive stress varies along the arch calculated in ABAQUS. This can be compared with the stresses in Figure 5.15, which was calculated with Navier's formula using the arch section forces obtained from ABAQUS. Using the failure envelope model, the failure always occurred in the crown. This is also indicated by the figures below, which shows that the critical part of the arch is the crown.

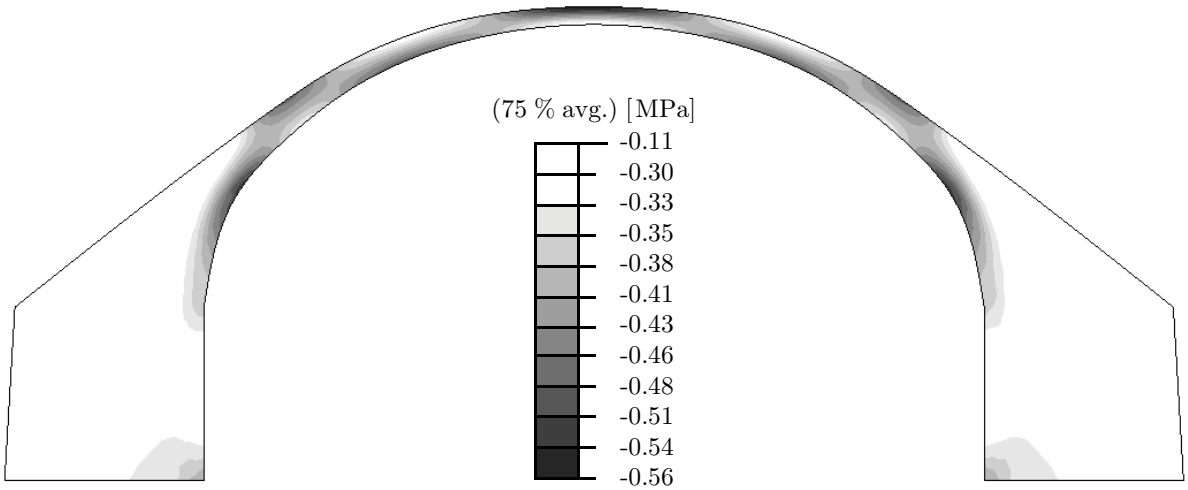

Figure 5.14: Principal compressive stress due to dead weight.

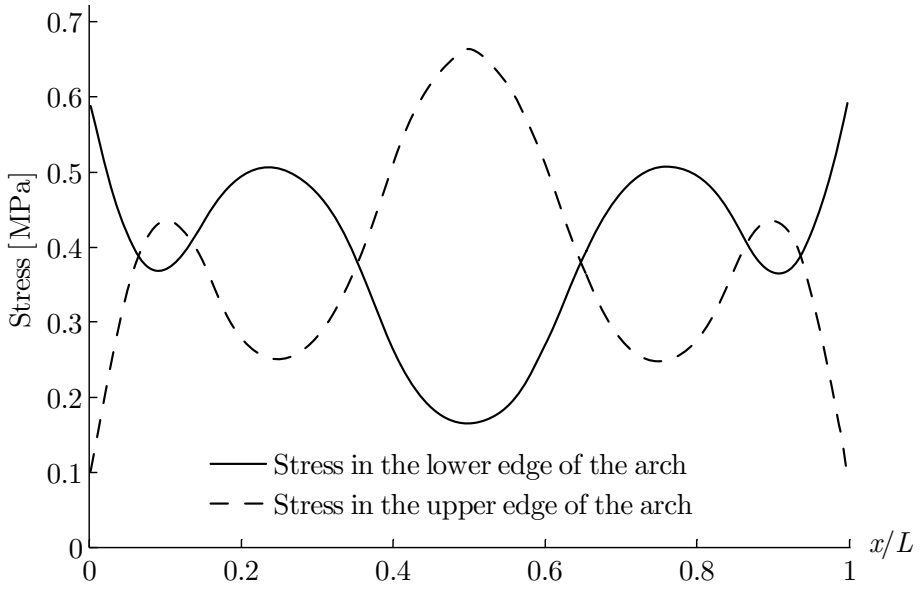

Figure 5.15: Compressive stress in the upper and lower edge of the arch due to deadweight.

5.4 Parametric survey

A survey was performed to investigate which parameters that influence the load carrying capacity the most. The considered parameters were the concrete compressive strength, the Young's modulus, the density and the Poisson's ratio. This was done for all four parts of the model. The survey was performed individually for the parameters, thus no correlation was considered. As for example, a higher compressive strength for the concrete would have resulted in a higher Young's modulus as shown in Figure 5.16. This was not taken into account. The parametric survey was performed with the design BK3 load. The load factors from the different parameters were compared with the reference case shown in Table 5.1.

The intervals of the studied parameters are shown in Table 5.5. The interval of the Poisson's ratio is the same for all parts.

The Young's modulus of the concrete was chosen to maximum 30 GPa since it seemed unlikely that the concrete would be of higher quality than C20/25 which corresponds to a Young's modulus of 30 GPa according to Boverket, 2004. The interval for the density of the concrete in the arch and abutments was chosen to include the density for unreinforced concrete as well as the density for reinforced concrete with some margin.

The interval for the Young's modulus of the backfill was chosen to 50-1000 MPa. Recommended values for sand and gravel are 50-500 MPa according to Flener, 2004. However, one extra unrealistically high value of 1000 MPa was chosen to see if the increase of the load factor diminishes.

The Young's modulus of the pavement can vary between 1-15 GPa, according to the Swedish Road Administration (Vägverket), depending on the temperature of the pavement. A reasonable value is 1 GPa which correspond to a temperature of 40 $^{\circ}$C,

because the pavement may reach this temperature during the summer. The pavement Poisson's ratio varies between 0.3-0.4 according to Huang, 2003. For this parameter survey, the interval was chosen to 0.1-0.4 to see if lower value would affect the load factor.

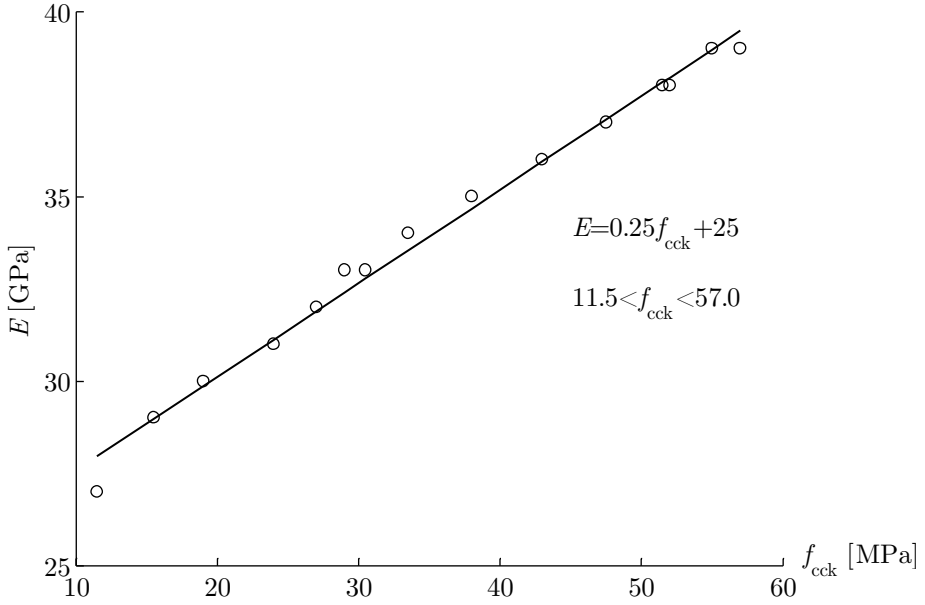

Figure 5.16: Relationship between the concrete compressive strength and the Young's modulus, according to BBK 04.

Table 5.5: Studied intervals in the parametric survey.

Studied intervals	Arch	Abutments	Backfill	Pavement
E – Young's modulus [GPa]	20-30	20-30	0.05-1	0.5-10
ρ - Density [kg/m^3]	2000-2600	2000-2600	1200-2200	1200-2000
ν - Poisson's ratio [-]	0.1-0.4	0.1-0.4	0.1-0.4	0.1-0.4
f_{cc} - Concrete compressive strength [MPa]	0.6-25	0.6-25	-	-

5.4.1 The backfill

As shown in Figure 5.17, the Young's modulus of the backfill had a very large influence on the load factor. With a higher stiffness in the backfill comes a wider load distribution. Hence, the point load does not affect the arch locally as much as if the fill has a lower stiffness. Due to elasticity, the fill has the ability to manage bending moment. With increased stiffness follows that the fill deals with a larger bending moment and therefore unloads the arch. A reasonable value for The Glomman Bridge is probably 200-400 MPa.

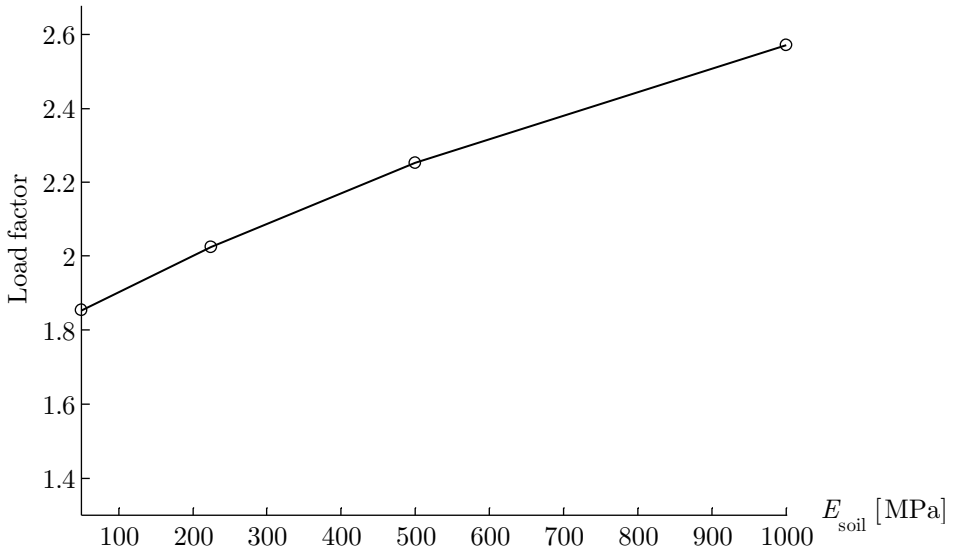

Figure 5.17: Load factor as a function of the Young's modulus in the backfill.

The effect of the Poisson's ratio for the backfill is shown in Figure 5.18. As seen in the figure, it has a large influence on the load factor. This is probably because an increased Poisson's ratio makes the coefficient for the horizontal passive earth pressure increase. Its importance may be exaggerated due to the tie constraints between the arch and the backfill, which lock the translations and rotations. A reasonable value of Poisson's ratio in the backfill is 0.2 – 0.3.

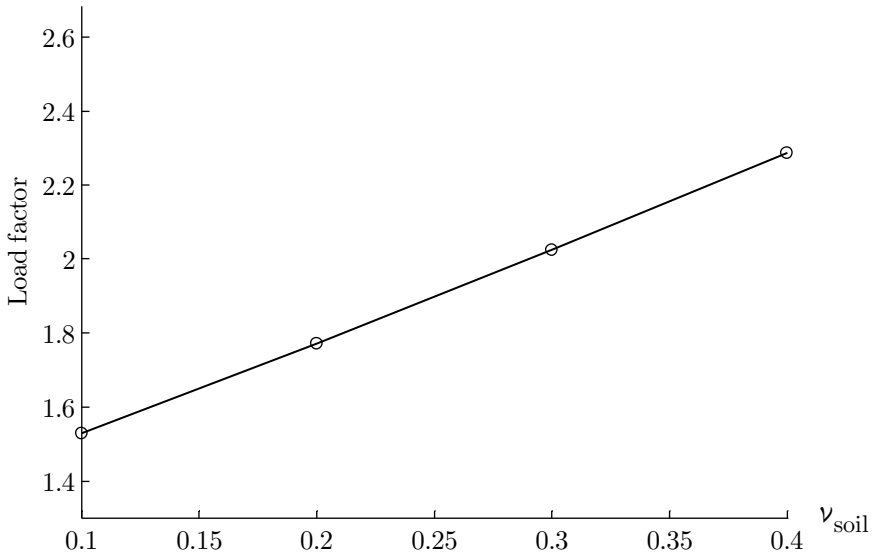

Figure 5.18: Load factor as a function of Poisson's ratio in the backfill.

The density of the backfill has a clear effect on the load factor as shown in Figure 5.19. As mentioned in Chapter 2.1, arch bridges have always been made heavy to increase the strength. The deadweight will mainly increase the normal force in the arch. Increasing the normal force will change the inclination of the load line in Figure 5.9. The load line will rotate counter-clockwise and the load factor will increase up to a certain point. A reasonable value should be 1800-2000 kg/m^3.

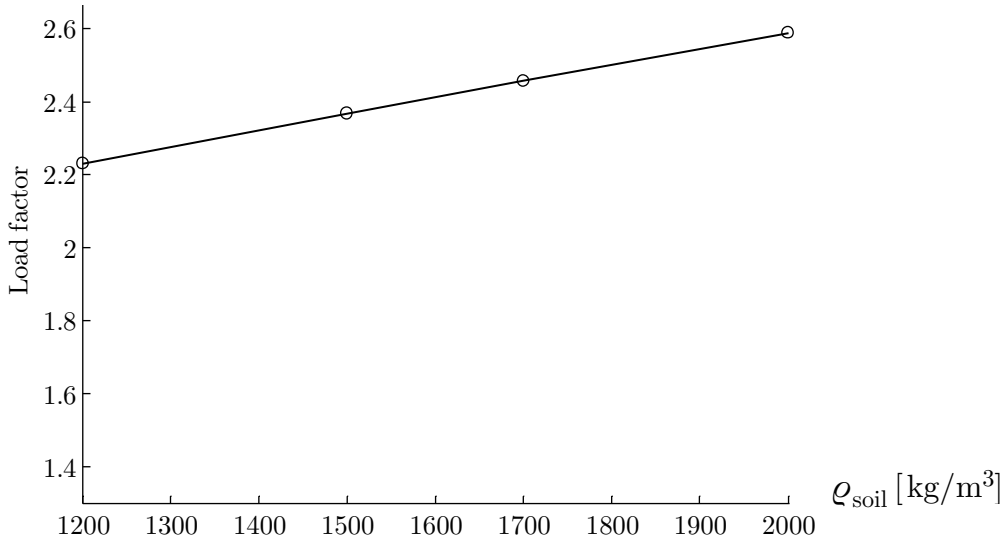

Figure 5.19: Load factor as a function of backfill density.

Figure 5.20 and Figure 5.21 show the effect of a non-resistant backfill. The curve for the resistant backfill was calculated by loading the arch with the backfill as an element. The curve for the non-resistant backfill was calculated by applying concentrated forces to the arch corresponding to the deadweight of the backfill. As seen in the figures the resistance of the fill has a minor effect on both the bending moment and the normal force. However, this is only valid for the deadweight. It is possible that the resistance of the backfill has a larger influence on the cross section forces when a live load is applied to the bridge.

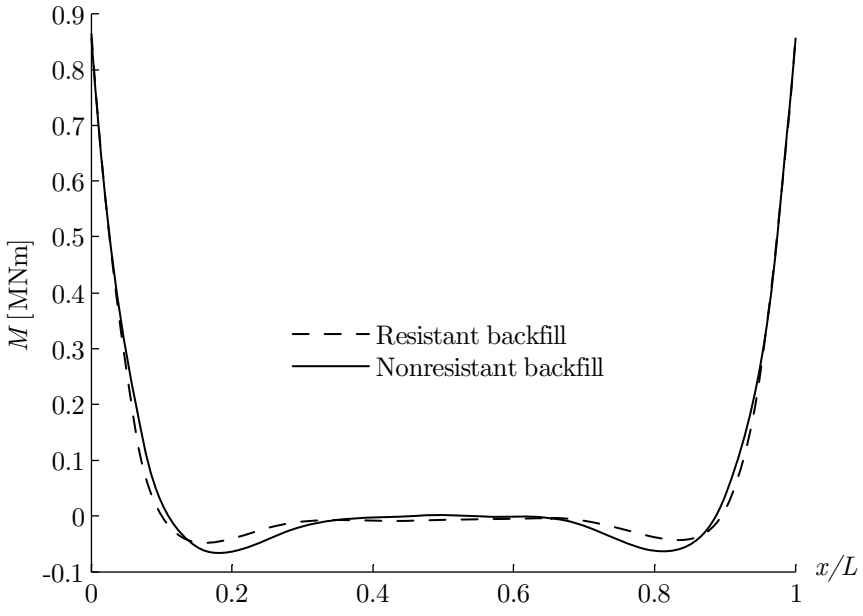

Figure 5.20: Bending moment in the arch due to deadweight.

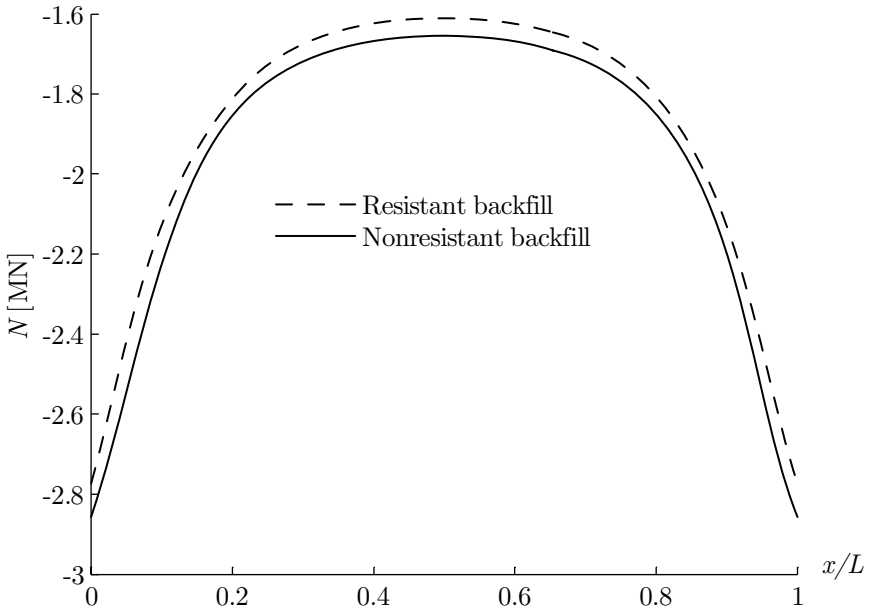

Figure 5.21: Normal force in the arch due to deadweight.

5.4.2 The pavement

Due to the shallow thickness of the pavement, the parameters have no significant effect on the load factor. The Poisson's ratio has no effect at all. The pavements contribution to the deadweight is so small compared to the backfill and arch, hence the density has negligible influence. The Young's modulus has the most effect. A higher stiffness in the pavement distributes the load better. However, the effect of the pavements stiffness is rather small even though the Young's modulus can vary between 1-15 GPa depending on the temperature of the pavement.

5.4.3 The arch

In this linear elastic model, the backfill can manage tensile forces and therefore moment. In this case, the arch and backfill cooperate to manage the moment. If a higher stiffness is applied to the arch, it will give a lower load factor as shown in Figure 5.22. This is because a higher stiffness in the arch exposes it to a higher bending moment and the backfill to a lower, without increasing the moment capacity. A reasonable value is 25-30 GPa.

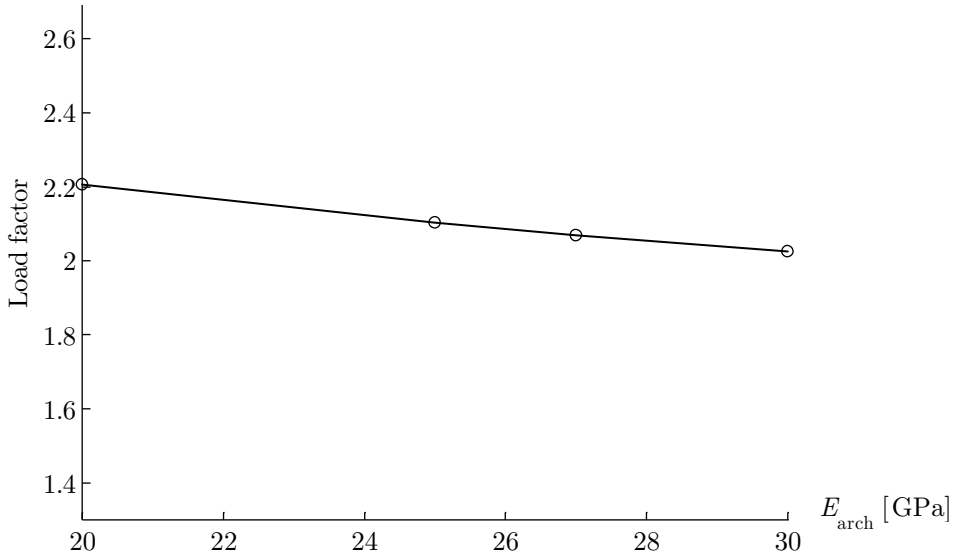

Figure 5.22: The load factor as a function of the Young's modulus for the arch.

The Poisson's ratio for the arch has no effect on the load factor. When increasing the density of the arch, the load factor increases as seen in Figure 5.23. This is the same effect as the increased density of the fill. The increased deadweight rotates the load line counter-clockwise and increases the load factor.

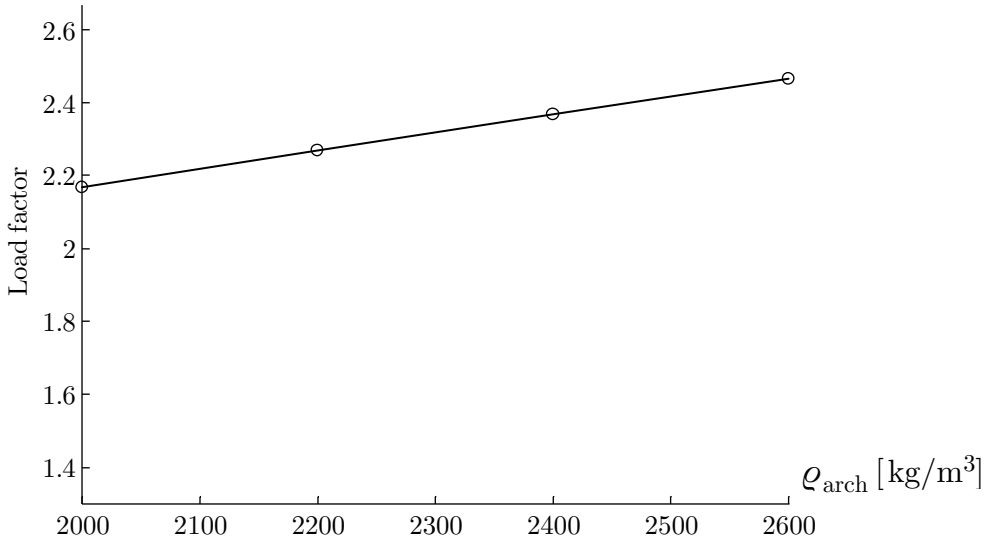

Figure 5.23: The load factor as a function of the density of the arch.

5.4.4 The abutments

The parameters for the abutments has very little or no effect on the load factor. In this model, the abutments were assumed fixed due to the presumed high density of the abutments together with the earth pressure, which would counteract the movement of the abutments. The Young's modulus affects the degree of restraint in the springing by making it harder for the rigid beam, mentioned in Chapter 4.2, to deform the abutments.

5.4.5 Restraint of the springing

Hinges were inserted in the springing to examine how the degree of restraint influenced the load factor. Figure 5.24 and Figure 5.25 shows the bending moment and normal force in the arch due to deadweight with and without hinges in the springing. The hinges were made with a coupling constraint between the arch and the rigid beam. The coupling had locked translational degrees of freedom and free rotational degrees of freedom. As seen in Figure 5.24 there is some moment in the springing for the case with hinges. This is particularly odd, because it should of course be zero. This was probably caused by some numerical inaccuracy of the model.

In the case of hinges, a load factor of 2.44 was calculated. The corresponding load factor without hinges was calculated to 2.37. The critical load case was when the load was placed in the crown. That was also where the failure appeared. As seen in Figure 5.24 and Figure 5.25, the hinges do not influence the moment and normal force due to deadweight very much in the crown. In Figure 5.26, the influence for moment in the crown is shown with and without hinges. As seen, the difference is rather small between the lines, which show that the moment and normal force in the crown due to a moving load is affected very little by hinges in the springing. This makes it possible to draw the conclusion that the degree of restraint in the springing has very little influence on the load carrying capacity of the bridge.

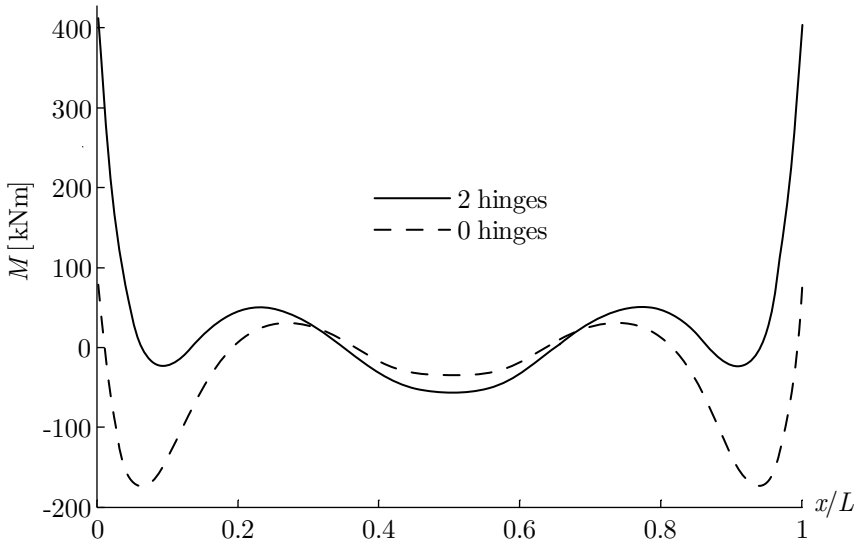

Figure 5.24: Bending moment in the arch, with and without hinges in the springing, due to deadweight.

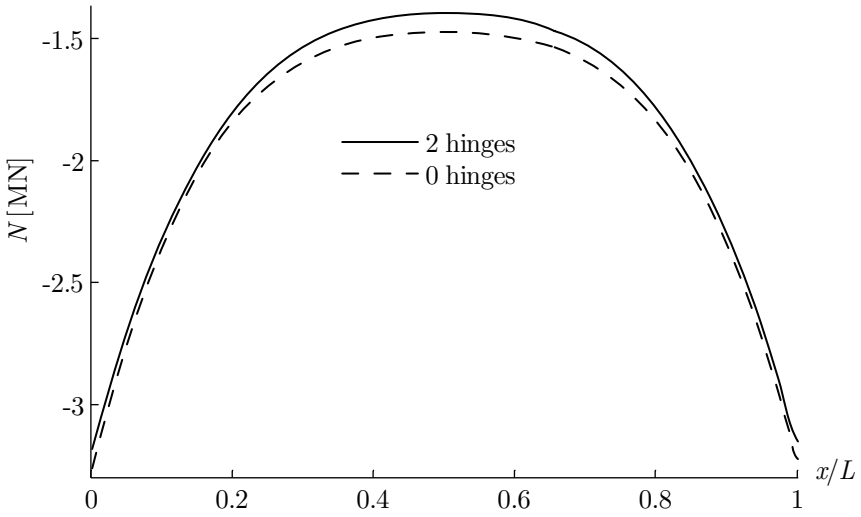

Figure 5.25: Normal force in the arch, with and without hinges in the springing, due to deadweight.

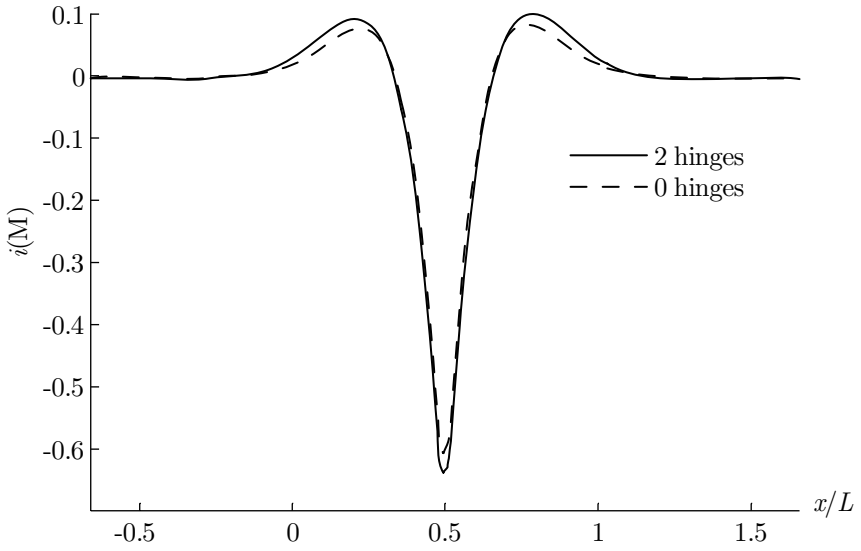

Figure 5.26: Influence lines for moment in the crown with and without hinges in springing.

5.5 Worst-case scenario

In Table 5.6, the parameter values were chosen to give as large negative effect on the load factor as possible, within reasonable limits. These values are probably overestimated. For example, the density of unreinforced concrete is well known as 2200 kg/m^3 and would be even higher with rocks embedded. Since the Poisson's ratio of the pavement does not affect the load factor, it can be set to any value between 0.1-0.4. Neither does the pavement density have any effect, thus was the density set to its reference value. Even though the values were overestimated, it gave a picture of how bad the conditions could be for the bridge to still carry some load. When the bridge was loaded with a BK3 bogie, it needed a minimum concrete compressive strength of

2.3 MPa to give a load factor of 1.0. For a two-axle bus, the load factor will not reach a value of 1.0 for any concrete compressive strength, as shown in Figure 5.27.

Table 5.6: Values for the parameters that gave a BK3 bogie load factor of 1.0.

Worst-case scenario	Arch	Abutments	Backfill	Pavement
E - Young's modulus [GPa]	30	25	0.05	0.5
ρ - Density [kg/m^3]	2000	2000	1200	1200
ν - Poisson's ratio [-]	0.1	0.1	0.1	0.3

Provided that the concrete compressive strength is set to 6.4 MPa, a maximum axle- and bogie load could be calculated by multiplying the given load factors from Figure 5.27 with the used pressures from Table 4.3 and Table 4.4. The load factors for the axle- and bogie load were both found to be 1.3. That gave the maximum axle- and bogie load, 1.3·8 tonnes=10.4 tonnes and 1.3·11.5 tonnes=15.0 tonnes corresponding to 102 kN and 147 kN respectively.

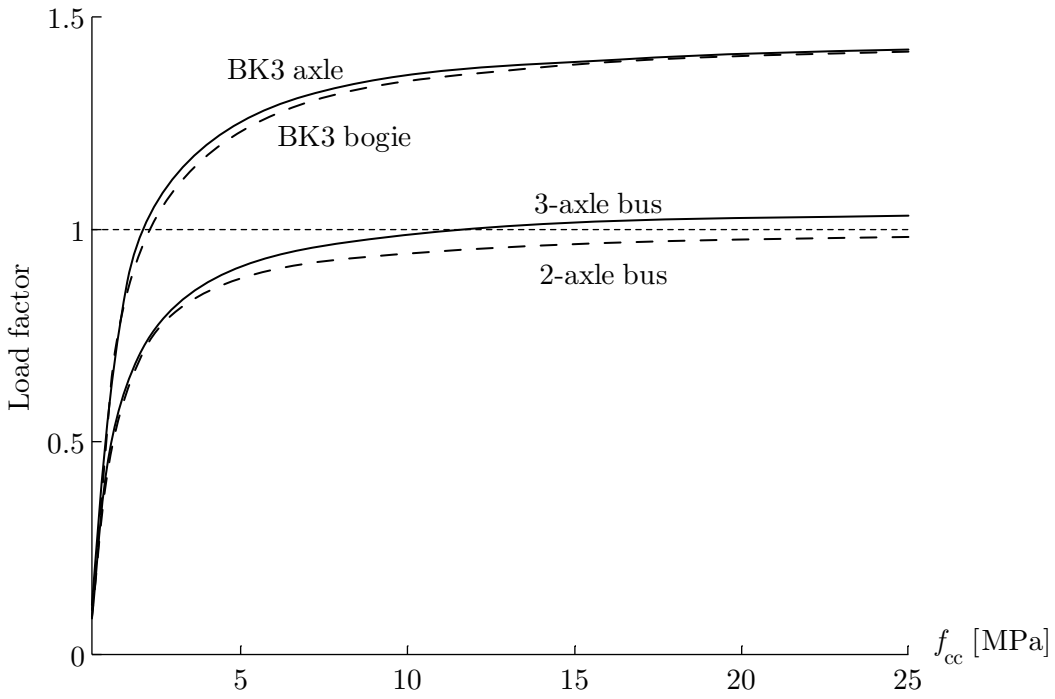

Figure 5.27 The load factor for the worst-case scenario.

In reality, the two-axle bus is allowed to pass over the bridge. This means that the bridge cannot be as poor as in the worst-case showed in Table 5.6. However, the curves in Figure 5.27 were calculated including partial coefficients for the safety class and uncertainties in the material. This, together with the overestimated poorness of the values for the parameters makes it possible for the bridge to resist a higher load than the calculations show.

5.6 Comparison with results from Reinertsen

According to Reinertsen, 2006, the maximum loads on an axle and bogie were calculated to be 108 kN and 152 kN respectively. These values can be compared to the results calculated in the worst-case scenario in Chapter 5.5, 102 kN and 147 kN. The method using the failure envelope thus gives almost the same results when using the least favourable parameters. When using the parameters from the reference case the corresponding maximum loads are 181 kN and 226 kN respectively, thus 30-40% higher than the results in Reinertsen, 2006. The parameters in the reference case should not be seen as a fact. They are most likely more similar to the actual bridge than the worst-case scenario though. A difference between the studied method and the method used in Reinertsen, 2006 is that the latter uses a three-dimensional model. However, the major difference between the methods is the failure mode. The failure criteria used in Reinertsen, 2006 is that the concrete arch collapses as soon as the tensile stress in one cross section exceeds its tensile strength or half of its tensile strength, depending on which restrictions that are used. The failure criteria used in this study was that failure occurred when the eccentric normal force did not manage to balance the bending moment.

5.7 The Prestwood Bridge

The Prestwood Bridge is a single span masonry arch bridge with backfill, located in the United Kingdom. It has a span length of 6.55 m, a rise of 1.43 m, a fill depth of 0.16 m and a constant arch thickness of 0.22 m. The bridge has been subject to an experimental test where it was loaded to collapse. In the experiment, the load was applied in the quarter point on the entire width of the bridge and on a length of 0.3 m. The collapse load from the experiment was $P_{\text{exp}} = 228$ kN.

A finite element model of the Prestwood Bridge was created. The model shown in Figure 5.28 is rather similar to the model of the Glomman Bridge. It is a linear elastic two-dimensional model, which consists of three parts, arch, backfill and a rigid plate. The arch and rigid plate consist of 2D beam elements while the backfill consist of 2D solid plane stress elements. Between the parts, there were tie constraints with locked translational and rotational degrees of freedom. The boundary conditions were roller bearings both vertically and horizontally for the soil and rigid restraint for the arch. The load was applied on the rigid plate to simulate the experimental test. The material properties shown in Table 5.7 were chosen according to Cavicchi and Gambarotta, 2004.

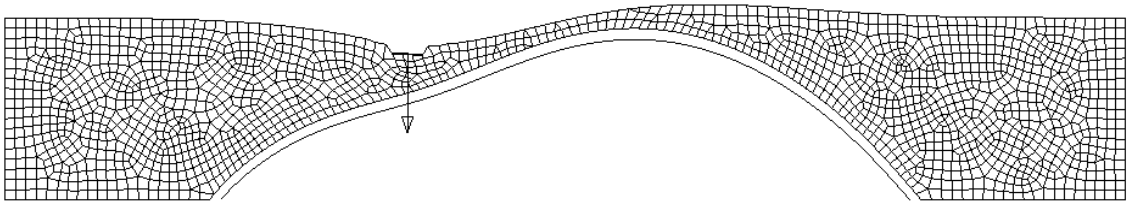

Figure 5.28: FE-model of the Prestwood Bridge. The load was applied to the rigid plate.

Table 5.7: Material properties for the Prestwood Bridge.

Material properties	Arch	Backfill
E - Young's modulus [GPa]	15	0.3
ρ - Density [kg/m^3]	2000	2000
ν - Poisson's ratio [-]	0.3	0.3
f_{cc} - Concrete compressive strength [MPa]	4.5	-

The failure envelope for the Prestwood Bridge is shown in Figure 5.29. As seen in the figure, the critical design load for the Prestwood Bridge, using the parameters shown in the table above, is 136 kN. This correspond to 60% of the experimental value, which is comparable to Cavicchi and Gambarotta, 2004, where a cohesion for the fill of 1 kPa resulted in a critical design load of 149 kN or 65% of the experimental load.

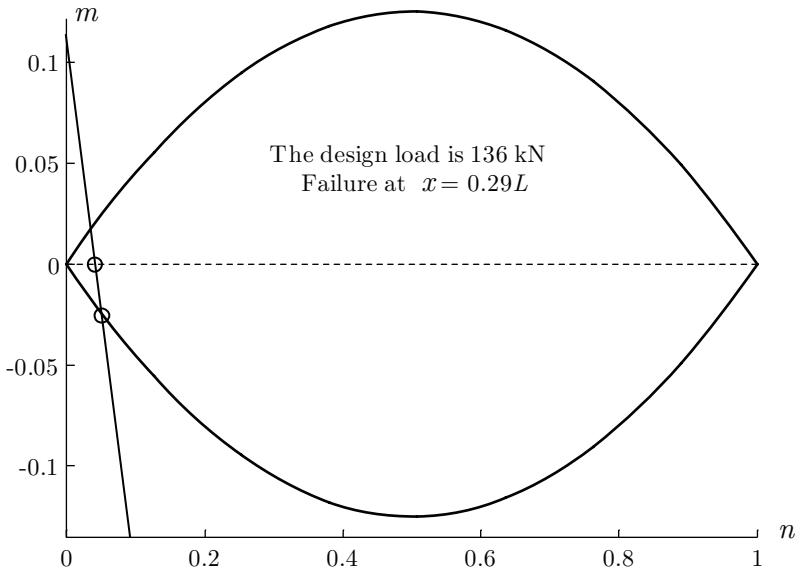

Figure 5.29: Failure envelope, showing the design load for the Prestwood Bridge.

A small parameter survey was performed for the Prestwood Bridge where the Young's modulus for the fill and the concrete compressive strength was studied. These parameters were chosen because they were found to have a large influence on the load factor of the Glomman Bridge. In addition, only one parameter at the time was changed. As shown in Figure 5.30, the Young's modulus for the fill has a clear effect on the load factor. The critical design load will not reach higher than 145 kN for any concrete compressive strength, as shown in Figure 5.31.

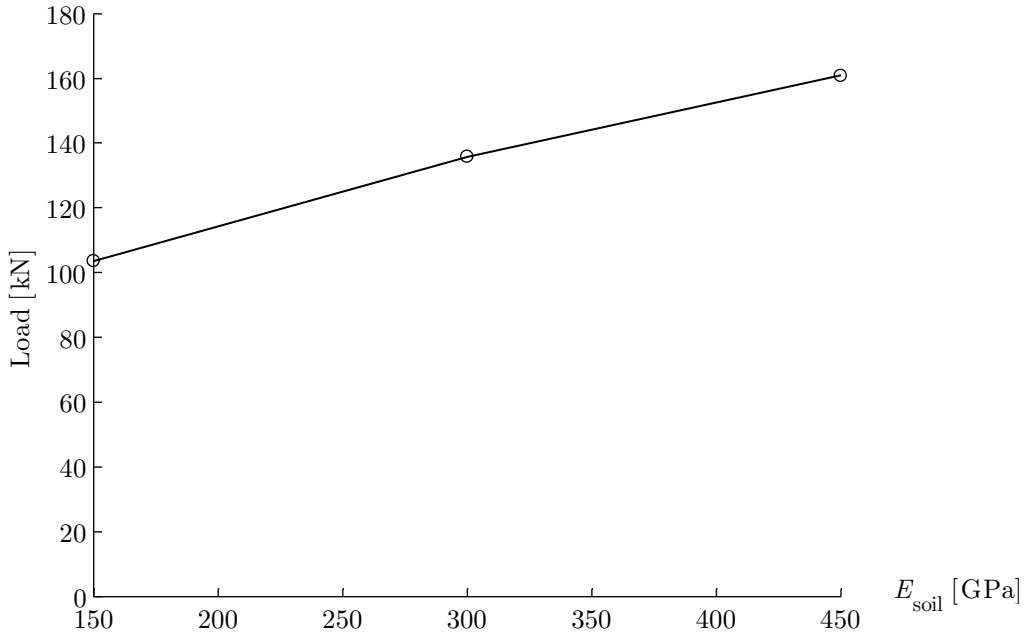

Figure 5.30: Load factor as a function of the Young's modulus for the fill.

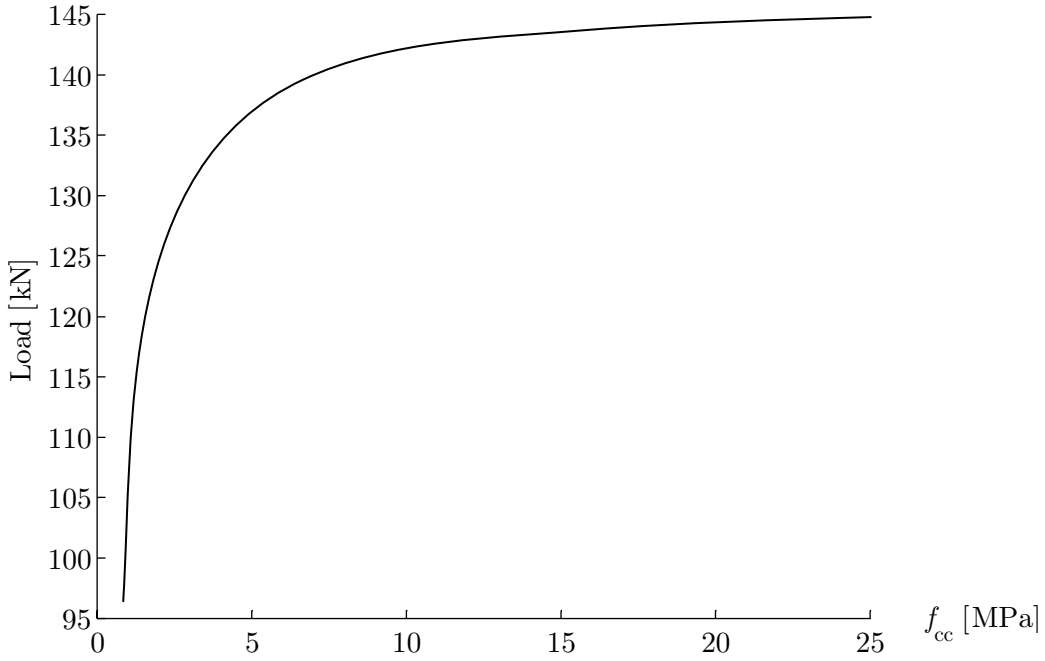

Figure 5.31: Load factor as a function of the concrete compressive strength.

5.8 Analysis using RING 2.0

An analysis using the commercial software RING 2.0 was performed for both the Glomman Bridge and the Prestwood Bridge. This was done in order to compare the failure envelope model to an alternative model. The complete reports from the RING-analyses are presented in Appendix B.

5.8.1 The Glomman Bridge

The bridge was modelled with a span of 17.27 m, a rise of 3.95 m and a fill depth of 0.40 m. The arch ring was modelled as bonded brick consisting of 40 units as seen in Figure 5.32. The model was simplified by having a horizontal carriageway at the level of the backfill upper edge in the crown. The real bridge has a lower carriageway in the abutments and a crest in the crown. This is probably a negligible simplification because it gives a larger fill height outside the arch. Another simplification in the model was that the arch thickness varied linearly between the springing and the crown. In reality, the thickness variation is almost identical to a Strassner arch. A movable load was run along the bridge to find the worst load factor and load position.

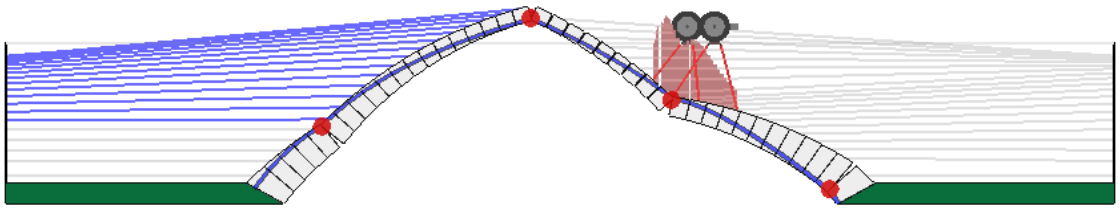

Figure 5.32: Model of the Glomman Bridge in RING 2.0.

The analysis was performed with the parameters shown in Table 5.8, which corresponds to the parameters in the reference case in Chapter 5.3. As seen in the table, the Young's modulus and Poisson's ratio are not used in the program. The cohesion was found to have a marginal influence on the load factor.

Table 5.8: Parameters used for the Glomman Bridge.

Material properties	Arch	Backfill
E - Young's modulus [GPa]	-	-
ρ - Density [kg/m^3]	2400	1500
ν - Poisson's ratio [-]	-	-
f_{cc} - Concrete compressive strength [MPa]	6.4	-
Friction coefficient	0.6	0.6
Angle of internal friction	-	37
Cohesion	-	0

Using the parameters in the table above, the load factors in Table 5.9 were obtained. As seen in the table, the critical design load is the three-axle bus. The minimum load factor was obtained when the bus was positioned so that the rear axle alone stood on the bridge. For all load types, failure occurred in the quarter point of the arch.

Table 5.9: Load factors for the reference case computed with RING 2.0.

Load type	Load factor	Load position
BK3 Bogie	7.0	Quarter point
BK3 Axle	9.4	Quarter point
Bus 3-axles	6.3	Quarter point
Bus 2-axles	6.5	Quarter point

A small parametric survey, shown in Figure 5.33, was performed for the concrete compressive strength and the horizontal earth pressure. The survey was done for the BK3 bogie load. The horizontal earth pressure increased the load factor by approximately 0.5 for the concrete compressive strength 6.4 MPa.

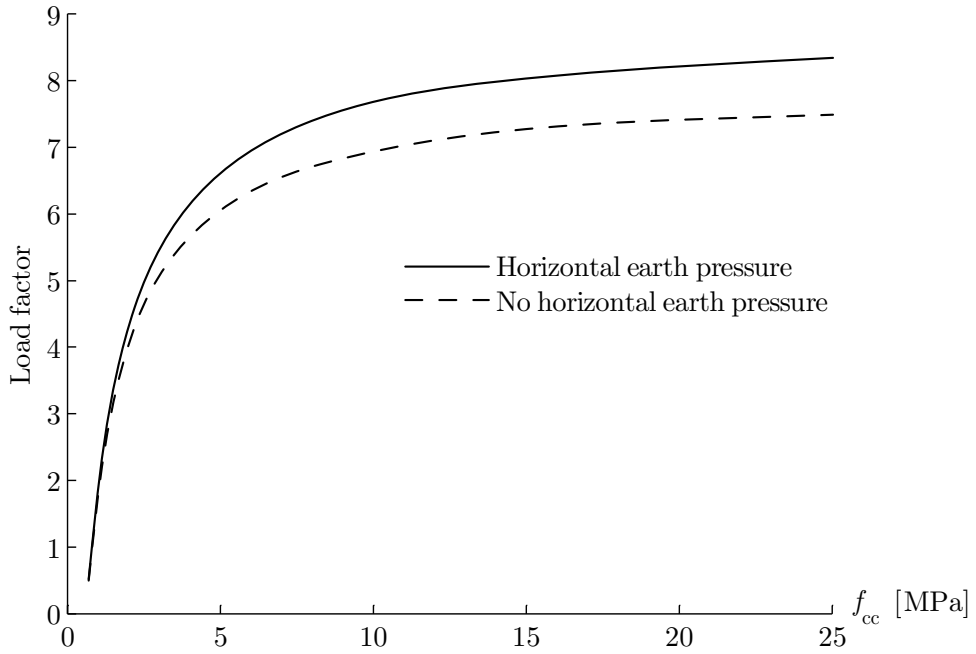

Figure 5.33: The load factor for the Glomman Bridge as a function of concrete compressive strength, with and without horizontal earth pressure.

5.8.2 The Prestwood Bridge

The Prestwood Bridge was modelled with a span length of 6.55 m, a rise of 1.43 m and a fill depth of 0.16 m. The arch ring was modelled as bonded brick with 50 units, as seen in Figure 5.34, having a constant thickness of 0.22 m. The load was applied in the quarter point of the bridge.

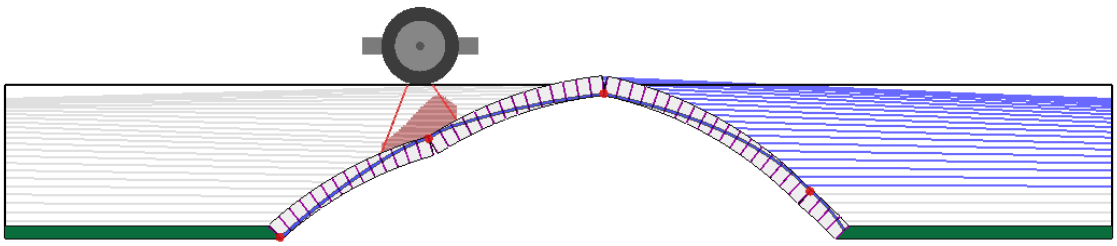

Figure 5.34: Model of the Prestwood Bridge in RING 2.0.

The analysis was performed with the parameters in Table 5.10. The parameters were chosen according to Cavicchi and Gambarotta, 2004.

Table 5.10: Material properties for the Prestwood Bridge.

Material properties	Arch	Backfill
E - Young's modulus [GPa]	-	-
ρ - Density [kg/m^3]	2000	2000
ν - Poisson's ratio [-]	-	-
f_{cc} - Concrete compressive strength [MPa]	4.5	-
Friction coefficient	0.6	0.6
Angle of internal friction	-	37
Cohesion	-	10

Using the parameters in the table above gives a critical design load of 152 kN which corresponds to 67% of the experimental collapse load.

A similar parametric survey that was performed in the previous chapter was also done for the Prestwood Bridge, shown in Figure 5.35. As seen in the figure, the horizontal earth pressure has a major effect on the critical design load.

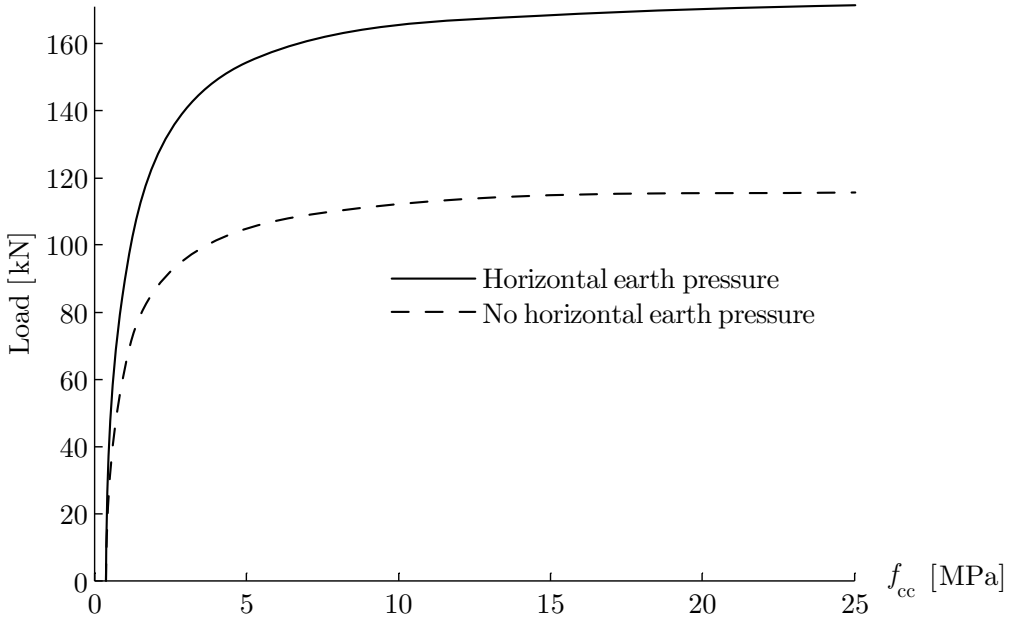

Figure 5.35: Load factor as a function of concrete compressive strength, with and without horizontal earth pressure.

5.9 Comparison between the studied model and RING 2.0

5.9.1 The Glomman Bridge

RING 2.0 gives a design load factor of 6.3 for the three-axle bus while the failure envelope method gives a design load factor of 1.6 for the two-axle bus. Hence, RING 2.0 gives a load factor, which is four times the load factor obtained from the failure envelope. Part of this difference may be because RING 2.0 considers that the arch has to form a mechanism with four hinges to collapse. The studied method assumes that the bridge collapse when one hinge has appeared. When using RING 2.0, failure occurred in the quarter point when the load was positioned in the quarter point. Using the failure envelope model, the failure occurred in the crown when the load was positioned in the crown. One reason for this change of critical load position may be the peak in the influence line for the normal force, mentioned in Chapter 5.2. This peak grows larger in magnitude closer to the crown and therefore the decrease in normal force is larger in the crown than in the quarter point.

5.9.2 The Prestwood Bridge

The critical design load for the Prestwood Bridge using the failure envelope model was 137 kN which corresponds to 60% of the experimental collapse load. When RING 2.0 was used, a critical design load of 152 kN was obtained, which corresponds to 67% of the experimental collapse load. This can be compared with the critical design load of 149 kN, or 65% of the experimental collapse load, for the cohesion of 1 kPa according to Cavicchi and Gambarotta, 2004.

The results for the Prestwood Bridge from the two different methods correspond better than the different results for the Glomman Bridge. This is probably because the load is fixed in the Prestwood Bridge. Therefore, no influence lines needs to be used and the peak in the influence lines for the normal force, which appears for the Glomman Bridge, does not affect the result. The difference between 60% from the failure envelope and 67% from RING 2.0 may be explained by the mechanism failure mode in RING 2.0.

Chapter 6

Discussion and conclusions

6.1 Factors of uncertainty

Due to the considerable high age of the bridge, the uncertainties in material data and functionality are very large.

In this thesis, the arch was analysed as comparable to a concrete arch. It is however shown in Figure 3.10 that the arch consists of large plums. It seems like the design drawing gives a rather good view over the content of the arch, see Figure 3.3. If the entire arch consists of these large plums, it may seem like a rough estimation to compare it with concrete. However, the compressive strength of the arch should increase due to the higher compressive strength of the plums. The most critical sections in the arch should then be the joints between the plums, spaced irregularly along the arch.

When Grontmij AB, formerly known as Carl Bro AB, performed the concrete inspection, all of the core samples were taken from a rather small area. According to Figure 3.6 the highest point from where a sample was taken, was 1.70 m. The samples covered almost the entire width of the bridge, but were only taken at the abutments. Some samples should have been taken from a higher point in the arch since the largest uncertainties is about the arch. To get more data and to determine if the concrete has the same quality in the entire arch, the tests should be completed with some core samples taken higher in the arch. Convenience could be a possible explanation why the samples were taken from the lower part of the arch; it might take a lot of time to arrange a way to reach the higher parts of the arch from below. Another possible explanation could be that the train services would have been interrupted.

When the load combination routines were created, the number of studied cases was limited to four, see Chapter 4.3. It would of course be better to study every single load position for every element. However, during the development of this thesis, the routines have been run through hundreds of times and such an alternative would have been too time-consuming. The four examined cases should however cover some of the worst cases. For each element only one bending moment and one normal force was stored as the least favourable cross section forces, regarding only the traffic load. Not until these forces caused by the traffic were compared to the forces caused by the deadweight could the load factors be calculated. As an example, the reference case

could be mentioned. When the two-axle bus was run along the bridge, the largest value for each element was stored in a matrix. The values for the different elements were then compared and element no. 101 was found to have the largest value from the traffic load. When the forces were put into the failure envelope and compared to the forces caused by the deadweight, element no.108 was found to cause the failure.

The standardized pressures on the bogie axles vary with the axle distance according to Boverket, 2004. The shortest axle distance in a bogie must be longer than the diameter of the tires. Vehicles heavy enough to need a bogie generally have large tires. The question is how small the tires in a bogie can be. The standardization does not say anything about the shortest axle distance. Because there is a standardized pressure for axle distances shorter than 1.0 m, the shortest axle distance in this thesis was set to 0.8 m. The shortest distance is rather important to consider because the shorter the distance is set, the larger the influence will be, compare with Figure 5.7. The bridge was also tested with a shortest axle distance of 1.0 m of the bogie. The routine in MATLAB was run with different compressive strengths of the concrete. The result showed that a longer axle distance gave a much higher load factor than with the shorter axle distance. The load factor in this case was even higher than the one from the single axle load.

The largest negative bending moment and adherent normal force were the design case for every single run. The largest negative value for the bending moment was found and then the adherent normal force with the load in the same position. When examining e.g. the two-axle bus, the rear axle hits the peak in the normal force diagram, which causes MATLAB to use this lower normal force. Inside the failure envelope, a lower normal force from the traffic load will cause a steeper load line, which in its turn will cause a lower load factor. This error thus underestimates the carrying capacity and is therefore on the safe side. The largest risk with this peak is if the crown becomes the dimensioning cross section due to a much lower normal force instead of another section, which maybe in reality is the most critical.

In this thesis, no attention has been paid to a possible correlation between the input parameters, they were only changed individually. This was done to limit the calculation time. To make conclusions concerning correlation effects would require much more work in both ABAQUS and MATLAB. A known correlation effect is the one between the concrete compressive strength and the Young's modulus, that has an almost linear relation, as seen in Figure 5.16.

A good examination of the condition of the bridge has not been made. Even if not every damage separately seems that serious, maybe they all together could cause grave degradation.

6.2 Discussion of the obtained results

The results in this thesis show that the design load type is the two-axle bus. That the bridge can manage the two-axle bus is also evident, knowing that the same is passing the bridge today. It may then seem a bit odd to limit the weight of the allowed vehicles to 3.5 tonnes. The design axle distance for the largest negative moment was either 0.8 m or 1.0 m in every case, depending on which influence line that was studied. The

corresponding pressures on the bogie for a BK3 load are then 11.5 tonnes and 12.0 tonnes respectively. In the case with the two-axle bus, the pressure on the rear axle is 11.29 tonnes, a pressure almost equal to the total bogie pressure that is. It seems like loads classified as BK3 could be allowed when this load type in each case had a higher load factor than the two-axle bus. Problems concerning fatigue would though need further investigation.

The calculated maximum axle- and bogie pressures are 102 kN and 147 kN respectively. The worst conceivable parameters, see Table 5.6, were used when calculating the maximum pressure. These values were determined with a compressive strength of the concrete of 6.4 MPa, the strength that was calculated from the core samples in Chapter 3.4.

The most important part of the bridge is the backfill. Depending on which modulus of elasticity that is chosen, widely differing load factors are obtained. What seems to have a greater effect on the load factor is the choice of the Poisson's ratio. The interval used in Figure 5.18 is though unrealistic when in fact the Poisson's ratio has a rather narrow span of variation.

The accuracy of the results from this work can be discussed since the comparison between the studied method and RING 2.0 shows a large difference in the results for the Glomman Bridge. RING 2.0 gives a load factor four times the load factor from the failure envelope model. The results calculated in RING 2.0 seem rather unrealistic when it would mean that the Glomman Bridge would manage the load of six two-axle buses. An important difference between the two methods is that RING 2.0 allows further loading until a fourth hinge occurs while the failure envelope model gives the load factor when the first hinge is developed.

6.3 Further research

A suitable continuation to the work carried out within this thesis would be to create a three-dimensional model of the Glomman Bridge. The spandrels could then be considered in a way that was not possible with the two-dimensional model used in this thesis. As discussed in Chapter 3.2, there is some uncertainty regarding the effect of the spandrels regarding the load capacity of the bridge. The spandrels would probably have a strengthening effect on the bridge and therefore increase the load factor. However, they would also increase the deadweight, which would have an uncertain effect on the load factor and therefore need further investigation.

To use non-linear FEM would probably give a model that resembles more of the real bridge. The model described in this work does not use any friction between the backfill and the concrete arch, which of course is the case in reality. The linear elastic model in this thesis allows the backfill to manage tensile forces, which is unrealistic.

Further analyses may concern effects of the passive earth pressure. In this thesis, the earth pressure was considered by modelling the fill as an elastic medium in the FE-model.

Bibliography

Betti, M., Drosopoulos, G. A. and Stavroulakis, G. E., 2008. Two non-linear finite element models developed for the assessment of failure of masonry arches. *Comptes Rendus Mechanique, Vol. 336, pp. 42-53.*

Boverket (The National Board of Housing, Building and Planning), 1994. Dimensionering genom provning (handbook).

Boverket (The National Board of Housing, Building and Planning), 2004. Boverkets handbok om betongkonstruktioner, BBK 04.

Cavicchi, A. and Gambarotta, L., 2004. Collapse analysis of masonry bridges taking into account arch-fill interaction. *Engineering Structures, Vol. 27, pp. 605-615.*

Cernica, J. N., 1995. Geotechnical Engineering Soil Mechanics. *John Wiley & Sons, Inc, USA.*

Flener, E., 2004 Soil-Structure Interaction for Integral Bridges and Culverts. *Bulletin 74, Licentiate Thesis in Structural Design and Bridges, the Royal Institute of Technology (KTH).*

GeotechniCAL, http://environment.uwe.ac.uk/geocal/geoweb.htm

Holmgren, J., Lagerblad, B., and Westerberg, B., 2007. Reinforced Concrete Structures. *Compendium on reinforced concrete. Report 115, the Royal Institute of Technology, division of Concrete Structures.*

Howe, M. A., 1897. A Treatise on Arches. *John Wiley & Sons, New York.*

Huang, Y. H., 2003. Pavement Analysis and Design. *Prentice Hall, 2^{nd} edition.*

LimitState Ltd, 2007. Theory & Modelling Guide, Version 2.0h. *User manual for the Ring 2.0 software, LimitState Ltd, Sheffield, U.K.*

Reinertsen, 2006. Klassningsberäkning av vägbro vid Glomman. *Dokument nr. 21000990-01, uppdrag åt Banverket Östra Banregionen.*

Sowden, A.M., 1990. The Maintenance of Brick and Stone Masonry Structures. *Taylor & Francis.*

Sundquist, H., 2007. Arch Structures. *Compendium on structural design of bridges. Report 107, the Royal Institute of Technology, division of Structural Design and bridges.*

Sustainable Bridges, http://www.sustainablebridges.net

Trafikförordningen, 1998. 1998:1276, Sveriges Rikes Lag (Swedish Law).

Vägverket (Swedish Road Administration), 1998. Publ. 1998:78 Klassningsberäkningar av vägbroar.

Appendix A

Evaluation of concrete strength

A.1 Dimensionering genom provning

Six core samples

$$x := \begin{pmatrix} 23.0 \\ 45.0 \\ 20.5 \\ 16.0 \\ 13.5 \\ 25.0 \end{pmatrix} \cdot MPa$$

$$n := \text{length}(x)$$

$$x_{mean} := \frac{\sum_{i=1}^{n} x_i}{n}$$

$$x_{mean} = 23.8\ MPa$$

$$s := \sqrt{\frac{\sum_{i=1}^{n} (x_i - x_{mean})^2}{n-1}}$$

$$s = 11.2\ MPa$$

$$V := \frac{s}{x_{mean}}$$

$$k_{pn} := 2.33$$

$$x_{k1} := x_{mean} \cdot (1 - k_{pn} \cdot V)$$

$$x_{k1} = -2.3\ MPa$$

Four core samples

$$x_2 := \begin{pmatrix} 23.0 \\ 20.5 \\ 16.0 \\ 25.0 \end{pmatrix} \cdot MPa$$

$$n_2 := \text{length}(x_2)$$

$$x_{2.mean} := \frac{\sum_{i=1}^{n_2} x2_i}{n_2}$$

$$x_{2.mean} = 21.1\ MPa$$

$$s_2 := \sqrt{\frac{\sum_{i=1}^{n_2} (x2_i - x_{2.mean})^2}{n_2 - 1}}$$

$$s_2 = 3.9\ MPa$$

$$V_2 := \frac{s_2}{x_{2.mean}}$$

$$k2_{pn} := 2.68$$

$$x2_{k1} := x_{2.mean} \cdot (1 - k2_{pn} \cdot V_2)$$

$$x2_{k1} = 10.7\ MPa$$

Five core samples

$$x_3 := \begin{pmatrix} 23.0 \\ 20.5 \\ 16.0 \\ 13.5 \\ 25.0 \end{pmatrix} \cdot MPa$$

$$n_3 := \text{length}(x_3)$$

$$x_{3.mean} := \frac{\sum_{i=1}^{n_3} x3_i}{n_3}$$

$$x_{3.mean} = 19.6\ MPa$$

$$s_3 := \sqrt{\frac{\sum_{i=1}^{n_3} (x3_i - x_{3.mean})^2}{n_3 - 1}}$$

$$s_3 = 4.8\ MPa$$

$$V_3 := \frac{s_3}{x_{3.mean}}$$

$$k3_{pn} := 2.46$$

$$x3_{k1} := x_{3.mean} \cdot (1 - k3_{pn} \cdot V_3)$$

$$x3_{k1} = 7.8\ MPa$$

A.2 BBK 04, Appendix A

Six core samples

$$x := \begin{pmatrix} 23.0 \\ 45.0 \\ 20.5 \\ 16.0 \\ 13.5 \\ 25.0 \end{pmatrix} \text{MPa}$$

$$n := \text{length}(x)$$

$$k_1 := \begin{cases} 6\text{MPa} & \text{if } 3 \le n \le 6 \\ 5\text{MPa} & \text{if } 7 \le n \le 9 \\ 4\text{MPa} & \text{if } 10 \le n \le 14 \end{cases}$$

$$m \ge f_{KK} + k_1$$

$$m := \text{mean}(x)$$

$$f_{KK} \le m - k_1$$

$$x \ge f_{KK} - 4 \qquad f_{KK} \le x + 4$$

$$f_{KK} := \min\left(m - k_1, \min(x) + 4\text{MPa}\right)$$

$$f_{cck} := \frac{f_{KK}}{1.14} \qquad f_{cck} = 15.4\ \text{MPa}$$

Four samples

$$x_2 := \begin{pmatrix} 23.0 \\ 20.5 \\ 16.0 \\ 25.0 \end{pmatrix} \text{MPa}$$

$$n_2 := \text{length}\left(x_2\right)$$

$$k_{1.2} := \begin{cases} 6\text{MPa} & \text{if } 3 \le n \le 6 \\ 5\text{MPa} & \text{if } 7 \le n \le 9 \\ 4\text{MPa} & \text{if } 10 \le n \le 14 \end{cases}$$

$$m_2 \ge f_{KK.2} + k_{1.2}$$

$$m_2 := \text{mean}\left(x_2\right)$$

$$f_{KK.2} \le m_2 - k_{1.2}$$

$$x_{2_i} \ge f_{KK.2} - 4 \qquad f_{KK.2} \le x_{2_i} + 4$$

$$f_{KK.2} := \min\left(m_2 - k_{1.2}, \min\left(x_2\right) + 4\text{MPa}\right)$$

$$f_{cck.2} := \frac{f_{KK.2}}{1.14} \qquad f_{cck.2} = 13.3\ \text{MPa}$$

Five samples

$$x_3 := \begin{pmatrix} 23.0 \\ 20.5 \\ 16.0 \\ 13.5 \\ 25.0 \end{pmatrix} \text{MPa} \qquad n_3 := \text{length}\left(x_3\right)$$

$$k_{1.3} := \begin{cases} 6\text{MPa} & \text{if } 3 \le n \le 6 \\ 5\text{MPa} & \text{if } 7 \le n \le 9 \\ 4\text{MPa} & \text{if } 10 \le n \le 14 \end{cases}$$

$$m_3 \ge f_{KK.3} + k_{1.3} \qquad m_3 := \text{mean}\left(x_3\right)$$

$$f_{KK.3} \le m_3 - k_{1.3} \qquad x_{3_i} \ge f_{KK.3} - 4 \qquad f_{KK.3} \le x_{3_i} + 4$$

$$f_{KK.3} := \min\left(m_3 - k_{1.3}, \min\left(x_3\right) + 4\text{MPa}\right)$$

$$f_{cck.3} := \frac{f_{KK.3}}{1.14} \qquad f_{cck.3} = 11.9\ \text{MPa}$$

Appendix B

Report from RING 2.0 analysis

B.1 The Prestwood bridge

This report was generated by ring2.0.h.5262

Summary

Bridge name	Location	Reference No.	Map reference
Prestwood			

Bridge type	Name of assessor	Assessing organization	Date of assessment
Highway			to dec 11 2008

Analysis result
Failure load factor = 152.175, load case 1 (this is the critical load case)

Mode of response at current load case

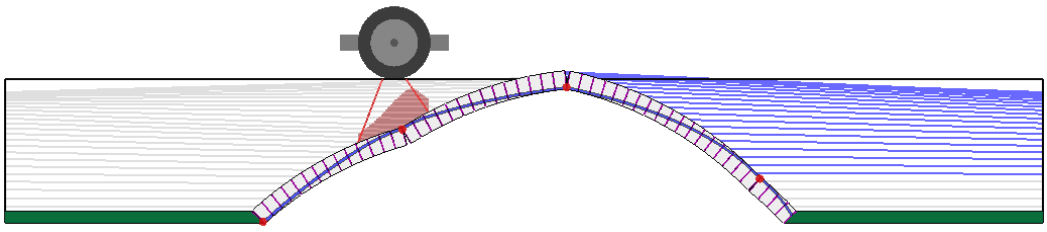

Units

Unless specified otherwise, the following units are used throughout this report:

Distance	Force*	Moment*	Angle	Unit weight	Material strength
mm	kN	kNmm	Degrees	kN/m3	N/mm2

* = *per metre width*

Geometry

Global:	No. Spans	Bridge width
	1	3800

Span 1:	Type	Shape	No. Rings	Span	Rise	Auto angle	LHS angle	RHS angle
	Bonded brick	Segmental	1	6550	1430	Yes	43	43

Ring 1:	No. Blocks	Ring thickness
	50	220

Fill Profile Properties

x	y	Surface fill depth
0	1810	0

Partial Factors

Factors applied to LOADS

Masonry unit weight	Fill unit weight	Surface unit weight	Axle load	Dynamic
1	1	1	1	1

Factors applied to MATERIALS

Masonry strength	Masonry friction
1	1

Backfill Properties

Unit weight	Angle of friction	Cohesion
20	37	10

Model dispersion of live load?	Model horizontal ' passive' pressures?
Yes	Yes
Dispersion type	**Cutoff angle**
Boussinesq	30
Soil arch interface, friction multiplier	**Soil arch interface, cohesion multiplier**
0.66	0.5
Mobilisation multiplier on Kp (mp)	**Mobilisation multiplier on cohesion (mpc)**
0.33	0.1
Keep mp.Kp > 1?	**Auto identify passive zones?**
Yes	Yes
Position	**Passive pressures?**
Abutment 0	Yes
Abutment 1	Yes

Surface Fill Properties

Basic properties

Unit weight	Load dispersion limiting angle
18	26.6

Load Cases

Load case	Vehicle	Position	Mirror?
Load Case1	Default 1kN Single Axle	1637	No

Vehicles

Name	Axle No.	Load magnitude	Axle position	Dynamic factor
Default 1kN Single Axle	1	1	0	No

B.2 The Glomman bridge

This report was generated by ring2.0.h.5262

Summary

Bridge name	Location	Reference No.	Map reference
Glomman2			

Bridge type	Name of assessor	Assessing organization	Date of assessment
Highway			fr dec 19 2008

Analysis result
Failure load factor = 6.34468, load case 122 (this is the critical load case)

Mode of response at current load case

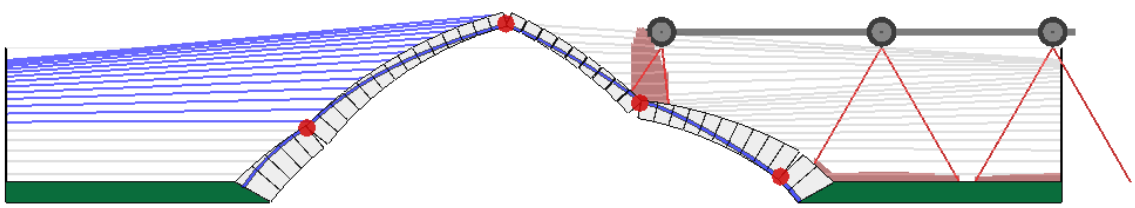

Units

Unless specified otherwise, the following units are used throughout this report:

Distance	Force*	Moment*	Angle	Unit weight	Material strength
mm	kN	kNmm	Degrees	kN/m3	N/mm2

* = per metre width

Geometry

Global:	No. Spans	Bridge width
	1	4200

Span 1:	Type	Shape	No. Rings	Bed joints normal to intrados
	Bonded brick	User defined	1	Yes

Intrados points:

x	y
0	0
8092	3952
16184	0

Extrados points of Ring 1:

x	y
-1082	604
8092	4352
17266	605

Ring 1:	No. Blocks
	40

Fill Profile Properties

x	y	Surface fill depth
8092	4702	50

Partial Factors

Factors applied to LOADS

Masonry unit weight	Fill unit weight	Surface unit weight	Axle load	Dynamic
1	1	1	1	1

Factors applied to MATERIALS

Masonry strength	Masonry friction
1	1

Backfill Properties

Unit weight	Angle of friction	Cohesion
15	30	0
Model dispersion of live load?	**Model horizontal ' passive' pressures?**	
Yes	Yes	
Dispersion type	**Cutoff angle**	
Boussinesq	30	
Soil arch interface, friction multiplier	**Soil arch interface, cohesion multiplier**	
0.66	0.5	
Mobilisation multiplier on Kp (mp)	**Mobilisation multiplier on cohesion (mpc)**	
0.33	0.1	
Keep mp.Kp $>$ 1?	**Auto identify passive zones?**	
Yes	Yes	
Position	**Passive pressures?**	
Abutment 0	Yes	
Abutment 1	Yes	

Surface Fill Properties

Basic properties

Unit weight	Load dispersion limiting angle
12	26.6

Appendix C

Results from the parametric survey

C.1 Load factors

Table C.1: Load factors for different loads with one parameter varying at the time and all other parameters equal to the reference case.

Young' s modulus - pavement (GPa)	Axle	Bogie 0.8 m	2-axle bus	3-axle bus
0.05	2.3	2.0	1.6	1.7
1	2.3	2.0	1.6	1.7
10	2.6	2.3	1.9	1.9
5	2.5	2.1	1.8	1.8

Young' s modulus - arch (GPa)	Axle	Bogie 0.8 m	2-axle bus	3-axle bus
20	2.5	2.2	1.7	1.8
25	2.4	2.1	1.7	1.7
30	2.3	2.0	1.6	1.7
27	2.4	2.1	1.7	1.7

Young' s modulus - abutments (GPa)	Axle	Bogie 0.8 m	2-axle bus	3-axle bus
20	2.3	2.0	1.6	1.7
25	2.3	2.0	1.6	1.7
30	2.3	2.0	1.6	1.7
250	2.5	2.3	1.7	1.8

Young' s modulus - backfill (GPa)	Axle	Bogie 0.8 m	2-axle bus	3-axle bus
0.05	2.2	1.9	1.5	1.6
0.5	2.6	2.3	1.8	1.9
0.225	2.3	2.0	1.6	1.7
1	2.8	2.6	2.0	2.0

Hinges in springing	Axle	Bogie 0.8 m	2-axle bus	3-axle bus
Yes	2.5	2.1	1.8	1.8
No	2.3	2.0	1.6	1.7

Poisson' s ratio - arch	Axle	Bogie 0.8 m	2-axle bus	3-axle bus
0.2	2.3	2.0	1.6	1.7
0.1	2.3	2.0	1.6	1.7
0.3	2.4	2.0	1.6	1.7
0.4	2.4	2.0	1.6	1.7

Poisson' s ratio - abutments	Axle	Bogie 0.8 m	2-axle bus	3-axle bus
0.2	2.3	2.0	1.6	1.7
0.1	2.3	2.0	1.6	1.7
0.3	2.3	2.0	1.6	1.7
0.4	2.4	2.0	1.6	1.7

Poisson' s ratio - backfill	Axle	Bogie 0.8 m	2-axle bus	3-axle bus
0.3	2.3	2.0	1.6	1.7
0.1	1.8	1.5	1.2	1.3
0.2	2.1	1.8	1.4	1.5
0.4	2.7	2.3	1.9	1.9

Poisson' s ratio - pavement	Axle	Bogie 0.8 m	2-axle bus	3-axle bus
0.3	2.3	2.0	1.6	1.7
0.1	2.3	2.0	1.6	1.7
0.2	2.3	2.0	1.6	1.7
0.4	2.3	2.0	1.6	1.7

Density - backfill (kg/m^3)	Axle	Bogie 0.8 m	2-axle bus	3-axle bus
1500	2.3	2.0	1.6	1.7
1200	2.2	1.9	1.5	1.6
1700	2.4	2.1	1.7	1.8
2000	2.6	2.2	1.8	1.9

Density - pavement (kg/m^3)	Axle	Bogie 0.8 m	2-axle bus	3-axle bus
1200	2.3	2.0	1.6	1.7
1000	2.3	2.0	1.6	1.7
1400	2.4	2.0	1.6	1.7
1600	2.4	2.0	1.6	1.7

Density - arch (kg/m^3)	Axle	Bogie 0.8 m	2-axle bus	3-axle bus
2400	2.3	2.0	1.6	1.7
2000	2.1	1.9	1.5	1.6
2200	2.2	1.9	1.6	1.6
2600	2.4	2.1	1.7	1.8

Density - abutments (kg/m^3)	Axle	Bogie 0.8 m	2-axle bus	3-axle bus
2400	2.3	2.0	1.6	1.7
2000	2.3	2.0	1.6	1.7
2200	2.3	2.0	1.6	1.7
2600	2.4	2.0	1.6	1.7

Appendix D

Code from ABAQUS and MATLAB

D.1 ABAQUS input file data

```
*HEADING
** Job name: Bridge Model name: Model-1
*PREPRINT, ECHO=NO, MODEL=NO, HISTORY=NO, CONTACT=NO
**
** PARTS
**
*PART, NAME=Abutment
*END PART
**
*PART, NAME="Arch_Frame line"
*END PART
**
*PART, NAME=Backfill_soil
*END PART
**
*PART, NAME=Pavement
*END PART
**
*PART, NAME=Rigid
*END PART
**
**
** ASSEMBLY
**
*ASSEMBLY, NAME=Assembly
**
*INSTANCE, NAME="Arch_Frame line-1", PART="Arch_Frame line"
*NODE
*ELEMENT, type=B21
**
**The Include command imports the text file to the analysis
**The ElSet-file group the elements of the arch into pairs
**symmetric around the crown
*INCLUDE, INPUT=H:\Exjobb Glomman\ABAQUS\081008\Bridge\Matlab\ElSet.txt
**The Section-file assign a different thickness for each element-pair
*INCLUDE, INPUT=H:\Exjobb Glomman\ABAQUS\081008\Bridge\Matlab\Section.txt
*END INSTANCE
**
*INSTANCE, NAME=Abutment-1, PART=Abutment
*NODE
*ELEMENT, TYPE=CPS4R
** Region: (Abutments:Picked)
** Section: Abutments
*SOLID SECTION, ELSET=_PickedSet2, MATERIAL=Concrete
8.4,
```

```
*END INSTANCE
**
*INSTANCE, NAME=Pavement-1, PART=Pavement
*NODE
*ELEMENT, TYPE=B21
** Region: (Pavement:Picked), (Beam Orientation:Picked)
** Section: Pavement  Profile: Pavement
*BEAM SECTION, ELSET=_PickedSet3, MATERIAL=Pavement, TEMPERATURE=GRADIENTS,
SECTION=RECT
8.4, 0.05
0.,0.,-1.
*END INSTANCE
**
*INSTANCE, NAME=Rigid-1, PART=Rigid
*NODE
*ELEMENT, TYPE=B21
** Region: (Rigid:Picked), (Beam Orientation:Picked)
** Section: Rigid  Profile: Arch
*BEAM SECTION, ELSET=_PickedSet2, MATERIAL=Rigid, TEMPERATURE=GRADIENTS,
SECTION=RECT
8.4, 0.4
0.,0.,-1.
*END INSTANCE
**
*INSTANCE, NAME=Backfill_soil-1, PART=Backfill_soil
*NODE
*ELEMENT, TYPE=CPS4R
** Region: (Soil:Picked)
** Section: Soil
*SOLID SECTION, ELSET=_PickedSet2, MATERIAL=Soil
8.4,
*End INSTANCE
**
**NSet.txt assign a name to each node in the pavement so they can be called in the
load module
*INCLUDE, INPUT=H:\Exjobb Glomman\ABAQUS\081008\Bridge\Matlab\NSet.txt
** Constraint: Abutment_left_rigid
*TIE, NAME=Abutment_left_rigid, adjust=YES
** Constraint: Abutment_right_rigid
*TIE, NAME=Abutment_right_rigid, adjust=YES
** Constraint: Arch_left_abutment
*TIE, NAME=Arch_left_abutment, adjust=YES, position tolerance=0.7
** Constraint: Arch_right_abutment
*TIE, NAME=Arch_right_abutment, adjust=YES, position tolerance=0.7
** Constraint: Backfill_left_abutment
*TIE, NAME=Backfill_left_abutment, adjust=YES
** Constraint: Backfill_right_abutment
*TIE, NAME=Backfill_right_abutment, adjust=YES
** Constraint: Pavement_soil
*TIE, NAME=Pavement_soil, adjust=yes, position tolerance=0.2
** Constraint: Soil_arch
*TIE, NAME=Soil_arch, adjust=YES, position tolerance=0.7
*END ASSEMBLY
**
**Amplitude.txt creates an amplitude function which activate one load in each time
increment
*INCLUDE, INPUT=H:\Exjobb Glomman\ABAQUS\081008\Bridge\Matlab\Amplitude.txt
**
** MATERIALS
**
*MATERIAL, NAME=Concrete
*DENSITY
2200.,
*ELASTIC
 3e+10, 0.2
*MATERIAL, NAME=Pavement
*DENSITY
1200.,
```

```
*ELASTIC
 5e+07, 0.3
*MATERIAL, NAME=Rigid
*ELASTIC
 1e+16,0.
*MATERIAL, NAME=Soil
*DENSITY
1500.,
*ELASTIC
 2e+08, 0.3
** ----------------------------------------------------------------
**
** STEP: Step-1
**
*STEP, NAME=Step-1, inc=309
*STATIC, direct
1., 309.,
**
** BOUNDARY CONDITIONS
**
** Name: Abutments Type: Displacement/Rotation
*BOUNDARY
_PickedSet263, 1, 1
_PickedSet263, 2, 2
** Name: Horizontal Type: Displacement/Rotation
*BOUNDARY
_PickedSet275, 1, 1
** Name: Vertical Type: Displacement/Rotation
*BOUNDARY
_PickedSet276, 2, 2
**
** LOADS
**
**Load.txt assign a load with the corresponding amplitude to each node in the
pavement
*INCLUDE, INPUT=H:\Exjobb Glomman\ABAQUS\081008\Bridge\Matlab\Load.txt
**
** OUTPUT REQUESTS
**
*RESTART, WRITE, frequency=0
**
** FIELD OUTPUT: F-Output-2
**
*OUTPUT, FIELD
*NODE OUTPUT
CF, RF, TF, U
*ELEMENT OUTPUT, directions=YES
E, S, SF
**
** FIELD OUTPUT: F-Output-1
**
*OUTPUT, FIELD, variable=PRESELECT
**
** HISTORY OUTPUT: H-Output-1
**
*OUTPUT, HISTORY, variable=PRESELECT
*END STEP
```

D.2 MATLAB code for Abaqus input data

```
clc, clear all

%Arch-nodes koordinates
A=[ ];


%Number of nodes in pavement
np=309;

%Number of nodes in outer part of pavement
npo=55;

%Number of nodes in inner part of pavemet
npi=100;

%Number of nodes in arch
na=201;

%% NSet grouping nodes in pavement into node sets
NSet=fopen('NSet.txt','wt');

k=1;
for i=1:np;
    if i==1
        fprintf(NSet,'*Nset, nset=_NPavementSet%g , internal, instance=Pavement-
1\n' , i);
        fprintf(NSet,'    %g ,  %g\n' , 1, 1);
    else if i==npo
        fprintf(NSet,'*Nset, nset=_NPavementSet%g , internal, instance=Pavement-
1\n' , i);
        fprintf(NSet,'    %g ,  %g\n' , 2, 2);
        else if i==round(np/2)
            fprintf(NSet,'*Nset, nset=_NPavementSet%g , internal,
instance=Pavement-1\n' , i);
            fprintf(NSet,'    %g ,  %g\n' , 3, 3);
            else if i==npo+2*npi
                fprintf(NSet,'*Nset, nset=_NPavementSet%g , internal,
instance=Pavement-1\n' , i);
                fprintf(NSet,'    %g ,  %g\n' , 4, 4);
                else if i==np
                    fprintf(NSet,'*Nset, nset=_NPavementSet%g , internal,
instance=Pavement-1\n' , i);
                    fprintf(NSet,'    %g ,  %g\n' , 5, 5);
                    else
                        fprintf(NSet,'*Nset, nset=_NPavementSet%g , internal,
instance=Pavement-1\n' , i);
                        fprintf(NSet,'    %g ,  %g\n' , k+5, k+5);
                        k=k+1;
                    end
                end
            end
        end
    end
end

fclose(NSet);

%% ElSet Grouping elements into element sets
ElSet=fopen('ElSet.txt','wt');
for i=1:na/2;
    fprintf(ElSet,'*Elset, elset=EArchset%g , internal, instance=Arch_Frame line\n'
, i);
    fprintf(ElSet,'    %g ,  %g\n' , i, na-i);
end
```

```
fclose(ElSet);

%% Section variation

for i=1:length(A)/2;
    x(i,2)=A(i,2)-A(1,2);
    x(i,1)=A(i,1);
end
for i=1:length(x);
    if x(i,2)<=3.019;
        h(i,2)=-0.0059545*x(i,2)^3+0.079294*x(i,2)^2-0.36068*x(i,2)+1.1;
    else
        h(i,2)=0.0025066*x(i,2)^2-0.059847*x(i,2)+0.72782;
    end
    h(i,1)=x(i,1);
end

Sect=fopen('Section.txt','wt');
for i=1:length(h);
    fprintf(Sect,'** Region: (Arch_Section-%g:Picked), (Beam
Orientation:Picked)\n', i);
    fprintf(Sect,'*Elset, elset=EArchSet%g, internal\n', i) ;
    fprintf(Sect,'%g,  %g\n', i, na-i);
    fprintf(Sect,'** Section: Arch_Section-%g  Profile: Arch_Profile-%g\n', i, i);
    fprintf(Sect,'*Beam Section, elset=EArchSet%g, material=CONCRETE,
temperature=GRADIENTS, section=RECT\n', i);
    fprintf(Sect,'%g, %g\n', 8.4, h(i,2));
    fprintf(Sect,'0.,0.,-1.\n');
end
fclose(Sect);


%% Generate Load
Load=fopen('Load.txt','wt');
for i=1:np;
    fprintf(Load,'** Name: Load- %g  Type: Concentrated force\n', i);
    fprintf(Load,'*Cload, amplitude=Amp- %g\n', i);
    fprintf(Load,'_NPavementSet%g , 2, -1\n', i);
    fprintf(Load,'**\n');
end
fclose(Load);

%% Amplitude
Amp=fopen('Amplitude.txt','wt');

%First node
fprintf(Amp,'*Amplitude, name=Amp- 1 , time=TOTAL TIME\n');
fprintf(Amp,'0, 0, 1 , 1,  2 , 0, %g, 0\n', np);

for i=2:np-2;
    fprintf(Amp,'*Amplitude, name=Amp- %g , time=TOTAL TIME\n',i);
    fprintf(Amp,'0, 0, %g , 0,  %g , 1,  %g , 0, %g, 0\n', i-1, i, i+1, np);
end

%2:nd last node
fprintf(Amp,'*Amplitude, name=Amp- %g , time=TOTAL TIME\n', np-1);
fprintf(Amp,'0, 0, %g, 0, %g, 1, %g,0 \n', np-2, np-1, np);

%Last node
fprintf(Amp,'*Amplitude, name=Amp- %g , time=TOTAL TIME\n', np);
fprintf(Amp,'0, 0, %g, 0, %g, 1, \n', np-1, np);
fclose(Amp);
```

D.3 MATLAB code for failure analysis

The following code from MATLAB calculates and plots the load factors and the failure envelope.

```
clear all, clc, clf

%% Reading of other files for input
influenser
xcor
%% Rupture envelope
for calc=1:4
    for i=1:length(nperm(:,1))
        if calc==1
            if csf(i,1)>=csf(i,4)
                Mlive(i,calc)=csf(i,1);
                Nlive(i,calc)=csf(i,2);
                node(i,calc)=csf(i,3);
                axelavs(i,calc)=0;
            else
                Mlive(i,calc)=csf(i,4);
                Nlive(i,calc)=csf(i,5);
                node(i,calc)=csf(i,6);
                axelavs(i,calc)=csf(i,7);
            end
        elseif calc==2
            if csf(i,8)<=csf(i,11)
                Mlive(i,calc)=csf(i,8);
                Nlive(i,calc)=csf(i,9);
                node(i,calc)=csf(i,10);
                axelavs(i,calc)=0;
            else
                Mlive(i,calc)=csf(i,11);
                Nlive(i,calc)=csf(i,12);
                node(i,calc)=csf(i,13);
                axelavs(i,calc)=csf(i,14);
            end
        elseif calc==3
            if csf(i,16)>=csf(i,19)
                Nlive(i,calc)=csf(i,16);
                Mlive(i,calc)=csf(i,15);
                node(i,calc)=csf(i,17);
                axelavs(i,calc)=0;
            else
                Nlive(i,calc)=csf(i,19);
                Mlive(i,calc)=csf(i,18);
                node(i,calc)=csf(i,20);
                axelavs(i,calc)=csf(i,21);
            end
        elseif calc==4
            if csf(i,23)<=csf(i,26)
                Nlive(i,calc)=csf(i,23);
                Mlive(i,calc)=csf(i,22);
                node(i,calc)=csf(i,24);
                axelavs(i,calc)=0;
            else
                Nlive(i,calc)=csf(i,26);
                Mlive(i,calc)=csf(i,25);
                node(i,calc)=csf(i,27);
                axelavs(i,calc)=csf(i,28);
            end
        end
    end

    nlive(:,calc)=1.8*Nlive(:,calc)*1.3;    %*2 because we want traffic in
    mlive(:,calc)=1.8*Mlive(:,calc)*1.3;    %both lanes
```

```
                                                %1.3 is the partial coefficient
    ntot(:,calc)=nperm(:,1)+nlive(:,calc);
    mtot(:,calc)=mperm(:,1)+mlive(:,calc);

    step=1E-3;
    n=[0:step:1]';
    m=n.*(0.5-(beta/alfa).*n);

    if calc==1
        figure
    end
    subplot(2,2,calc)
    plot([0 n(end)],[0 0],'k--')
    hold on
    plot(n,m,'k-')
    plot(n,-m,'k--')
    xlim([0 n(end)])
    ylim([-(max(m)+0.01) max(m)+0.01])

%% Plot the permanent loads (nperm,mperm) and the total loads (ntot,mtot)
    plot(nperm,mperm,'ro')
%_____________________________________________________________________________
    for i=1:length(nperm)

        if nperm(i)<0 || nperm(i)>1 || mperm(i)>nperm(i)*(0.5-...
                (beta/alfa)*nperm(i)) || mperm(i)<-nperm(i)*(0.5-...
                (beta/alfa)*nperm(i))
            disp(sprintf('Failure in node %g caused by the deadweight',i))
            plot(ntot(i,calc),mtot(i,calc),'bo')
            return

        else plot(ntot(i,calc),mtot(i,calc),'bo')
        end
    end
%_____________________________________________________________________________

%% Plot the extended line between the points

%y=kx+p
    p=0;
    k=inf;
    if nlive==0
        m2=-(max(m)+0.01):0.001:max(m)+0.01;
        n2=0*m2+nperm;
        plot(n2,m2,'k')
    elseif nlive~=0
        k=(mtot(:,calc)-mperm)./(ntot(:,calc)-nperm);    %k=the inclination
        p=mperm-k.*nperm;                                %of the line
        n2=n;                                            %the line crosses
        for j=1:length(k(:,1))                           %the y-axis  at p
            for i=1:length(n2)
                m2(i,j)=k(j)*n2(i)+p(j);
            end
            plot(n2(:),m2(:,j),'k')
            hold on
        end
    end

%% Find the point where the second degree polynomial and the extended line cross
    %m=m2   =>   n*(0.5-(beta/alfa)*n)=k*n2+p
    %if k*x+p=0, 0<x<1, search for "crosspoints" in both curves

    for i=1:length(k(:,1))  %(pos and neg)
        if p(i)>0 && (-p(i)/k(i)<=0 || -p(i)/k(i)>=1)
            n3=0.5*alfa/beta*(0.5-k(i))-sqrt((0.5*alfa/beta*...
                (0.5-k(i)))^2-alfa/beta*p(i));
            n4=0.5*alfa/beta*(0.5-k(i))+sqrt((0.5*alfa/beta*...
                (0.5-k(i)))^2-alfa/beta*p(i));
```

```
        n5=0;
        n6=0;
        kors(i,:)=[n3 n4 n5 n6];
    elseif p(i)<0 && (-p(i)/k(i)<=0 || -p(i)/k(i)>=1)
        n3=0.5*alfa/beta*(0.5+k(i))-sqrt((0.5*alfa/beta*...
            (0.5+k(i)))^2+alfa/beta*p(i));
        n4=0.5*alfa/beta*(0.5+k(i))+sqrt((0.5*alfa/beta*...
            (0.5+k(i)))^2+alfa/beta*p(i));
        n5=0;
        n6=0;
        kors(i,:)=[n3 n4 n5 n6];
    elseif p(i)>0 && -p(i)/k(i)>0 && -p(i)/k(i)<1
        n3=0.5*alfa/beta*(0.5-k(i))-sqrt((0.5*alfa/beta*...
            (0.5-k(i)))^2-alfa/beta*p(i));
        n4=0.5*alfa/beta*(0.5-k(i))+sqrt((0.5*alfa/beta*...
            (0.5-k(i)))^2-alfa/beta*p(i));
        n5=0.5*alfa/beta*(0.5+k(i))-sqrt((0.5*alfa/beta*...
            (0.5+k(i)))^2+alfa/beta*p(i));
        n6=0.5*alfa/beta*(0.5+k(i))+sqrt((0.5*alfa/beta*...
            (0.5+k(i)))^2+alfa/beta*p(i));
        kors(i,:)=[n3 n4 n5 n6];
    elseif p(i)<0 && -p(i)/k(i)>0 && -p(i)/k(i)<1
        n3=0.5*alfa/beta*(0.5-k(i))-sqrt((0.5*alfa/beta*...
            (0.5-k(i)))^2-alfa/beta*p(i));
        n4=0.5*alfa/beta*(0.5-k(i))+sqrt((0.5*alfa/beta*...
            (0.5-k(i)))^2-alfa/beta*p(i));
        n5=0.5*alfa/beta*(0.5+k(i))-sqrt((0.5*alfa/beta*...
            (0.5+k(i)))^2+alfa/beta*p(i));
        n6=0.5*alfa/beta*(0.5+k(i))+sqrt((0.5*alfa/beta*...
            (0.5+k(i)))^2+alfa/beta*p(i));
        kors(i,:)=[n3 n4 n5 n6];
    end
end

for i=1:length(kors(:,1))
    q=1;
    for j=1:length(kors(1,:))
        if nlive(i,1)~=0 && kors(i,j)>0 && kors(i,j)<1;
            korsny(i,q)=kors(i,j);
            q=q+1;
        end
    end
end

for i=1:length(nlive(:,1))

    if nlive(i,calc)>0

        if korsny(i,1)>nperm(i)
            korspkt(i,calc)=korsny(i,1);
        else
            korspkt(i,calc)=korsny(i,2);
        end
        mslut(i,calc)=k(i)*korspkt(i,calc)+p(i);
        plot(korspkt(i,calc),mslut(i,calc),'ko')

    elseif nlive(i,calc)<0

        if korsny(i,1)<nperm(i)
            korspkt(i,calc)=korsny(i,1);
        else
            korspkt(i,calc)=korsny(i,2);
        end
        mslut(i,calc)=k(i)*korspkt(i,calc)+p(i);
        plot(korspkt(i,calc),mslut(i,calc),'ko')
```

```
        elseif nlive(i,calc)==0

            korspkt(i,calc)=nperm(i);

            if mlive(i,calc)>0
                mslut(i,calc)=nperm(i)*(0.5-(beta/alfa)*nperm(i));
                plot(nperm(i),mslut(i,calc),'ko')
            else
                mslut(i,calc)=-(nperm(i)*(0.5-(beta/alfa)*nperm(i)));
                plot(nperm(i),mslut(i,calc),'ko')
            end
        end
    end

%% Calculates the load factor
    for i=1:length(nlive)
        if nlive(i,calc)==0
            psi(i,calc)=abs((mslut(i,calc)-mperm(i))/...
                (mtot(i,calc)-mperm(i)));
        else
            psi(i,calc)=abs((korspkt(i,calc)-nperm(i))/...
                (ntot(i,calc)-nperm(i)));
        end
    end

    [a kaka]=min(psi(:,calc));
    title(sprintf('The lowest safety factor is %1.3f in node %g',a,...
        brytnod(calc)))

    if calc==1
        xlabel('Mmax,Nadh')
    elseif calc==2
        xlabel('Mmin,Nadh')
    elseif calc==3
        xlabel('Nmax,Madh')
    else
        xlabel('Nmin,Madh')
    end
end

[minimumpsi psinodetemp]=min(psi);
[minpsi psinode]=min(minimumpsi);
breaknode=psinodetemp(psinode);
```

influences.m below organizes the largest influences from bogiepressure.m.

```
arch_height                 %Reads the arch_height file which gives...
                            %each element a thickness
%%                          %According to the Swedish road administration
                            %Vägverkets document "Bärighetsklasser"
BK=3;                       %BK-class on the road (1,2 or 3)
drivande=1;                 %Yes=1
                            %No=0
krav=0;                     %Demands according to table "2. Boggitryck" i
                            %"Grundregler i 4 kap. trafikförordningen"
                            %krav=0 if the demands are not fulfilled
                            %krav=0 if the demands are fulfilled

if BK~=1 && BK~=2 && BK~=3 && BK~=4
    disp('Incorrect choice of "BK"')
    return
end
if drivande~=0 && drivande~=1
    disp('Incorrect choice of "drivande"')
    return
end
```

```
if krav~=0 && krav~=1
    disp('Incorrect choice of "krav"')
    return
end

%% Normalise the influence lines

for i=1:length(mxy(:,1))
    for j=2:length(mxy(1,1:end))
        mxy(i,j)=mxy(i,j)/(b*h(j-1)^2*fcc);
        nxy(i,j)=nxy(i,j)/(b*h(j-1)*fcc);
    end
end

mxy(:,1)=pavexy(:,1);            %sets the first column in the influence
nxy(:,1)=pavexy(:,1);            %line vector as the real x-values

nperm=Nperm./(b.*h(:,1).*fcc);
mperm=Mperm./(b.*h(:,1).^2*fcc);

%%

for point=1:4
    for k=2:length(mxy(1,1:end))       %Which node we're looking at
        if point==1 || point==2

            [minfluensa,ninfluensa,mnoda,minfluensb,ninfluensb,mnodb,...
                maxelavs]=mboggietryck(mxy,nxy,BK,drivande,krav,k,point);

            M(k-1,1)=minfluensa;       %Moment (max or min depending on
                                       %choice of "point") for one axle
            M(k-1,2)=ninfluensa;       %Normal force in the same point
            M(k-1,3)=mnoda;            %The actual node
            M(k-1,4)=minfluensb;       %Moment (max or min depending on
                                       %choice of "point") for two axle
            M(k-1,5)=ninfluensb;       %Normal force in the same point
            M(k-1,6)=mnodb;            %The actual node for the left axle
            M(k-1,7)=maxelavs;         %Distance between the axles

            if point==1
                csf(k-1,1)=minfluensa;                    %point=1
                csf(k-1,2)=ninfluensa;
                csf(k-1,3)=mnoda;
                csf(k-1,4)=minfluensb;
                csf(k-1,5)=ninfluensb;
                csf(k-1,6)=mnodb;
                csf(k-1,7)=maxelavs;

                if k==length(mxy(1,1:end))
                    [storstmoma brytnoda]=max(csf(:,1));
                    [storstmomb brytnodb]=max(csf(:,4));
                    if storstmoma>=storstmomb
                        brytkraft(point)=storstmoma;
                        brytnod(point)=brytnoda;
                    else
                        brytkraft(point)=storstmomb;
                        brytnod(point)=brytnodb;
                    end
                end

            else

                csf(k-1,8)=minfluensa;                    %point=2
                csf(k-1,9)=ninfluensa;
                csf(k-1,10)=mnoda;
                csf(k-1,11)=minfluensb;
                csf(k-1,12)=ninfluensb;
                csf(k-1,13)=mnodb;
```

```
                csf(k-1,14)=maxelavs;

              if k==length(mxy(1,1:end))
                    [minstmoma brytnoda]=min(csf(:,8));
                    [minstmomb brytnodb]=min(csf(:,11));
                    if minstmoma<=minstmomb
                        brytkraft(point)=minstmoma;
                        brytnod(point)=brytnoda;
                    else
                        brytkraft(point)=minstmomb;
                        brytnod(point)=brytnodb;
                    end
                end
            end

        elseif point==3 || point==4
            [ninfluensa, minsfluensa,nnoda,ninfluensb,minfluensb,nnodb,...
                naxelavs]=nboggietryck(mxy,nxy,BK,drivande,krav,k,point);
            N(k-1,1)=ninfluensa;
            N(k-1,2)=minfluensa;
            N(k-1,3)=nnoda;
            N(k-1,4)=ninfluensb;
            N(k-1,5)=minfluensb;
            N(k-1,6)=nnodb;
            N(k-1,7)=naxelavs;

            if point==3
                csf(k-1,15)=minfluensa;                    %point=3
                csf(k-1,16)=ninfluensa;
                csf(k-1,17)=nnoda;
                csf(k-1,18)=minfluensb;
                csf(k-1,19)=ninfluensb;
                csf(k-1,20)=nnodb;
                csf(k-1,21)=naxelavs;
                if k==length(mxy(1,1:end))
                    [storstnfa brytkrafta]=max(csf(:,16));
                    [storstnfb brytkraftb]=max(csf(:,19));
                    if storstnfa>=storstnfb
                        brytkraft(point)=storstnfa;
                        brytnod(point)=brytnoda;
                    else
                        brytkraft(point)=storstnfb;
                        brytnod(point)=brytnodb;
                    end
                end
            else
                csf(k-1,22)=minfluensa;                    %point=4
                csf(k-1,23)=ninfluensa;
                csf(k-1,24)=nnoda;
                csf(k-1,25)=minfluensb;
                csf(k-1,26)=ninfluensb;
                csf(k-1,27)=nnodb;
                csf(k-1,28)=naxelavs;
                if k==length(mxy(1,1:end))
                    [minstnfa brytnoda]=min(csf(:,23));
                    [minstnfb brytnodb]=min(csf(:,26));
                    if minstmoma<=minstmomb
                        brytkraft(point)=minstnfa;
                        brytnod(point)=brytnoda;
                    else
                        brytkraft(point)=minstnfb;
                        brytnod(point)=brytnodb;
                    end
                end
            end
        end
    end
end
```

The file bogiepressure.m makes the load combination for the BK-loads and sends them back to influences.m. The load combination for a BK3-bogie is given below. The same routine was then repeated with different axle pressures for BK2 and BK1 . They, and the routine to find the largest influence from the axle load, are not given here though.

```
%----------------------------Bogie load----------------------------
                                        %bt is the matrix where all the
for j=1:length(x)                       %influences are stored
    i=1; w=1; q=1;                      %i, w and q are counters
    if BK==3
        if x(j)<1.0                     %Steps. y(i)=influence in pt. i
            while pavexy(i,1)<x(j)      %while the distance between the
                bt(i,j)=mxy(i,k)*5750*g;  %axles are larger than x(j),
                i=i+1; u(j)=i;          %only one axle acts on the arch
            end                         %u(j) remembers how many node
            while pavexy(w,1)<=...      %steps the axle distance
                    L-(x(1)+(j-1)*dx)   %corresponds to
                while pavexy(q,1)<pavexy(w,1)+...
                        (x(1)+(j-1)*dx)
                    q=q+1;
                end
                bt(i,j)=(mxy(w,k)+(mxy(q,k)-mxy(q-1,k))/(mxy(q,1)-...
                    mxy(q-1,1))*(mxy(w,1)+(x(1)+(j-1)*dx)-mxy(q-1,1))+...
                    mxy(q-1,k))*5750*g;   %the first term corresponds to
                i=i+1; w=w+1; v(j)=w;   %the left axle and the second
            end                         %term to the right
            while w<=length(pavexy(:,1))...%the influence for the second
                    && pavexy(w,1)<=L   %term is interpolated because the
                bt(i,j)=mxy(w,k)*5750*g;  %right axle stands between two
                i=i+1; w=w+1;           %nodes
            end
        elseif x(j)>=1.0
            while pavexy(i,1)<x(j)
                bt(i,j)=mxy(i,k)*6000*g;
                i=i+1; u(j)=i;
            end
            while pavexy(w,1)<=L-(x(1)+(j-1)*dx)
                while pavexy(q,1)<pavexy(w,1)+(x(1)+(j-1)*dx)...
                        && q<=length(pavexy(:,1))
                    q=q+1;
                end
                bt(i,j)=(mxy(w,k)+(mxy(q,k)-mxy(q-1,k))/(mxy(q,1)-...
                    mxy(q-1,1))*(mxy(w,1)+(x(1)+(j-1)*dx)-mxy(q-1,1))+...
                    mxy(q-1,k))*6000*g;
                i=i+1; w=w+1; v(j)=w;
            end
            while w<=length(pavexy(:,1)) && pavexy(w,1)<=L
                bt(i,j)=mxy(w,k)*6000*g;
                i=i+1; w=w+1;
            end
        end
if point==1                 %a=Vector with the maximum influences, one
    [a,b]=max(bt);          %  maximum influence for each distance between
    [minfluensb,d]=max(a);  %  the axles
elseif point==2             %b=Vector with all nodes where the maximum
    [a,b]=min(bt);          %  influences operate
    [minfluensb,d]=min(a);  %c=The maximum influence
end                         %d=The node where the maximum influence
                            %  operates
mnodb=b(d);                 %In which node the load should be placed to
                            %cause the least favourable bending moment
maxel=x(1)+(d-1)*dx;        %Distance between axles at the maximum
                            %influence
q=1; r=1;
while pavexy(q,1)<maxel
    q=q+1;                  %How many nodes an axle distance corresponds to
end
```

```
while pavexy(r,1)<L-maxel
    r=r+1;
end

if mnodb<q-1
    maxel=0;
    ninfl=nxy(mnodb,k);     %Corresponding influence for normal force
elseif mnodb>=q-1 && mnodb<=r
    mnodb=mnodb-(u(d)-1);   %Subtracts the number of nodes that corresponds
    q=1;                    %to an axle diatnce
    while pavexy(q,1)<pavexy(mnodb,1)+maxel;
        q=q+1;
    end
    ninfl=nxy(mnodb,k)+((nxy(q,k)-nxy(q-1,k))/(nxy(q,1)-nxy(q-1,1)))*...
        ((nxy(mnodb,1)+maxel)-nxy(q-1,1))+nxy(q-1,k);
elseif mnodb>r
    mnodb=mnodb-(2*(u(d)-1));
    maxel=0;
    ninfl=nxy(mnodb,k);
end

if BK==3
    if maxel<1.0
        ninfluensb=ninfl*5750*g;    %Calculation of the normal force
    else ninfluensb=ninfl*6000*g;
    end
elseif BK==2
    if maxel<1.0
        ninfluensb=ninfl*5750*g;
    else ninfluensb=ninfl*8000*g;
    end
elseif BK==1
    if maxel<1.0
        ninfluensb=ninfl*5750*g;
    elseif maxel>=1.0 && maxel<1.3
        ninfluensb=ninfl*8000*g;
    elseif maxel>=1.3 && maxel<1.8
        if krav==0
            ninfluensb=ninfl*9000*g;
        elseif krav==1
            ninfluensb=ninfl*9500*g;
        end
    elseif maxel>=1.8
        ninfluensb=ninfl*10000*g;
    end
end
```

Each element is given a specific thickness in archheight.m.

```
thickness       %-----------------------------------------------------------%
M_perm          %thickness.m calculates the thickness variation of the arch
N_perm          %M_perm and N_perm give the cross section forces caused by
mkoordinater    %the deadweight of the different parts of the bridge
nkoordinater    %mkoordinater and nkoordinater give the influences from the
                %traffic load
xproj           %reads the real co-ordinates of the arch
pavement_koordinater   %the co-ordinates of the pavement
                %-----------------------------------------------------------%
%% Input
%Concrete properties
fcck=11.5E6;
alfa=0.8;
beta=0.4;
gammam=1.5;
gamman=1.2;
fcc=fcck/(gamman*gammam);
```

```
%depth of the bridge
b=8.4;

%% The different thicknesses for each element of the arch
 L=pavexy(end,1);
i=1; j=1; k=0;

while xy(i,1)<xx(bpoint);
    h(i,1)=-0.0059545*xy(i,1)^3+0.079294*xy(i,1)^2-0.36068*xy(i,1)+1.1;
    i=i+1; c=i;
end
while xy(i,1)<=xy(floor(length(xy(:,1))/2))
    h(i,1)=0.0025066*xy(i,1)^2-0.059847*xy(i,1)+0.72782;
    i=i+1; d=i;
end

while i<2*d-1-c
    h(i,1)=h(d-j);
    i=i+1; j=j+1;
end

while i<=2*(d-1)
    h(i,1)=h(c-k);
    i=i+1; k=k+1;
end
```

The thickness variation is calculated in thickness.m.

```
xproj   %Reads the file with the coordinates of the center line
        %Origin in the left springing
%% Breakpoint
bpoint=3;   %Breakpoint, the two curve parts meet
%----------------------%
polydeg1=3;             %Degree of polynomials
polydeg2=2;
%----------------------%
%% The arch shape
dx=0.001;   %step length in meter
xx=[        %% x-coordinates
    ];
t=[         %% Thickness of the arch in the given x-coordinates
   ];

%% x-coordinates
q=1;
while xy(q,1)<xx(bpoint)
    q=q+1;
end

xy1=xy(1:q-1,1);
xy1(q,1)=xx(bpoint);
xy2(1,1)=xx(bpoint);

for i=1:ceil(length(xy(:,1))/2)+1-q
    xy2(i+1,1)=xy(q,1);
    q=q+1;
end

%% Second part of the arch
t2=t(bpoint:end,1);

for j=1:polydeg2+1                      %column
    for i=1:length(t(bpoint:end))       %row
        T2(i,j)=xx(bpoint-1+i)^(j-1);
    end
```

```
end
fmat2=(T2'*T2)^(-1)*(T2'*t2);   %Calculates our coefficients
                                %"a0 a1 a2..."
%% Thickness of the arch
for j=1:length(fmat2)           %Calculates the thickness in every single
    for i=1:length(xy2)         %point in the right part of the arch
        thickness2(i,j)=fmat2(j)*xy2(i)^(j-1);
    end
end

for i=1:length(thickness2(:,1))
    sumthick2(i,1)=sum(thickness2(i,:));
end

%% Derivative of the arch thickness in the breakpoint
for i=1:polydeg2            %(second part of the arch)
    tprimbryt(i,1)=i*(fmat2(i+1)*xx(bpoint)^(i-1));
end

sumtprim=sum(tprimbryt);
%% First part of the arch
t1=t(1:bpoint-1,1);
t1(bpoint,1)=sumthick2(1);
t1(bpoint+1,1)=sumtprim;

for j=1:polydeg1+1                  %column
    for i=1:length(t(1:bpoint))     %row
        T1(i,j)=xx(i)^(j-1);
    end
    T1(i+1,j)=(j-1)*xx(bpoint)^(j-2);        %Adds another row so that the
end                                          %second part of the arch
fmat1=(T1'*T1)^(-1)*(T1'*t1);                %has the same derivative as
                                             %the first in the breakpoint
for j=1:length(fmat1)            %Calculates the y-values for the left part
    for i=1:length(xy1(:,1))
        thickness1(i,j)=fmat1(j)*xy1(i)^(j-1);
    end
end

for i=1:length(thickness1(:,1))
    sumthick1(i,1)=sum(thickness1(i,:));
end

%% The right half of the hole arch

for i=1:length(xy2)
    xy3(i,1)=2*xx(end)-xy2(end+1-i);
    sumthick3(i,1)=sumthick2(end+1-i);
end

for i=1:length(xy1)
    xy4(i,1)=2*xx(end)-xy1(end+1-i);
    sumthick4(i,1)=sumthick1(end+1-i);
end


%% Plot
axis([xx(1) xx(end)*2 min(t)-0.05 max(t)+0.05])
hold on
plot(xy1,sumthick1,'b')
plot(xy2,sumthick2,'r')
plot(xy3,sumthick3,'r')
plot(xy4,sumthick4,'b')
plot([0 xy(end,1)],[0 0],'--')
title('Thickness of the arch','fontsize',12,'fontname','latex serif')
xlabel('\itL\rm/2','fontsize',12,'fontname','latex serif')
ylabel('\itt \rm[mm]','fontsize',12,'fontname','latex serif')
set(gca,'fontsize',12,'fontname','latex serif')
```

TRITA-BKN. Master Thesis 271,
Structural Design and Bridges 2009
ISSN 1103-4297
ISRN KTH/BKN/EX-271-SE

www.kth.se